SPATIAL ASSOCIATION BETWEEN THE LOCATIONS OF ROOTS AND WATER FLOW PATHS IN HIGHLY STRUCTURED SOIL

A Thesis

by

NATHAN T. GARDINER

Submitted to the Office of Graduate Studies of
Texas A&M University
in partial fulfillment of the requirements for the degree of

MASTER OF SCIENCE

December 2003

Major Subject: Soil Science

SPATIAL ASSOCIATION BETWEEN THE LOCATIONS OF ROOTS AND WATER FLOW PATHS IN HIGHLY STRUCTURED SOIL

A Thesis

by

NATHAN T. GARDINER

Submitted to Texas A&M University
in partial fulfillment of the requirements
for the degree of

MASTER OF SCIENCE

Approved as to style and content by:

Kevin McInnes (Chair of Committee)	James Heilman (Member)
Bradford Wilcox (Member)	Mark Hussey (Department Head)

December 2003

Major Subject: Soil Science

ABSTRACT

Spatial Association Between the Locations of Roots And Water Flow Paths in Highly Structured Soil. (December 2003)

Nathan T. Gardiner, B.S., Brigham Young University

Chair of Advisory Committee: Dr. Kevin McInnes

Considerable evidence exists that the majority of low tension water flow through highly structured clayey soil occurs in a small fraction of total pore space and that the flow paths converge as depth increases. In structured clayey soils, water tends to flow in locations where macroporosity is high and roots tend to enjoy this condition as well. Water reduces the strength and mechanical impedance of the soil. Mechanical impedance of clayey soils tends to be extremely high when the soils are dry so one might expect that there would be a positive spatial correlation between the location of roots and the location of water flow paths in highly structured clayey soils. Understanding the relationship between the location of roots in soil relative to the location of water flow paths is important in understanding how plants obtain nutrients and water for growth, and it would also be of considerable importance in phytoremediation research and research into the prevention of groundwater contamination. This experiment was designed to map the locations of flow paths and roots and then measure the spatial association of the two.

A pasture on Ship's clay along the Brazos River was chosen as the research site. Three plots were irrigated with an Erioglaucine dye solution used to stain flow paths.

After irrigation the soil was excavated to a depth of 25 cm. On the resulting horizontal plane the dye stain pattern was mapped using photography. The locations of roots were mapped on clear plastic sheets. During mapping the roots were categorized by size. The mapping procedure was repeated at depth of 45 cm and 75 cm for all plots. The root maps were overlaid on the photographic images and analyzed for a spatial association.

There was no evidence the smallest (> 1 mm diameter) roots were not randomly distributed. The results did show that the larger roots were not randomly distributed, and evidence pointed to a clustering of roots in and around the dye stained flow paths. However, the data fell short of establishing a spatial association. The lack of more conclusive data was likely the result of inaccuracies in the mapping.

ACKNOWLEDGMENTS

There are a number of people I would like to thank for help. Without their assistance this thesis could never have been put together.

First, I would like to thank Dr. Kevin McInnes for taking me on as an employee and student, and also for his patience and funds on a project that seemed like it would never end. Secondly, I would like to thank Drs. Heilman and Wilcox for teaching excellent classes and serving on my committee. And third, I need to thank Dr. Bobby McMichael for his assistance in our root analysis.

This project could also not have been completed without the help of Dr. Maria Nobles, my fellow grad students, and student workers, specifically, Faith Ann Heinsch, Nick Laskowski, Euc Jasso, and Brad Melton.

I must also pass along a special thanks to my parents, especially my father, Dr. Duane Gardiner, for his advise and support.

TABLE OF CONTENTS

LIST OF FIGURES

FIGURE Page

FIGURE Page

FIGURE Page

LIST OF TABLES

CHAPTER I

INTRODUCTION AND OBJECTIVES

Considerable evidence exists that the majority of low tension water flow through highly structured clayey soil occurs in a small fraction of total pore space (Shaffer et al., 1979; Bouma, 1984; Watson and Luxmoore, 1986; Lin and McInnes, 1995; Lin et al., 1996) and that the fraction of soil that transmits water significantly decreases with depth (Heuvelman and McInnes, 1997). This implies that flow velocity increases with depth so that the time for water and contaminants that escape the rootzone to reach groundwater might be significantly less than previously expected.

In structured clayey soils, water tends to flow in locations where macroporosity is high (Lin et al., 1998) and roots tend to enjoy this condition as well (Taylor and Gardner, 1963; Whiteley and Dexter, 1983; Bengough and Mullins, 1990). Water reduces the strength and mechanical impedance of the soil, further enhancing the environment for root growth (Taylor and Ratliff, 1969). In addition, root channels themselves may act as paths for water flow (Mitchell et al., 1995; Gish et al., 1998). Mechanical impedance of clayey soils tends to be extremely high when the soils are dry so one might expect that there would be a positive spatial correlation between the location of roots and the location of water flow paths in highly structured clayey soils. One might also expect that this relationship would be of significant importance in understanding water and nutrient uptake

---

This thesis follows the format and style of the Soil Science Society of America Journal

by plants in these soils. Despite this, little detailed research has been done to determine either the correlation or the spatial association between root densities and water flow paths.

Not only would the knowledge of the location of roots in soil relative to the location of water flow paths be important in understanding how plants obtain nutrients and water for growth (Tardieu and Manichon, 1986; Tardieu, 1987; Clothier and Green 1997), it would also be of considerable importance in phytoremediation research (Cunningham et al., 1996) and research into the prevention of groundwater contamination (Gish et al., 1998). If plant roots were to prefer to follow water flow paths (or vice versa), contaminants may have less chance of escaping the root zone than they would otherwise. This is especially significant if water velocities increase with depth. Efforts to model the phytoremediation process (e.g., Chang and Corapciglu, 1998) would benefit from knowledge of the spatial association or correlation between contaminant concentration and root density. The ability to simulate the fate of contaminants is essential in designing technically sound and cost-effective, plant-aided remediation strategies. Knowledge of the spatial association between contaminants and roots is thus essential to sound phytoremediation strategies.

Most models of water and nutrient uptake by roots, assign a specific volume of soil to a specific length of root (Gardner, 1960; Passioura, 1991). These are termed single-root models. Roots and water are considered to be evenly distributed in the soil, at least for a given layer of soil. The radius b of soil surrounding the root, to which the root has effectively sole access to water and nutrients, is calculated as $b = (\pi L)^{-1/2}$, where L, the

rooting density, is the length of root per unit volume of soil. With this assumption of uniform distribution of roots, some simple calculations regarding root uptake may be made based on water flow theory. For example, when the soil is dry enough for it to limit water uptake, the change in average water content $\bar{\theta}$ with time *t* may be expressed as:

$$\frac{d\bar{\theta}}{dt} = \frac{D(\bar{\theta} - \theta_a)}{2b^2} \tag{1}$$

where *D* is the diffusivity of soil water, and θ_a is the soil water content at the surface of the root. If θ_a is constant (say that associated with a given water potential, θ_d, the difference between $\bar{\theta}$ and θ_a, may be expressed:

$$\theta_d = \theta_{d0} e^{(-t/\tau)} \tag{2}$$

where θ_{d0} is the difference between $\bar{\theta}$ and θ_a at $t = 0$, and $\tau = 2b^2/D$ is a time constant. Equations [1 and 2] allow an analysis of water uptake with time. When roots are considered to be evenly distributed, τ (the time to extract 63% of the available water) is on the order of days. However, when roots are considered to be clustered in sparse locations, similar equations may be used, but τ is in the order of weeks or months (Passioura, 1991).

The simple analysis described above considers water to be uniformly distributed in soil. Uncertainty in the location of water flow paths, i.e., a non-uniform distribution of water, could affect the significance of root clustering. In his discussion of simulation models, Passioura (1996) commented that sometimes the assumptions about the physical nature of the problem are so wrong that no amount of adjustment of the parameters will make them work. He discussed problems in trying to predict water and nutrient uptake

that arise from wide variations in local conditions throughout the rootzone. Two situations where problems may arise are when roots are not uniformly distributed throughout the rootzone (e.g., root clustering) and when water is not uniformly distributed throughout the rootzone (e.g., bypass flow). If there were a strong positive correlation between the location of the clusters and the water flow paths, water, nutrients, and contaminants might be more readily available to the plant. Conversely, if there were a strong negative correlation between the location of the roots and the flow paths, water, nutrients, and contaminants might be much less accessible. Between, would be the case of little or no correlation, perhaps the case of uniform water content analyzed above if water distribution is uniform but root distribution is not (Passioura, 1991).

Development of plant root systems is affected by soil macroporosity and soil strength or mechanical impedance (Wang et al., 1986). Water and chemical flow paths are located in discrete regions of the soil (Keys et al., 1997), as are many plant roots. Roots prefer relatively high porosity and low soil strength or mechanical impedance. Soil strength or mechanical impedance in part depends on water content (Taylor and Ratliff, 1969), decreasing with increasing water content. The flow of water and chemicals in these clayey soils is quite different from that in lighter textured soils. Desiccation cracks, interpedal pores, and biopores provide the major avenues for water movement. The presence or absence of water flow paths influences the spatial distribution of water content in structured soil after irrigation or rainfall. Transport of water and chemicals in these soils usually depends on the soils' macroporosity (Lin et al., 1998). Water flow is greater where porosity is higher. Water content and porosity are greater in water flow paths than

in the surrounding soil so soil strength and mechanical impedance should be lower. This leads to a reasonable hypothesis that roots in highly structured soil will have a greater density (total length per unit volume) in soil associated with water flow paths than in soil not initially wetted.

Plant roots influence the fate of water and chemicals in soils (Clothier and Green, 1997). This is one of the principles behind phytoremediation of contaminated soils (Cunningham et al., 1996). Most plant growth and phytoremediation models ignore the spatial association or correlation between root distributions and water flow path distributions. Passioura (1991) theorized that in a uniformly wet soil, there would be a significant difference in water uptake between clustered roots and uniformly distributed roots. Inspection of experimental observations (Tardieu and Manichon, 1986) and model results (Tardieu et al., 1992; and Pellerin and Pagès, 1996) places serious doubt on models that do not account for the spatial distribution of roots. Similarly, it is possible to speculate that in a uniformly rooted soil, there would be a significant difference in water uptake from flow paths and non-wetted areas. Actually the most realistic scenario is a combination of these into the case of a non-uniformly rooted and non-uniformly wetted soil.

I am aware of very little quantitative data on the spatial association between roots and bypass flow paths in structured soils. The overall goal of this project is to determine the degree of spatial association between the locations of pasture-grass roots and the location of water flow paths in a structured clay soil. To meet this goal, the experiment had several objectives. The first objective was to accurately map the location and size of

roots intersecting horizontal planes at given depth of soil. The second objective was to accurately map the patterns of water flow paths through the same horizontal planes where the roots were mapped. The third objective was to compare these two maps and determine the degree of spatial association between the water flow path patterns and the location of the roots. This research will lead to a better understanding of how plants interact with the natural soil environment. This information will improve the ability to predict the fate of water and chemicals in soil, and provide for considerable information on root-soil interactions.

CHAPTER II

LITERATURE REVIEW

Growth and development of plant root systems is affected by soil macroporosity and soil strength or mechanical impedance (Wang et al., 1986). Since transport of water and chemicals in structured clayey soils usually depends on the soils' macroporosity (Lin et al., 1998) water and chemical flow paths tend to be located in discrete regions of the soil (Keys et al., 1997), as are many plant roots. Water tends to flow in locations where macroporosity is high (Lin et al., 1998), reducing the strength and mechanical impedance of the soil. This combination of high porosity, available water, and reduced impedance creates very favorable conditions for roots (Taylor and Gardner, 1963; Whiteley and Dexter, 1983; Bengough and Mullins, 1990; Taylor and Ratliff, 1969). Roots may also act as flow channels further improving the environment (Mitchell et al., 1995; Gish et al., 1998).

Knowledge of how roots and soils interact, and the location of roots in relation to flow paths is key to understanding how plants obtain nutrients and water for growth (Tardieu and Manichon, 1986; Tardieu, 1987; Clothier and Green 1997). This relationship is also an important consideration when studying the effectiveness of any phytoremedition techniques (Cunningham et al., 1996), and research into the prevention of groundwater contamination (Gish et al., 1998). Efforts to model the phytoremediation process (e.g., Chang and Corapciglu, 1998) would benefit from knowledge of the spatial association or correlation between contaminant concentration and root density. Roots may collect and

transport organic and inorganic contaminants (de Souza et al., 1998; Clothier and Green, 1997), and they may stimulate mineralization of organic contaminants (Burken and Schnoor, 1996). The ability to simulate the fate of contaminants is essential in designing technically sound and cost-effective, plant-aided remediation strategies. Knowledge of the spatial association between contaminants and roots is thus essential to sound phytoremediation strategies.

Hasegawa and Sato (1987) demonstrated that roots clustered in cracks were very important to crop water uptake in a clayey soil, but that not all cracks had roots. The fact that not all cracks contained roots was important and they suggested that more information on the distributions of roots and cracks was needed before detailed analysis of the effect of root clustering could be made. Perhaps the cracks that contain roots are also the cracks that transmit water and solutes through the soil. Logsdon and Allmaras (1991) and Tardieu (1987, 1988a, 1988b) mapped roots and found statistically significant clustering, but neither attempted to locate water flow paths in relation to the clustered roots. Without knowledge of the water distribution, one is left assuming a horizontally uniform water distribution for root uptake, but in structured soil this assumption of a uniform water distribution is known to be false (Heuvelman and McInnes, 1997). Bouma and Dekker (1978) suggested that root growth and macropore water flow might be related after observing roots growing in cracks stained with dye marking water flow paths. Unfortunately they failed to quantify the relationship. In an apparent attempt to address this problem, Logsdon and Allmaras (1991) analyzed 23 root density data sets and found no correlation between root length density and hydraulic conductivity in 22 of the 23 sets.

This, however, is not surprising in light of the Hasegawa and Sato (1987) findings. Many of the potential flow paths are not active because of surface features that prevent water influx (Keys et al., 1997).

Tardieu et al. (1992) simulated the difference in the ratio of evapotranspiration (ET) to potential evapotranspiration (PET) with depletion of transpirable soil water between cases involving uniformly distributed roots and clustered roots. Both cases started with uniformly distributed water. They found that the ratio ET/PET dropped below 1 at a much smaller amount of depleted water for the case with clustered roots. In their model, clustered roots were not able to access all of the potentially available water. If there were a high positive correlation between root clusters and water flow paths, though, we expect that their simulated results of the drop in ET/PET might be reversed for the two cases. Essentially, clustered root would effectively access more of the available water than uniformly distributed roots. ET/PET would drop below 1 when more water was depleted for the case with clustered roots than the case with uniformly distributed roots. This difference demonstrates the need to quantify the association between root density patterns and water flow patterns so that models may accurately simulate soil-plant-atmosphere interactions.

Indirect evidence suggests a positive correlation between the location of water flow paths and roots might exist. Positive correlation between root growth and soil penetration resistance (Ehlers et al., 1983) suggests a positive correlation because water reduces soil strength. Also, measurements have shown that roots tend to preferentially explore the soil soaked with water differentially wet by drip or furrow irrigation (e.g., Kamara et al., 1991).

CHAPTER III

RESEARCH METHODS

The objectives were to map the preferential flow paths and the location of roots. In general this was done by irrigating plots with a dye solution that stained the flow paths. After irrigation, soil was excavated to expose horizontal planes and the dye stain pattern and root locations were mapped on these. We began by choosing a research site.

Research Site

The research site was located in a pasture on the Texas A&M University farm along the Brazos River. The coordinates to locate the site were N 30˚ 33.281' W 96˚ 25.567'. The soil at the site was Ships clay (Very-fine, mixed, thermic Chromic Hapluderts), a soil of moderate extent in Texas, mainly along the Colorado and Brazos Rivers.

Ships clay was chosen because the soil is highly structured, its color is suitable for dye staining water flow paths, and it is used extensively for both crops and pasture. Pasture was chosen because the grass roots were well established. A well developed root system was essential to ensure that sufficient root density existed beyond the surface horizon, and to allow root growth an opportunity to respond to the flow paths.

The subsoil contains moderate coarse angular blocky structure parting to moderate fine angular blocky structure with common roots on the ped faces. Intrapedal pores in the subsoil are mostly root channels. Large pores and fissures dominate water

flow near saturation in the Ships soil. Data from Lin et al. (1998) show the mean hydraulically active pore size (diameter of cylindrical pore or width of crack) for saturated flow to be about 1 mm.

The research site had been in pasture for many years, and aside from occasional mowing, the field was unmanaged. The pasture vegetation was predominantly common bermudagrass (*Cynodon dactylon*) and Johnsongrass (*Sorghum halepense*). The pasture was nearly level and vegetation was homogeneous in stand composition. Groundcover was nearly complete and the plant height at the time of this experiment was between 25 and 30 cm.

Collection of Field Data

Three 4 m by 4 m plots were established in the pasture. The areas chosen were level, and uniform in plant composition and cover. The plots were unmowed and unwatered until the time of the experiment.

Erioglaucine (Brilliant Blue FCF), which provides good color contrast in the Ships soil, was chosen as a dye marker. Erioglaucine is an environmentally friendly dye frequently used to expose flow paths in soil (Flury and Flühler, 1994, 1995).

Dye was applied using a rain simulator, having a 4 m by 4 m footprint. The rainfall simulator used was built on a 4 m by 4 m wide by 3 m tall frame of aluminum pipe. A nozzle at a height of 2.75 m produced a uniform square pattern of applied water over the research plot. A small gasoline pump powered the system. The sides were covered with tarps to minimize the wind interfering with uniformity of application.

The rainfall simulator was used instead of flood irrigation so that flow artifacts from unnatural ponding of water on the surface would be minimized. Water was applied at a rate of 2.5 cm/h, which was below the maximum infiltration rate. In each plot, 7.5 cm of water was applied, followed by 7.5 cm of dye solution containing 30 g/L erioglaucine. Water was applied before the dye solution to saturate the meso- and micropores in the upper soil horizons. The goal was to map the macropore flow paths where the vast majority of water is transported (Lin et al, 1998). Erioglaucine is slightly sorbed to clay and organic material so a relatively high dye concentration was chosen to insure sufficient dye followed the water to depth.

After irrigation with the dye solution, vegetation was cleared, and a horizontal plane at a depth of 25 cm was exposed by excavation with hand tools. A square grid of sixteen 0.5 m by 0.5 m sections was established in the center of each 4 m by 4 m plot. As reference markers, steel rods were placed at the corners of the 2 m by 2 m inner square, and corners of individual grid squares were marked with pushpins. Loose soil and debris were removed from the exposed soil plane with a leaf blower.

Previous work had shown that the majority of infiltration pathways converge at depths of 20 to 30 cm. Based on this knowledge the decision was made to begin at a depth of 25 cm.

To map the dye stain pattern exposed by excavation, photographs of the soil surface were taken. Photographs were taken with an Olympus D-600L digital camera for the first two plots, and a Sony DSC –S75 digital camera on the third plot. Photographs of each 0.5 m by 0.5 m grid section were taken at 1280 by 1024 pixel

resolution, which represents a physical resolution of about 0.2 mm^2 per pixel. One picture was taken for each grid unit. The camera was mounted on a tripod to keep it at a consistent height during photography.

Root distributions were mapped for the 2 m by 2 m area by marking, on clear plastic sheets, the location and size of roots intersecting the plane. Root mapping was done on 1.0 m by 1.0 m squares, four of the photographed squares. To prevent bias, the same individual mapped all roots on all three plots. During mapping, roots were classified by diameter as < 1mm, 1 to 2 mm, 2 to 5 mm, and > 5 mm. Because root mapping yielded both root count data and location data, mapping produced more realistic areal densities than simple counting (Böhm and Köpke, 1977).

The excavation and mapping procedure was repeated at depths of 45 cm and 75 cm on each plot. Repeating the mapping procedure at 25 cm, 45 cm and 75 cm allowed us to collect data at three different points in the soil profile, and assess clustering at three different depths.

Data Analysis

The digital photographs of dye-stained flow-path patterns on each exposed plane were combined and then converted to black and white images using Adobe Photoshop (Adobe Systems, Inc.). This was done by first by setting the photos to CMYK color mode. Then the cyan color channel was isolated by turning off the other color channels. The images were then converted to black and white using the threshold command. The

resulting black and white images were converted to an x-y grid binary format with Dyeye (Borland International, Inc., Scotts Valley, CA). The root maps recorded on plastic sheets were converted to numeric locations with a digitizer table (model #AC32 Altek Corporation, Silver Spring, MD) using Quantum Mechanic (Ziatek Inc. Santa Fe, NM). The resulting x-y root location and size data from the digitizer was spatially referenced to the binary flow path data from the photographs.

As the dye infiltrates downward in the preferential flow channels, it is absorbed and seeps out into the surrounding soil producing the patterns that were mapped. Conceptually, the centerline of these dye patches is indicative of the location of the crack, or flow channel. My analysis involves two sets of roots, those found within the dye stained areas, and those outside the dye stain. If a positive association exists between the roots and the flow paths, on average, the roots located in the stained areas ought to be closer to the center of the dye patches than their randomly located counterparts. This would indicate that the roots were in or immediately adjacent to the flow paths.

The unstained roots are obviously not located in flow paths, but if a positive association exists these unstained roots ought to be closer to the dye stain patches than the randomly located unstained roots.

A custom computer program was written to determine a measure of spatial association of roots and dye-marked flow paths. For each root, the program determined the percent dye coverage in discs of expanding radii around the root (see Figure 1). For roots located in dye stained areas and at a radius of 0 pixels beyond the location of the root, the percent dye cover was 100%. For roots in unstained areas and at a radius of 0

pixels beyond the location of the root, the percent dye cover was 0%. The program used discs of radii 0, 1, 2, 4, 8, 16, 32, 64, 128, 256, and 512 pixels beyond the pixel containing the root. This translates into radii of 0, 0.04, 0.09, 0.18, 0.36, 0.72, 1.4, 2.9, 5.7, 11.5, and 22.9 cm.

For a root in a stained location of the map, the percent dye cover decreased as the radius increased. The percent dye cover computed for that root point should approach the percent dye cover for the entire plot when the radius was large. For roots in an unstained location, the computed percent dye cover increased as the area analyzed increased until it too approached the percent dye cover for the entire plot. This procedure produced curves similar to that depicted in Figure 2. Values for each root were combined and averaged to produce a set of representative curves for each root set. A line for each size classification was produced for each plot.

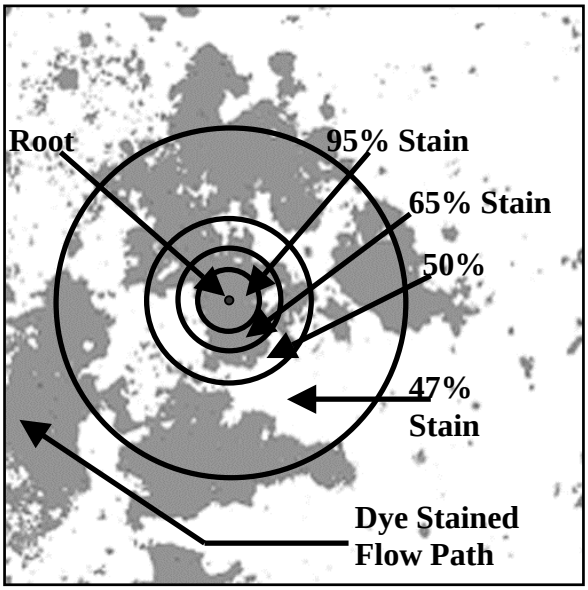

Figure 1. Schematic diagram showing procedure used to measure spatial association. Concentric were drawn circles around each root point, and the dye stain fraction inside each circle was calculated.

It would be possible to analyze each root individually for evidence of clustering and in so doing even determine a fraction of roots from a given root set that show evidence of clustering. However to determine the extent of clustering the data must be combined and averaged. Clustering is group behavior. We are interested in a root set as a set. In this case combining and averaging the root data gives an accurate representation of the root set.

As a conceptual example four root sets were plotted over a small dye stain pattern. In the first set (Figure 3) all the roots are located well within stained regions. In the second (Figure 4) the roots are located in unstained regions, but clustered along the periphery of stained regions. The third set (Figure 5) the roots are located in unstained regions with no association to the dye stained areas. The fourth set (Figure 6) is randomly distributed. These four root sets were analyzed using the computer program and the results are shown in Figure 7.

These are extreme examples where the roots were deliberately placed to show the different possible scenarios with regard to root clustering. The results from the randomly located root points form a baseline to which the data lines can be compared. The data sets positively associated with the dye stain, the stained and periphery roots, have data lines above their randomly located counterparts. While the data line of the negatively associated unstained roots is below the random distribution. If roots were clustering in and around the dye stain areas we would expect to find results similar to the stained and periphery data lines, albeit not quite as exaggerated.

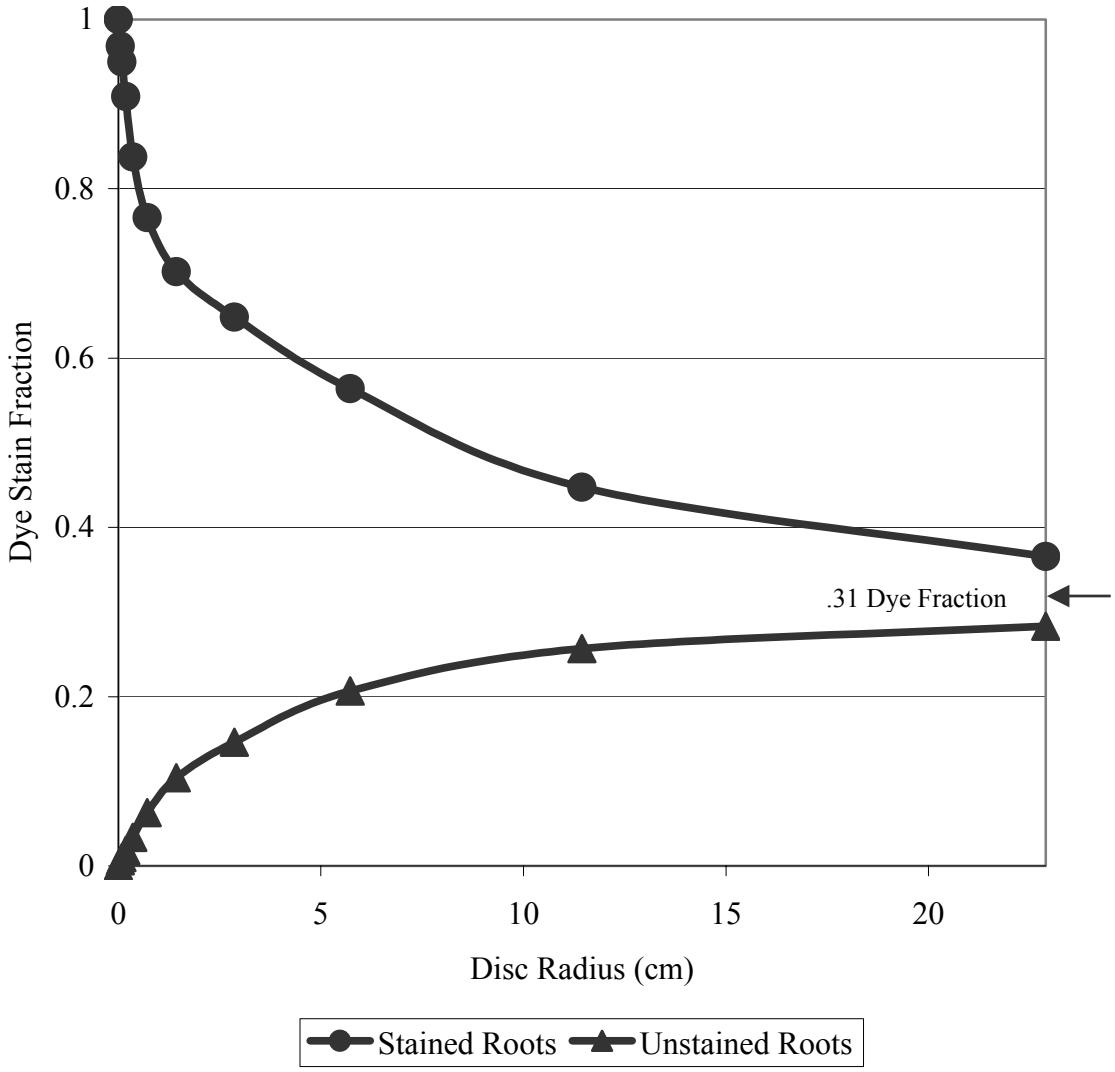

Figure 2. Conceptual example of data produced for each root from an area with a dye stain fraction of 0.31.

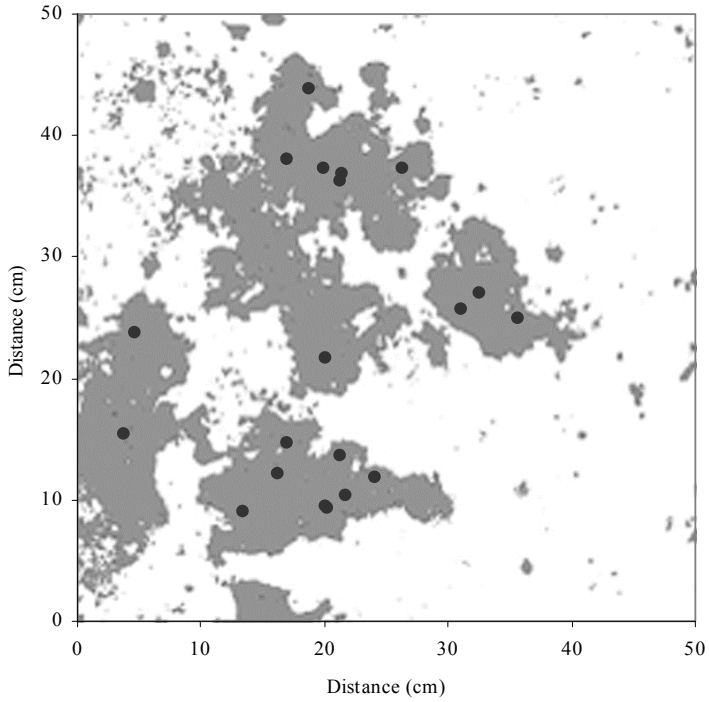

Figure 3. Stained roots.

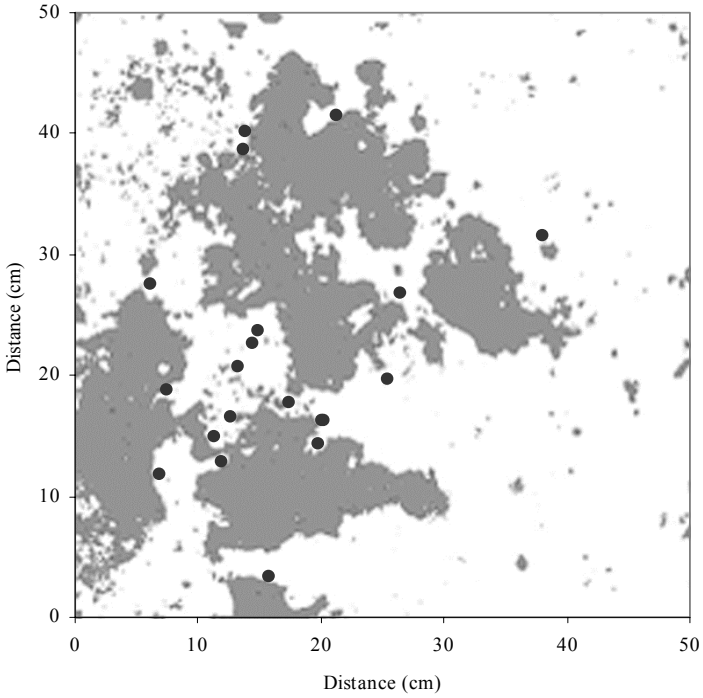

Figure 4. Unstained roots located along the periphery of stained regions.

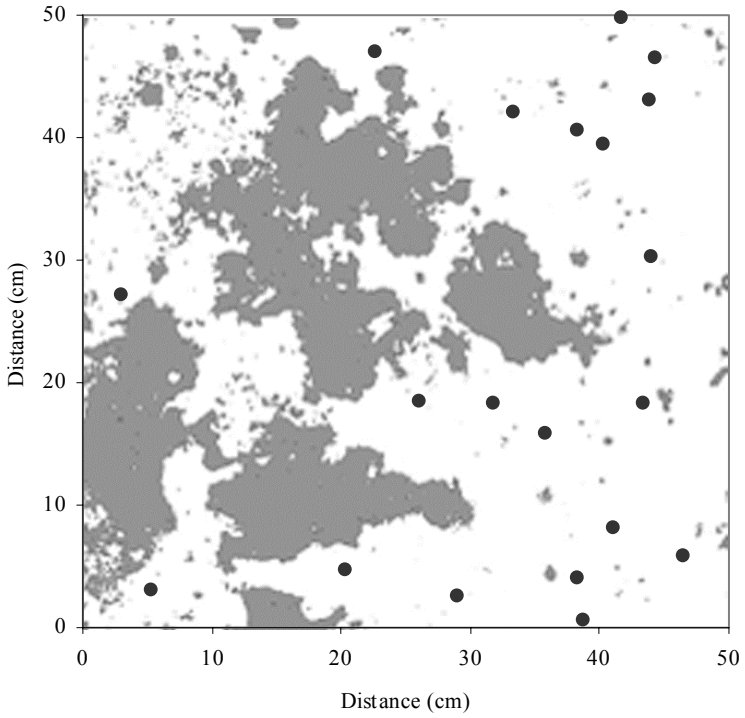

Figure 5. Unstained roots not associated with flow paths.

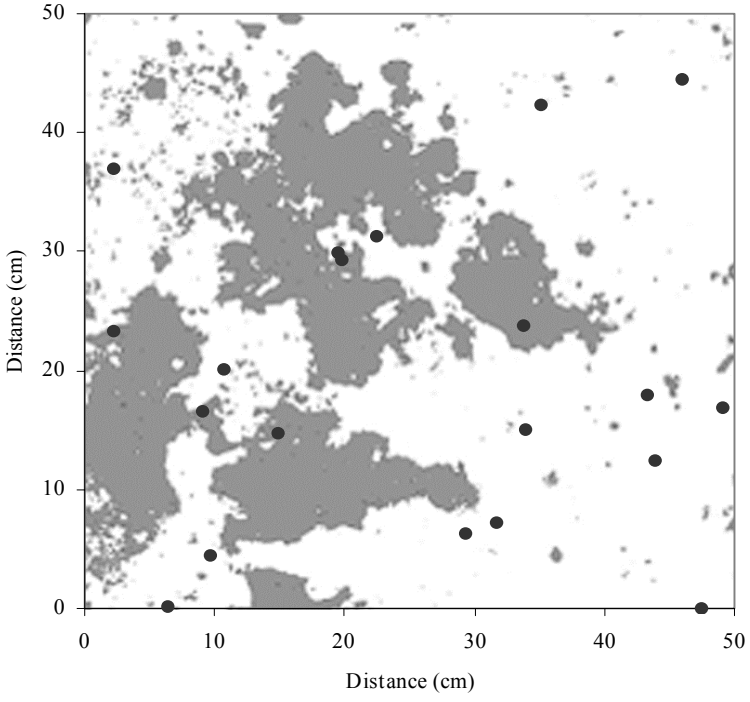

Figure 6. Roots located at random.

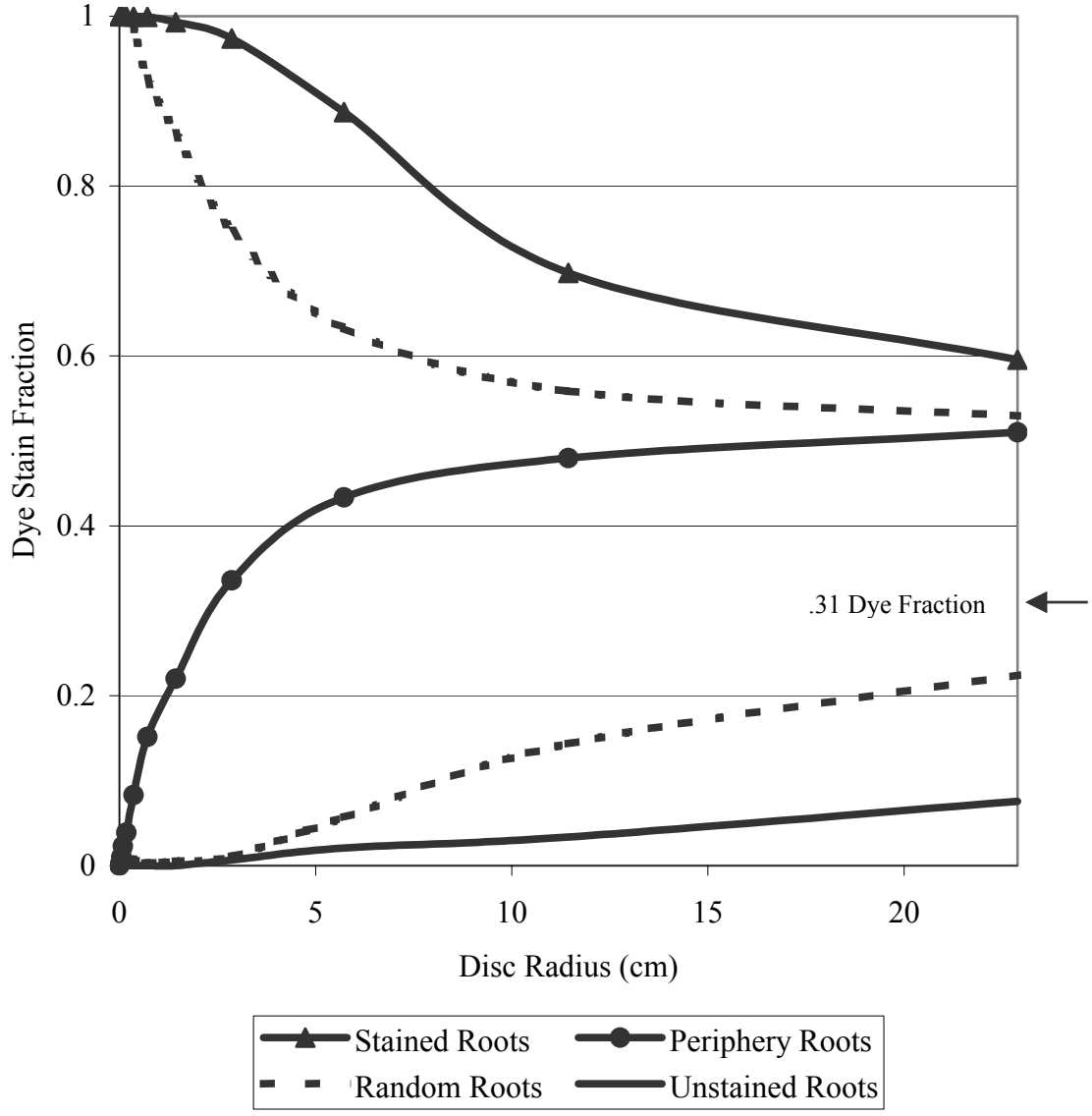

Figure 7. Distribution graph for conceptual example of analysis results.

For each set of roots, three random sets of the same number were created. Each random set was matched with the dye map and analyzed using the same program. The three random sets of each root set were averaged. The standard deviation was found and used to create a confidence interval ($\alpha = .05$). The curves from each root set and a corresponding confidence interval created from the random root set were compared.

Using randomly distributed roots to create such confidence intervals provides an objective method of comparing the actual root data to the randomly generated root data. By comparing the actual results to results obtained from randomly generated root data, it is possible to determine the relative average location for the different root sets. Data lines outside the confidence interval indicate a non-random distribution. Graphically, for both stained and unstained roots, data lines above the confidence interval indicate a positive association between the root distribution and the dye stain pattern.

CHAPTER IV

RESULTS AND DISSCUSIONS

Root Counts

This experiment is based on the premise that the dye solution stains the preferential flow paths. Because the water is more available and soil is generally softer in these flow paths, it seems logical that roots would prefer these areas. Based on this idea one would expect to find roots clustered in and around the dye stained portions of each plot.

It is informative to look first at the root count data. Root count data (Table 1) give a general indication as to whether the roots are clustering the in stained areas. If the root distributions were random with respect to the dye stain pattern the percent of roots found in the dye stained area ought to be very near the percent dye cover for the entire plot. Inspection of our maps showed a margin of error of about 5 mm with regards to the actual location of the roots. To account for this margin of error, unstained roots that showed a dye stain fraction of greater than 0.50 at disc radius of about 3.6 mm in the

Table 1. Root count data comparing the percent roots occurring in stained areas to the dye stain coverage area for the entire plot.

		Total Roots	<1 mm Roots	1-2 mm Roots	2-5 mm Roots	> 5 mm Roots
	% Dye Cover	(% in stained)	(% in stained)	(% in stained)	(% in stained)	(% in stained)
First Plot 25cm	37.74	9611 (27.8)	9354 (32.1)	164 (40.2)	91 (44.0)	2 (50.0)
First Plot 45cm	29.84	4345 (30.8)	4170 (35.3)	137 (35.0)	38 (34.2)	0 (0.00)
First Plot 75cm	25.06	2880 (24.7)	2828 (26.7)	34 (26.5)	18 (27.8)	0 (0.0)
Second Plot 25cm	44.37	7205 (44.8)	6879 (50.6)	202 (49.0)	116 (63.8)	8 (75.0)
Second Plot 45cm	25.44	4476 (23.6)	4349 (24.7)	90 (30.0)	36 (33.3)	1 (0.0)
Second Plot 75cm	33.32	2496 (34.1)	2441 (37.4)	39 (48.7)	15 (53.3)	1 (100.0)
Third Plot 25cm	17.54	8681 (16.4)	8122 (19.5)	399 (18.1)	140 (16.4)	20 (25.0)
Third Plot 45cm	11.54	4002 (11.0)	3866 (11.7)	116 (14.7)	20 (10.0)	0 (0.0)
Third Plot 75 cm	21.83	2249 (20.0)	2192 (21.6)	51 (25.5)	6 (50.0)	0 (0.0)

spatial analysis results, were counted as stained.

In comparing the total percentage of roots found in the stained areas to the percentage of dye coverage, it would appear that the root distribution is nearly random. With all root categories grouped together, the plot percent dye cover, and the percent of roots found in dye stained areas, are in fact very similar except for first plot at a depth of 25 cm.

The percentage of roots <1 mm found in the stained area is nearly identical to the dye stain coverage on nearly every plane. This is an indication that the distribution of these smallest roots is essentially random. In addition the number of roots <1 mm is so much larger than the number of larger roots that they swamp out any effect these larger roots may have on the total percentages.

When viewed separately, these larger roots do show a tendency toward higher densities in the dye stained areas. The percentage of 1 to 2 mm roots found in the stained area is larger than the percentage of dye stained for the entire area on six of the nine planes. The same can be said for the 2 to 5 mm roots. Roots greater than 5 mm in diameter were only found on five of the nine plots, but three of those had more stained roots than would be expected based on the percent dye cover for the plane. This data provides weak evidence that some clustering of the larger roots did occur in the dye stained areas. For a given plane and root size category an expected value for the number of stained roots was found by multiplying the dye stain fraction by the total number of roots for the given category. Using this expected value and the actual count a chi square value was obtained for all roots categories on all planes. Summing the chi

square values for an entire roots size category produced a chi square value for the category across the entire experiment (Ott and Longnecker, 2001). Using this methodology, none of the four root categories proved to have a significantly ($\alpha = .05$) larger percentage of stained roots across the entire experiment than the expected percentages. The chi-square values were also grouped by depth. The <1 mm roots were excluded in the grouping by depth. Still, the results were similar with no depth showing statistically significant evidence of clustering.

It is important to remember, that the dye coverage area is partially dependent upon the amount of dye applied. Had more dye been applied the dye coverage area would have been larger. The dye stained areas were used to indicate preferential flow paths. As the amount of dye applied, and the dye stain area, increase, the connection between the dye stain pattern and the actual preferential flow path weakens. Since this analysis correlates root count with the dye pattern and not the actual flow path, some uncertainty exists regarding the spatial association.

Root Maps

The first steps in the spatial analysis produced a set of root maps (Figures 8- 16). These figures show the roots mapped together and separated by size class. These roots maps were overlaid on the mosaic dye pattern photos (see Appendix) to complete the data analysis. By themselves these graphs are not very telling, but they do give an indication of the number of roots that were mapped and their general distribution.

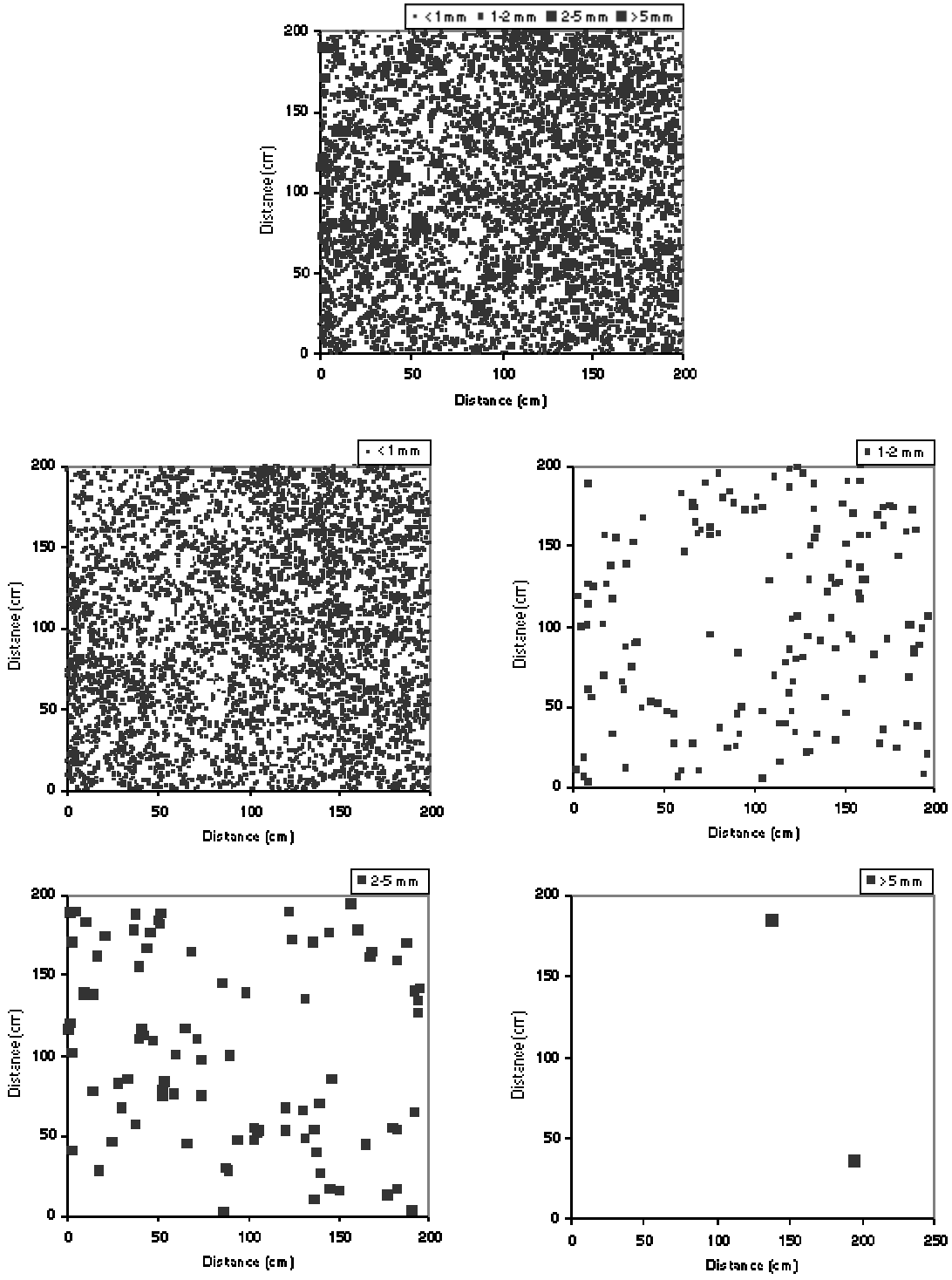

Figure 8. First plot at a depth of 25 cm.

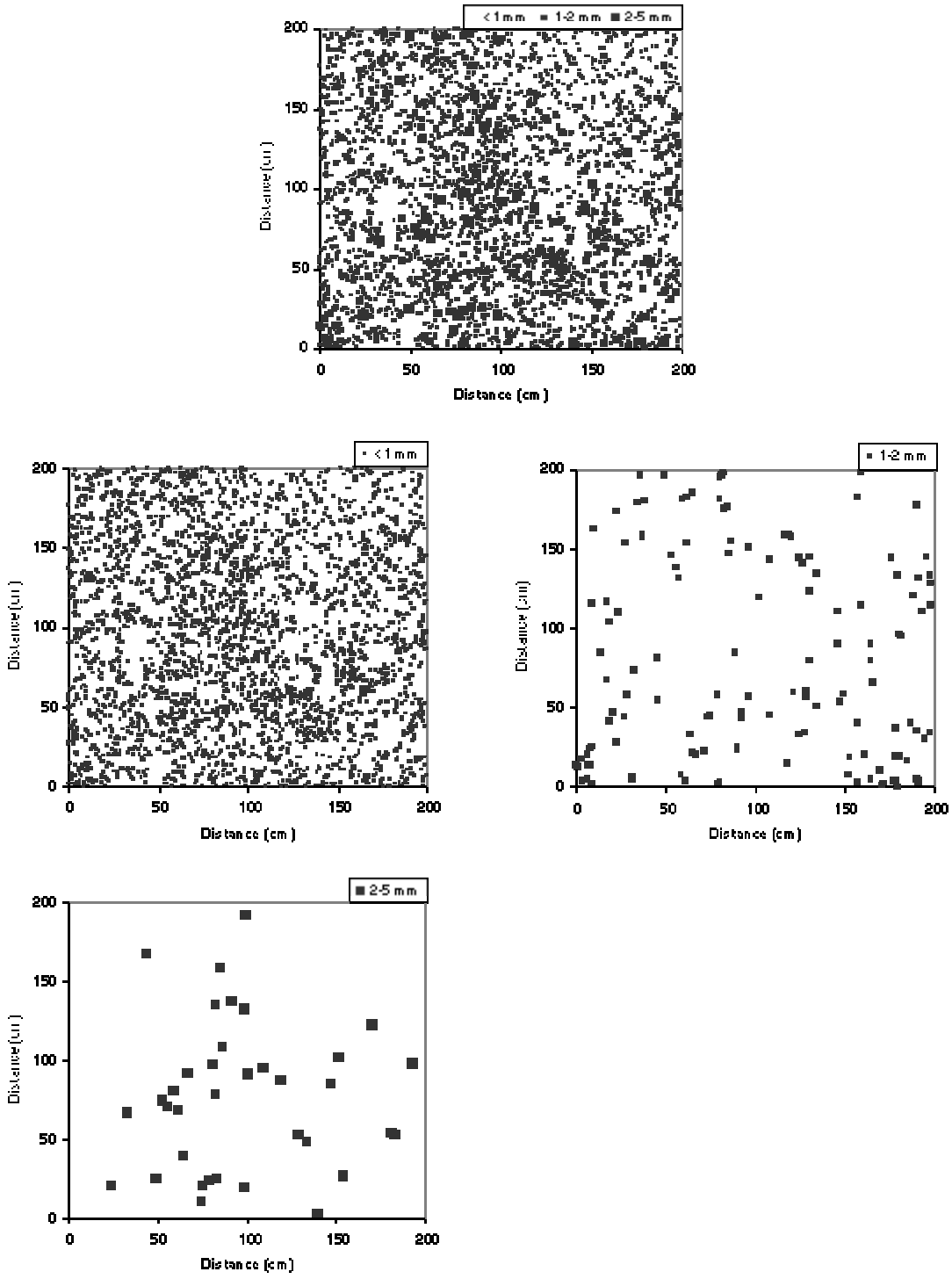

Figure 9. First plot at a depth of 45 cm.

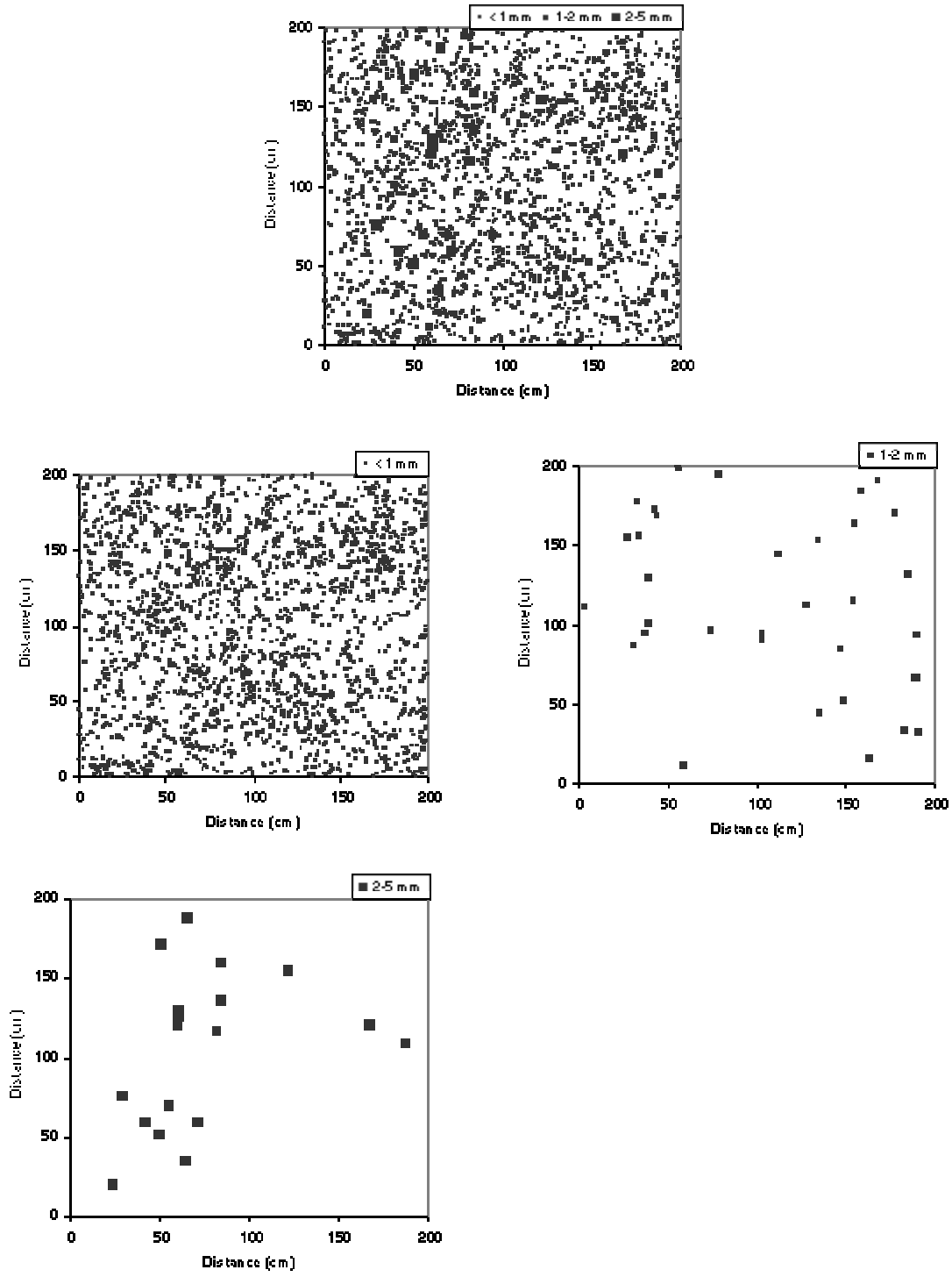

Figure 10. First plot at a depth of 75 cm.

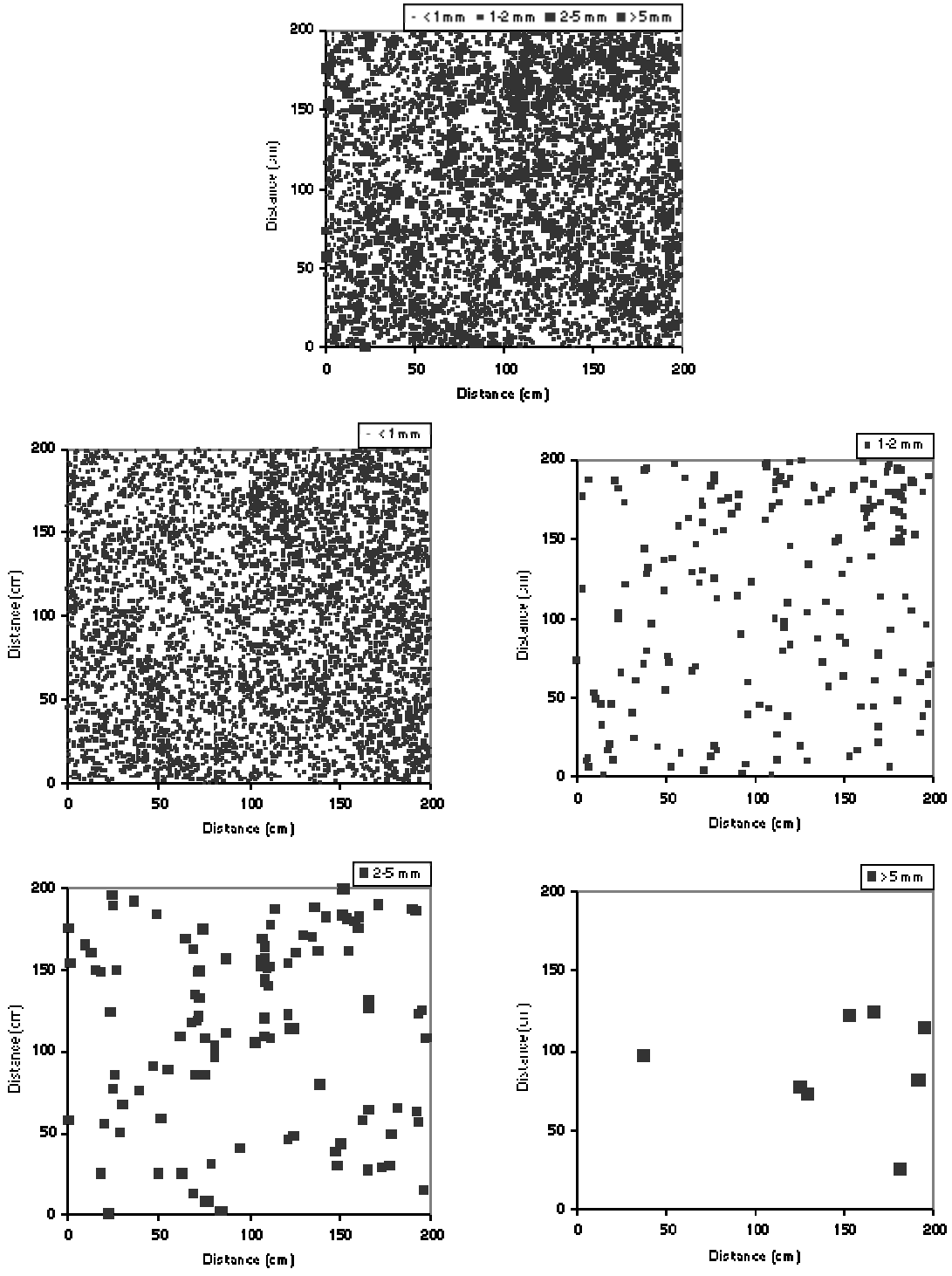

Figure 11. Second plot at a depth of 25 cm.

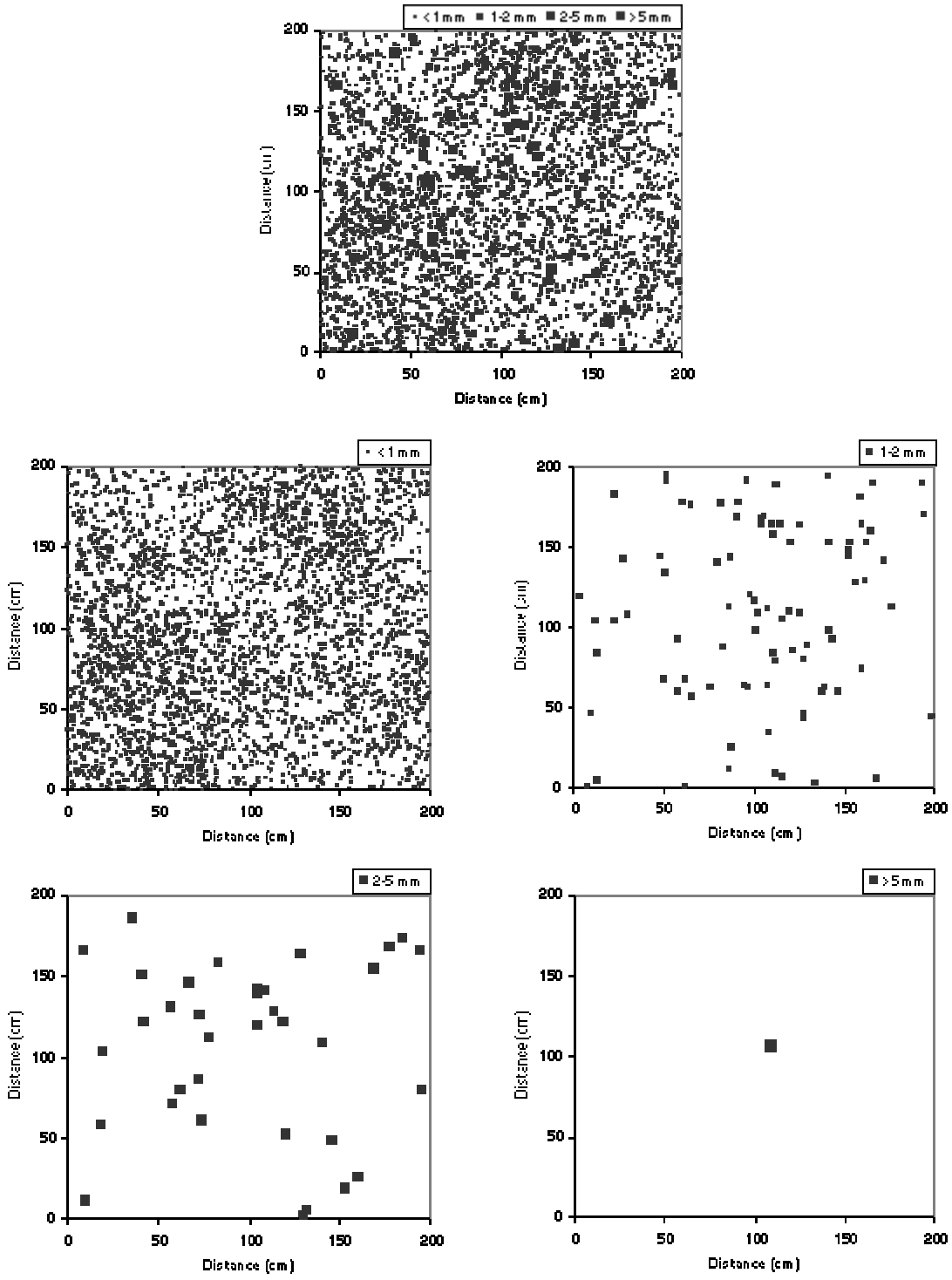

Figure 12. Second plot at a depth of 45 cm.

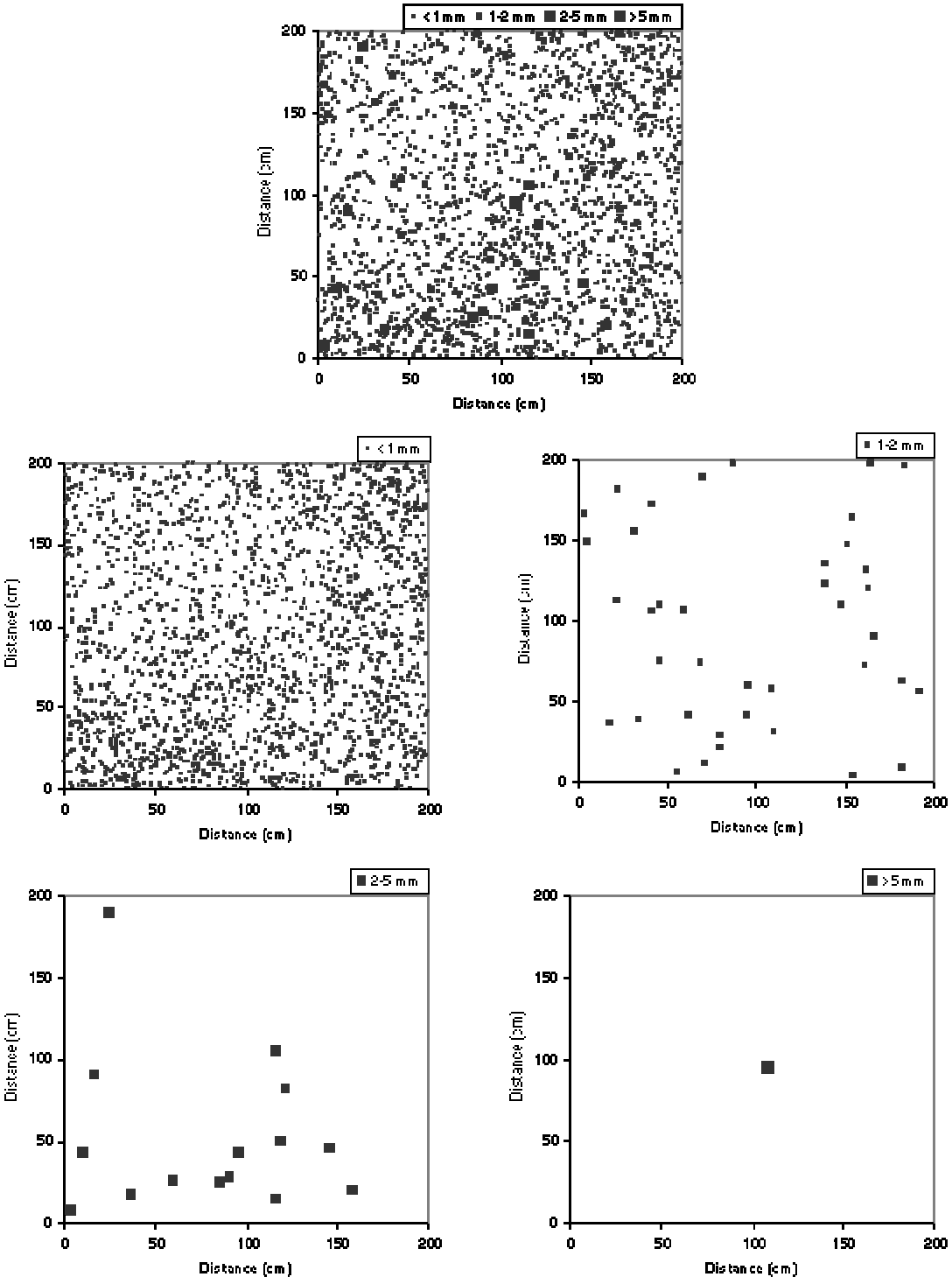

Figure 13. Second plot at a depth of 75 cm.

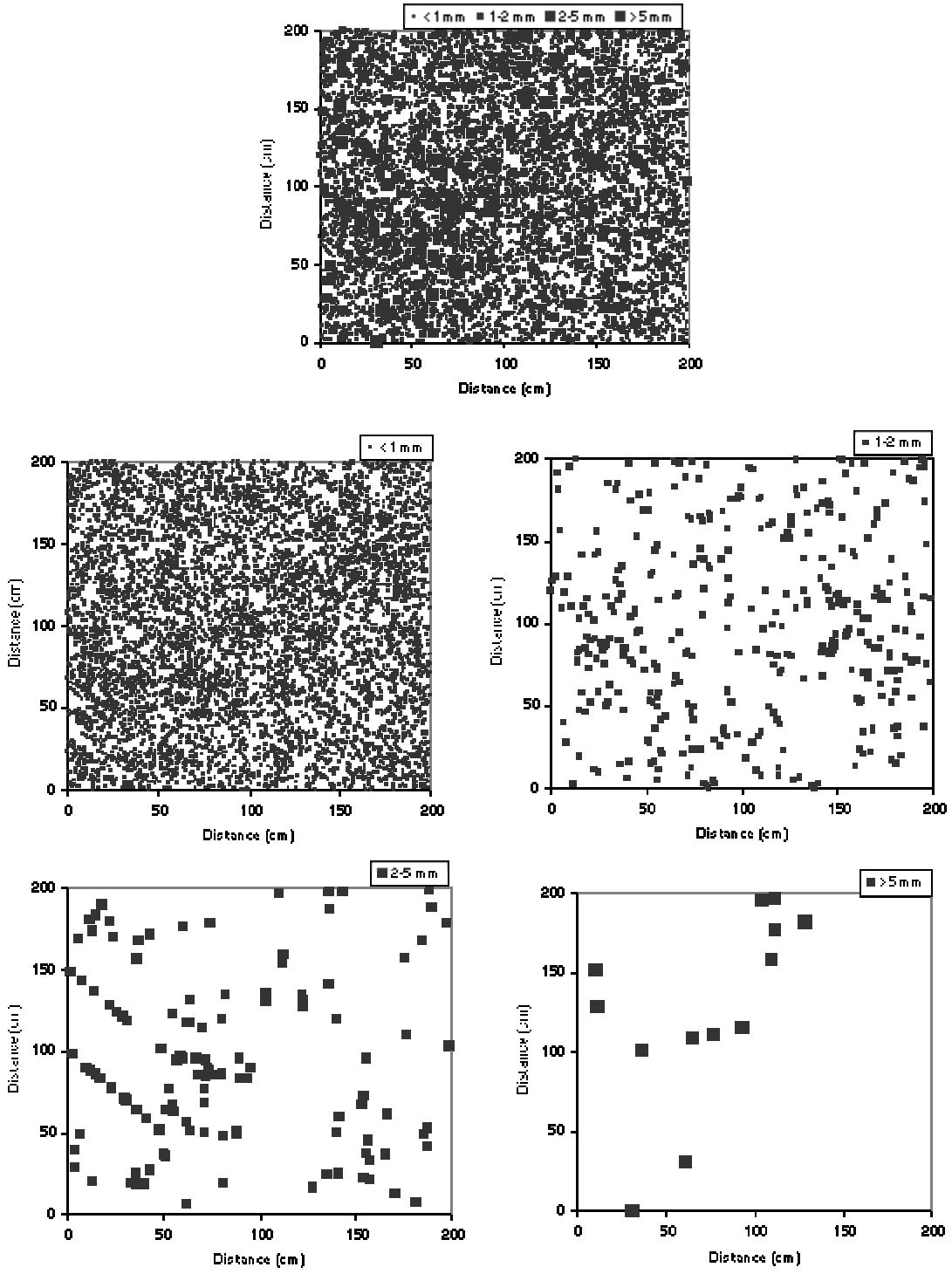

Figure 14. Third plot at a depth of 25 cm.

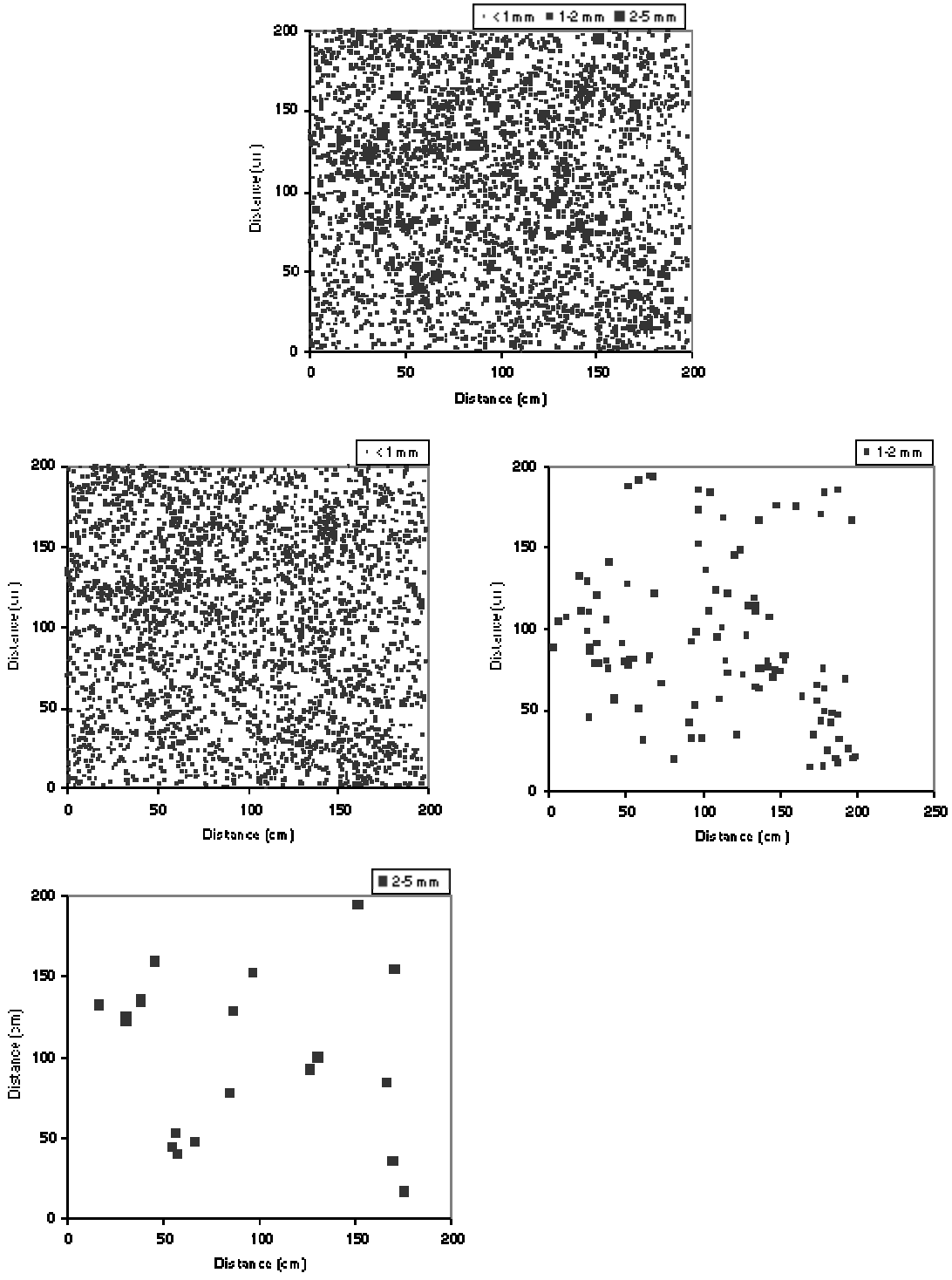

Figure 15. Third plot at a depth of 45 cm.

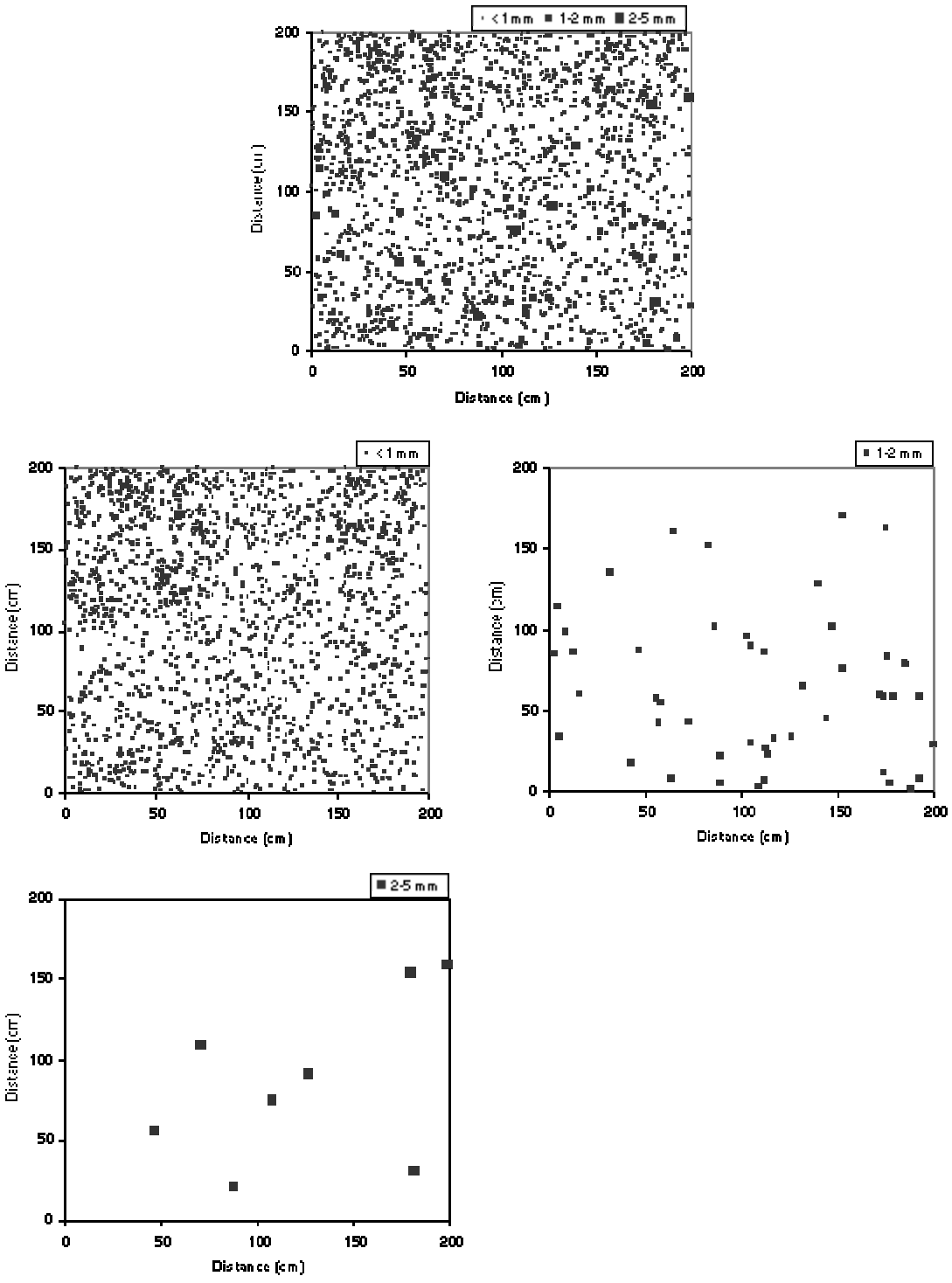

Figure 16. Third plot at a depth of 75 cm.

Spatial Association

In Figures 17 - 45 the results of the computer program written to measure spatial association between the root point and the dye stain pattern are graphed with confidence intervals created from three random root distributions.

As with the simple root count data, the <1 mm roots show little or no departure from results indicative of a random distribution. The upper and lower confidence interval lines and the actual data lines are nearly identical on all nine planes for the <1 mm roots (see Figures 17 and 20). There is no evidence to support the smallest category of roots being spatially associated with the flow paths. There is evidence that the distribution of the larger roots is not entirely random.

The number of data lines that fall outside the confidence intervals indicates that the distribution of these larger roots is not completely random with respect to the dye stain pattern. Two thirds of both the stained and unstained data lines fell outside the confidence intervals at some point. For the stained roots most of the larger deviations were above the confidence intervals (see Figures 19, 31, 34, and 38), indicating a positive association between the roots and dye stain pattern. There are some noteworthy exceptions (see Figures 25 and 45), which would seem to contradict the evidence supporting a positive spatial association. However, the data lines in these figures are based on only 5 and 3 roots respectively so their significance is small. There are relatively few larger roots especially at depths of 45 cm and 75 cm. These small sample sizes results in large confidence intervals, and data that is easily skewed by one or two outlying data points.

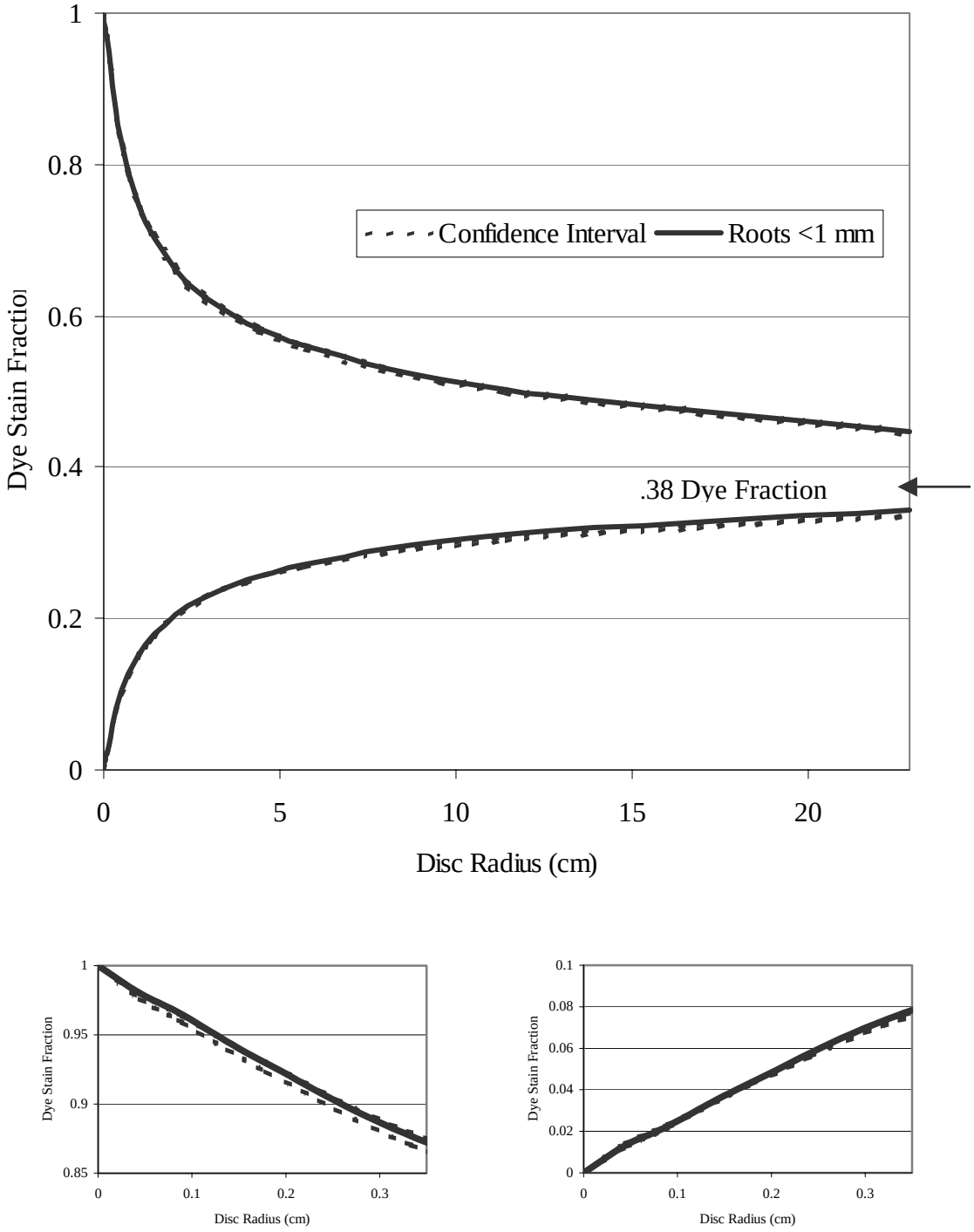

Figure 17. Fraction of area stained around roots in stained and unstained areas for roots <1 mm in the first plot at a depth of 25 cm. Plot had 0.38 m^2/m^2 stained.

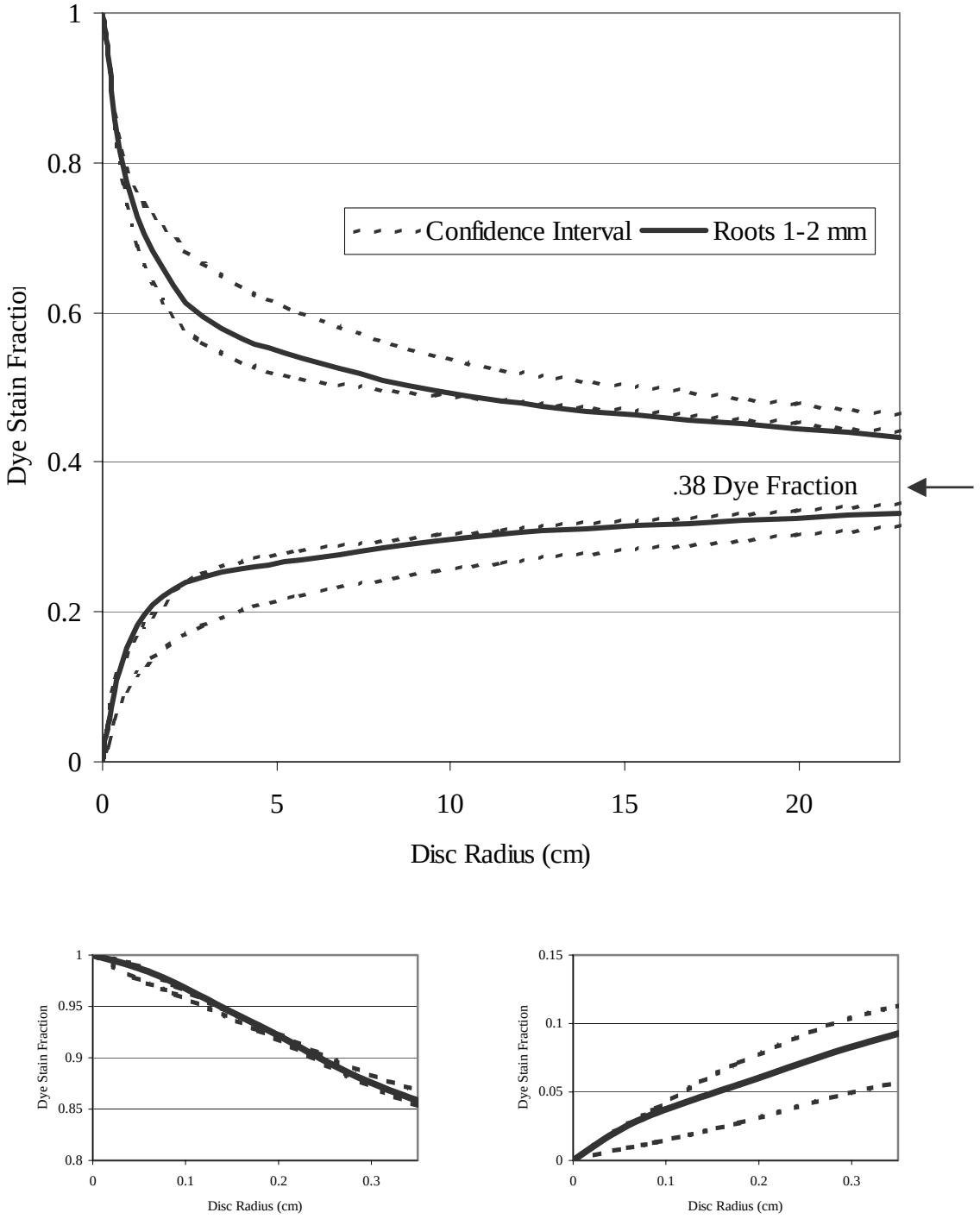

Figure 18. Fraction of area stained around roots in stained and unstained areas for roots 1-2 mm in the first plot at a depth of 25 cm. Plot had 0.38 m^2/m^2 stained.

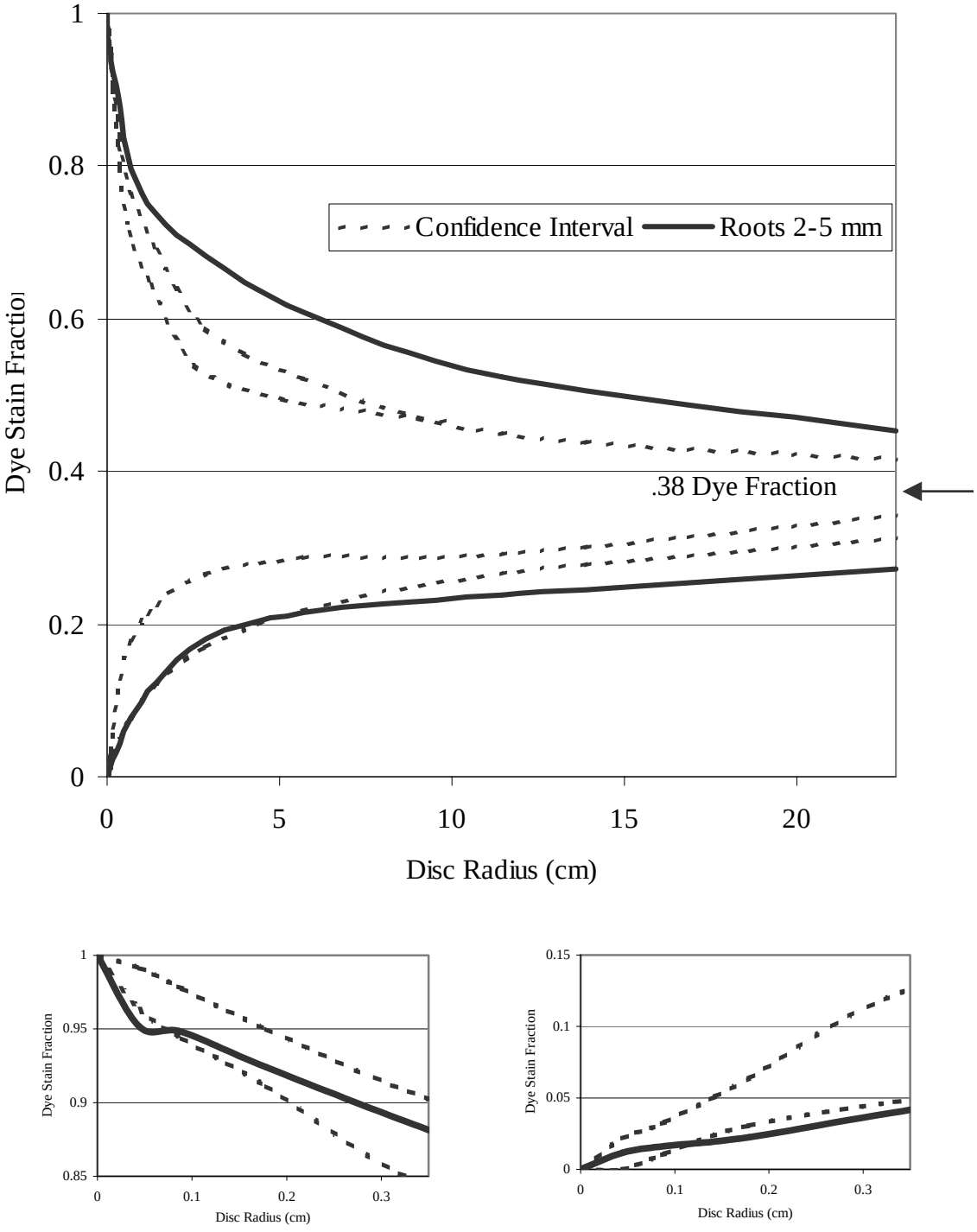

Figure 19. Fraction of area stained around roots in stained and unstained areas for roots 2-5 mm in the first plot at a depth of 25 cm. Plot had 0.38 m^2/m^2 stained.

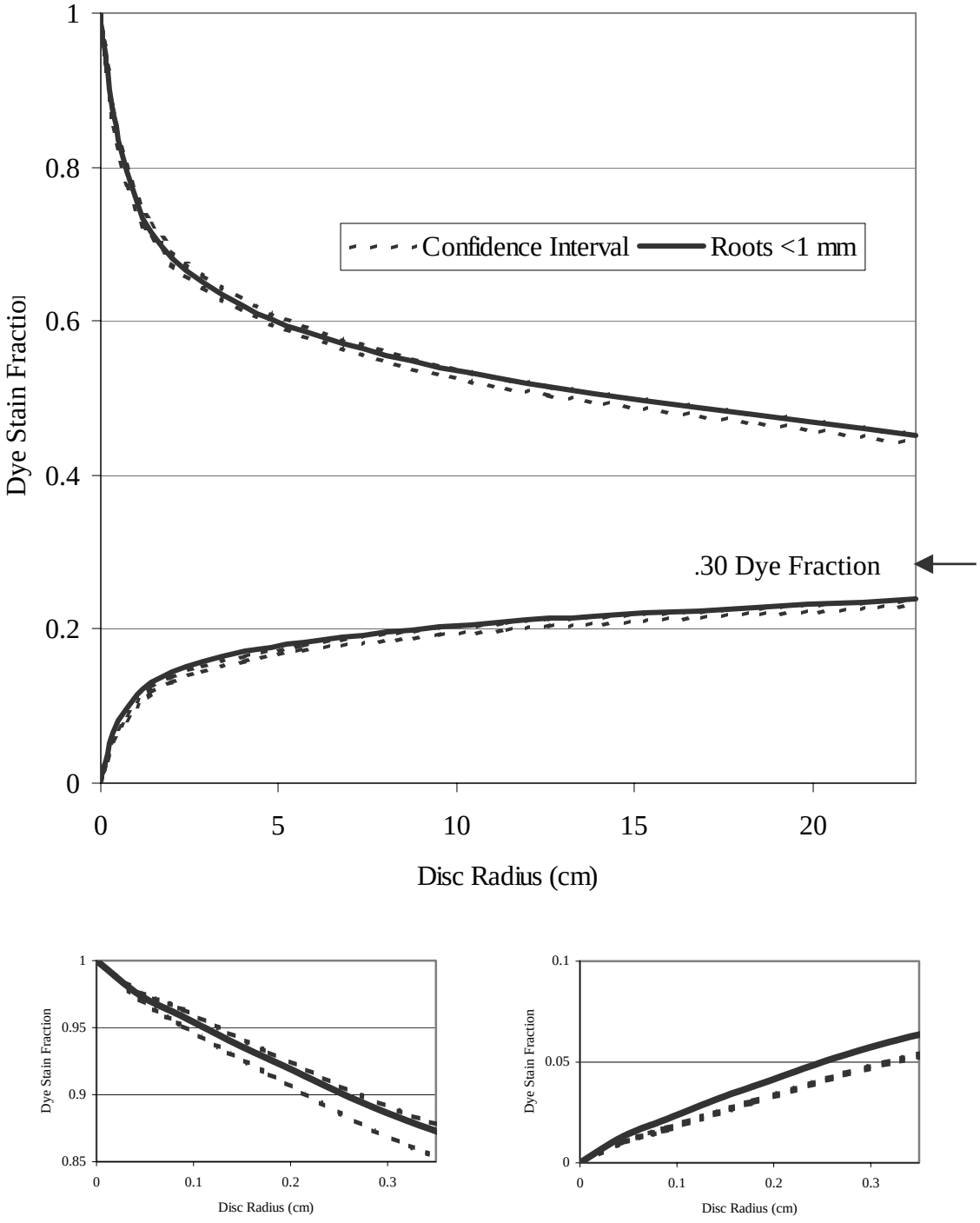

Figure 20. Fraction of area stained around roots in stained and unstained areas for roots <1 mm in the first plot at a depth of 45 cm. Plot had 0.30 m^2/m^2 stained.

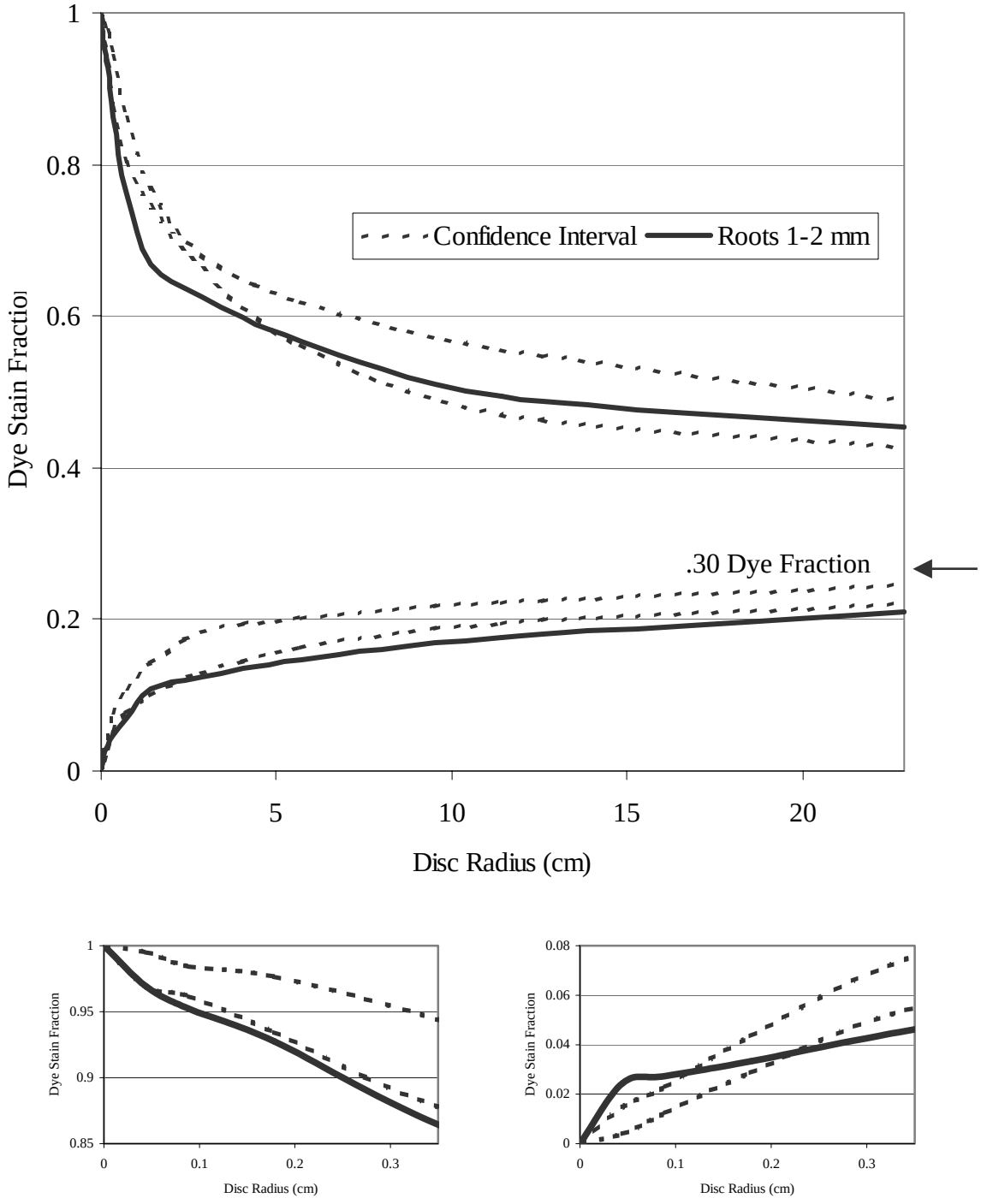

Figure 21. Fraction of area stained around roots in stained and unstained areas for roots 1-2 mm in the first plot at a depth of 45 cm. Plot had 0.30 m^2/m^2 stained.

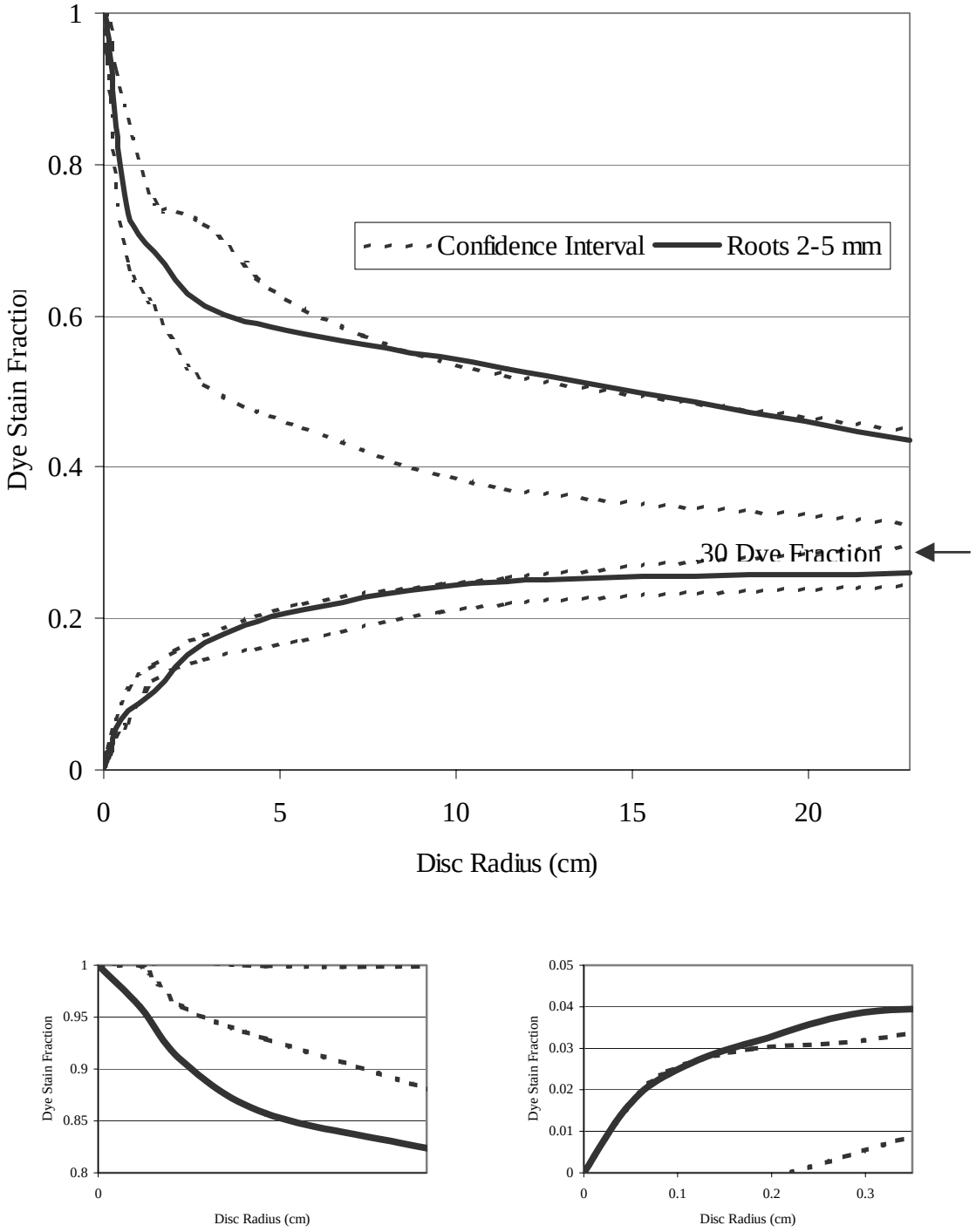

Figure 22. Fraction of area stained around roots in stained and unstained areas for roots 2-5 mm in the first plot at a depth of 45 cm. Plot had 0.30 m^2/m^2 stained.

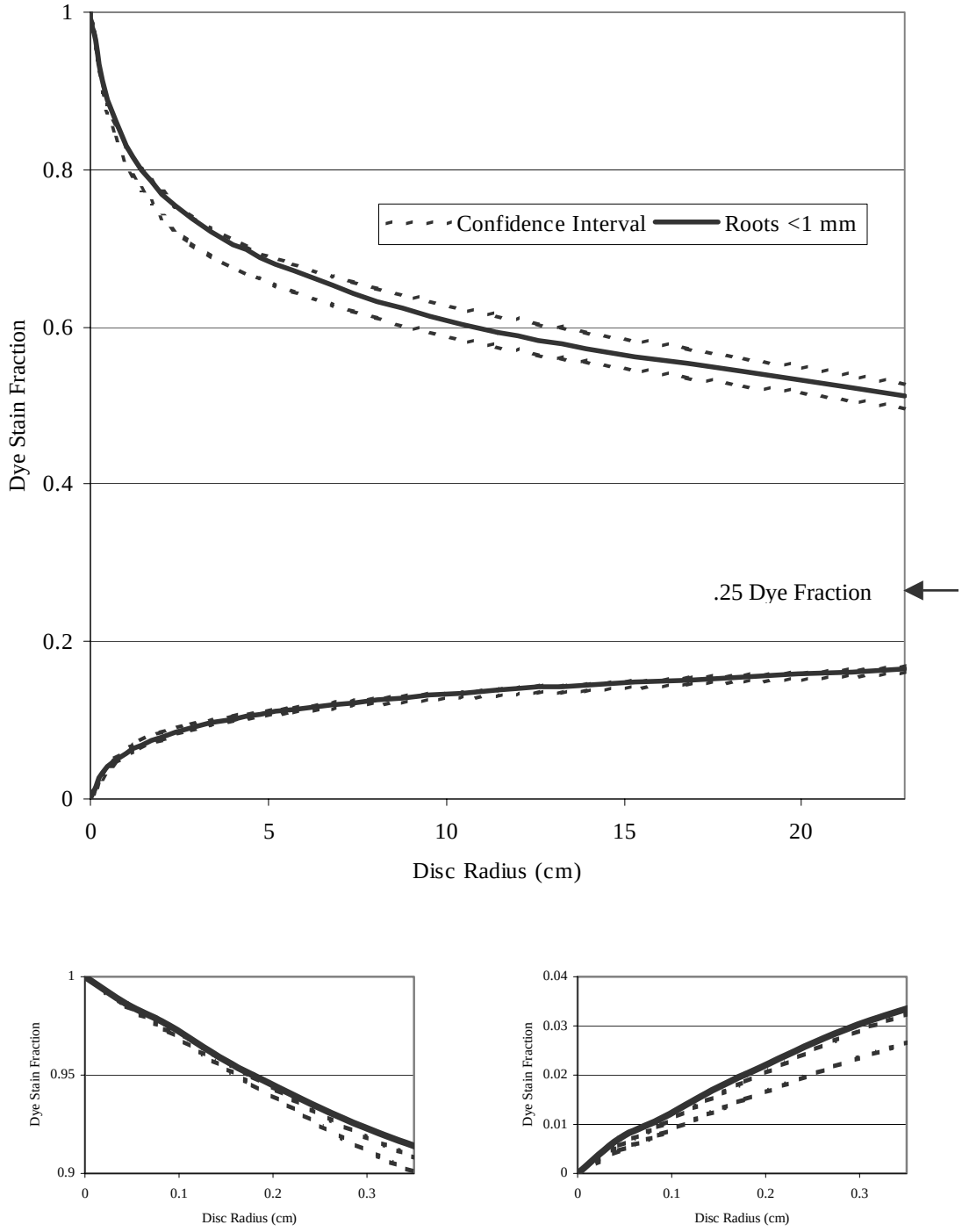

Figure 23. Fraction of area stained around roots in stained and unstained areas for roots <1 mm in the first plot at a depth of 75 cm. Plot had 0.25 m^2/m^2 stained.

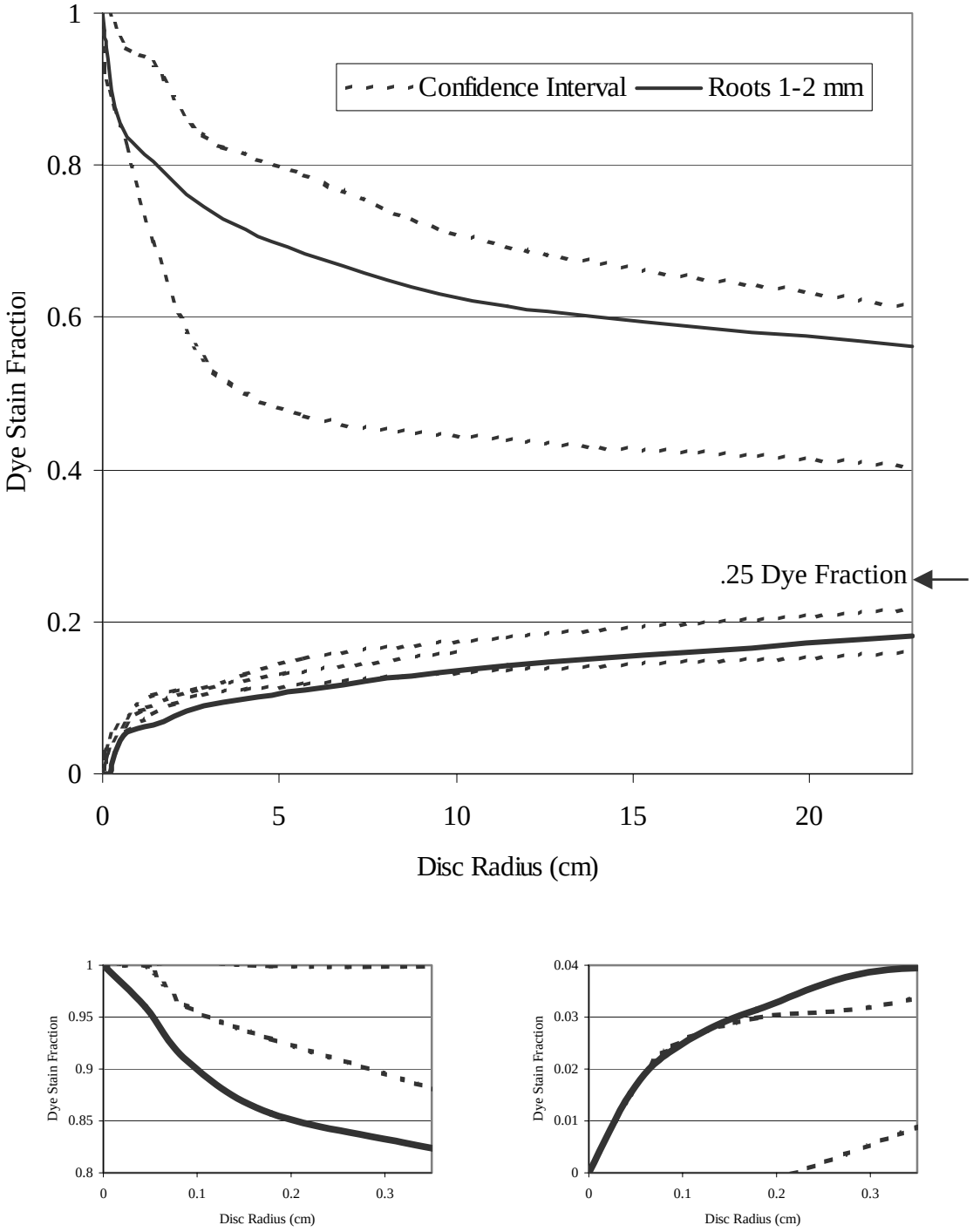

Figure 24. Fraction of area stained around roots in stained and unstained areas for roots 1-2 mm in the first plot at a depth of 75 cm. Plot had 0.25 m^2/m^2 stained.

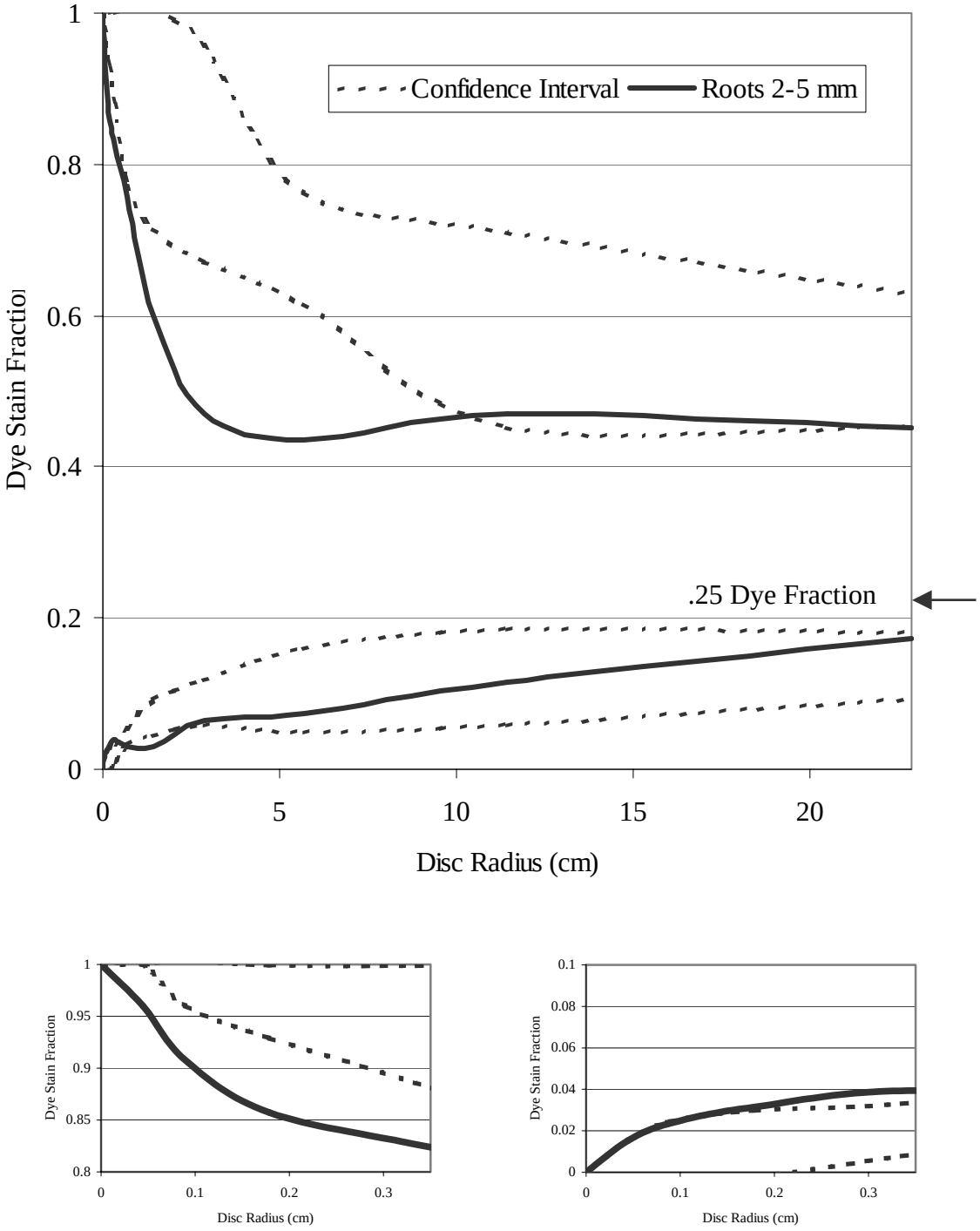

Figure 25. Fraction of area stained around roots in stained and unstained areas for roots 2-5 mm in the first plot at a depth of 75 cm. Plot had 0.25 m^2/m^2 stained.

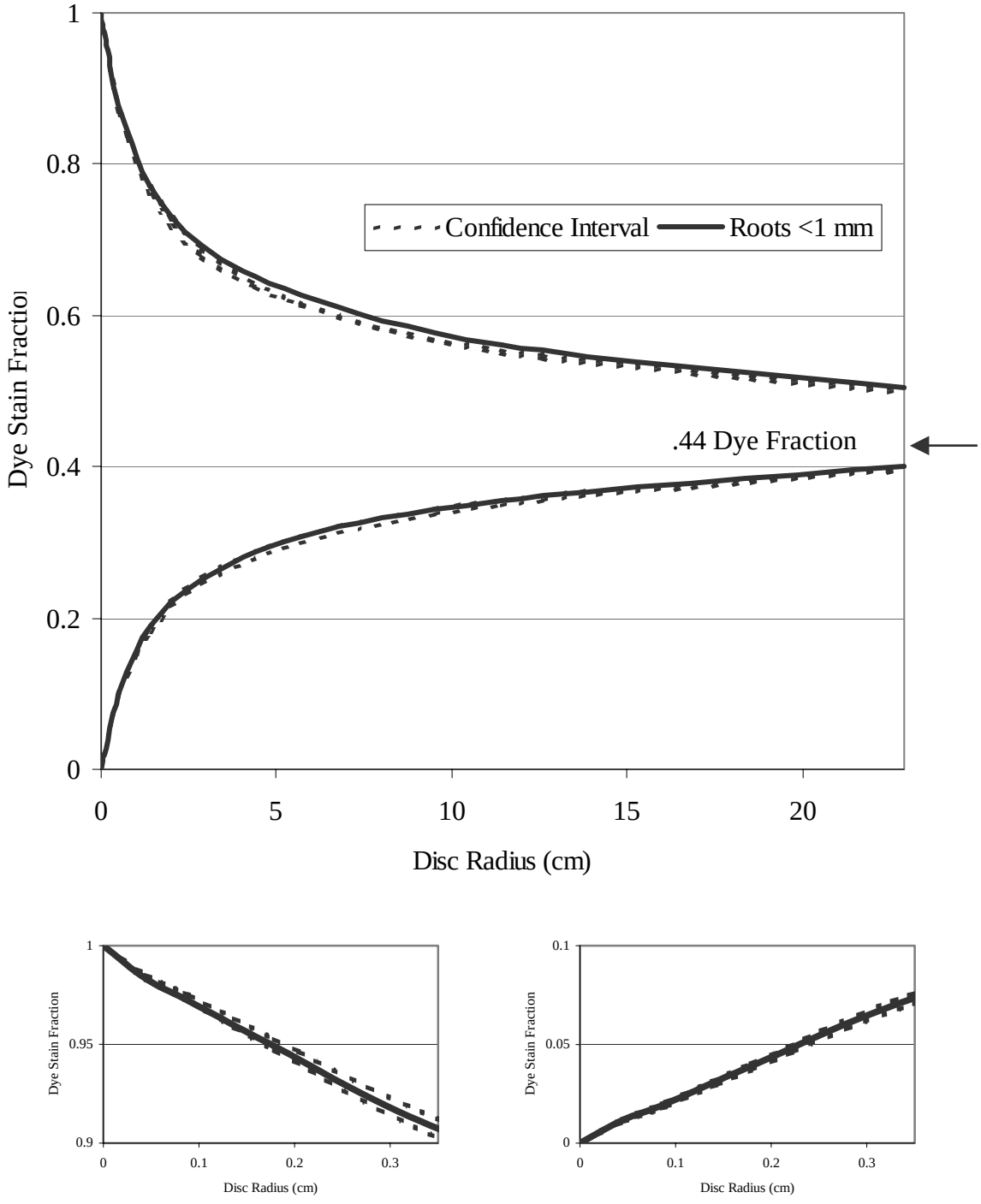

Figure 26. Fraction of area stained around roots in stained and unstained areas for roots <1 mm in the second plot at a depth of 25 cm. Plot had 0.44 m^2/m^2 stained.

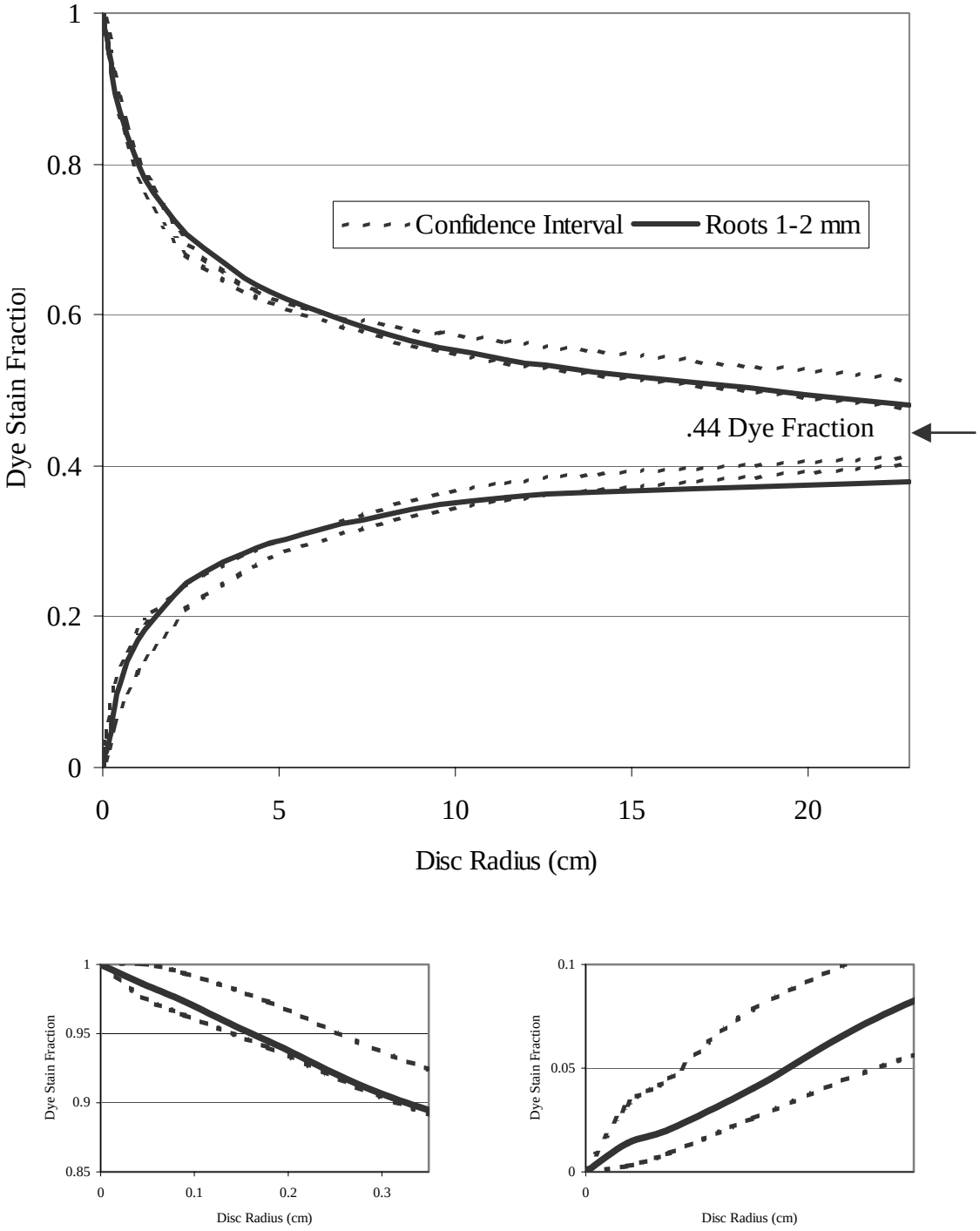

Figure 27. Fraction of area stained around roots in stained and unstained areas for roots 1-2 mm in the second plot at a depth of 25 cm. Plot had 0.44 m^2/m^2 stained.

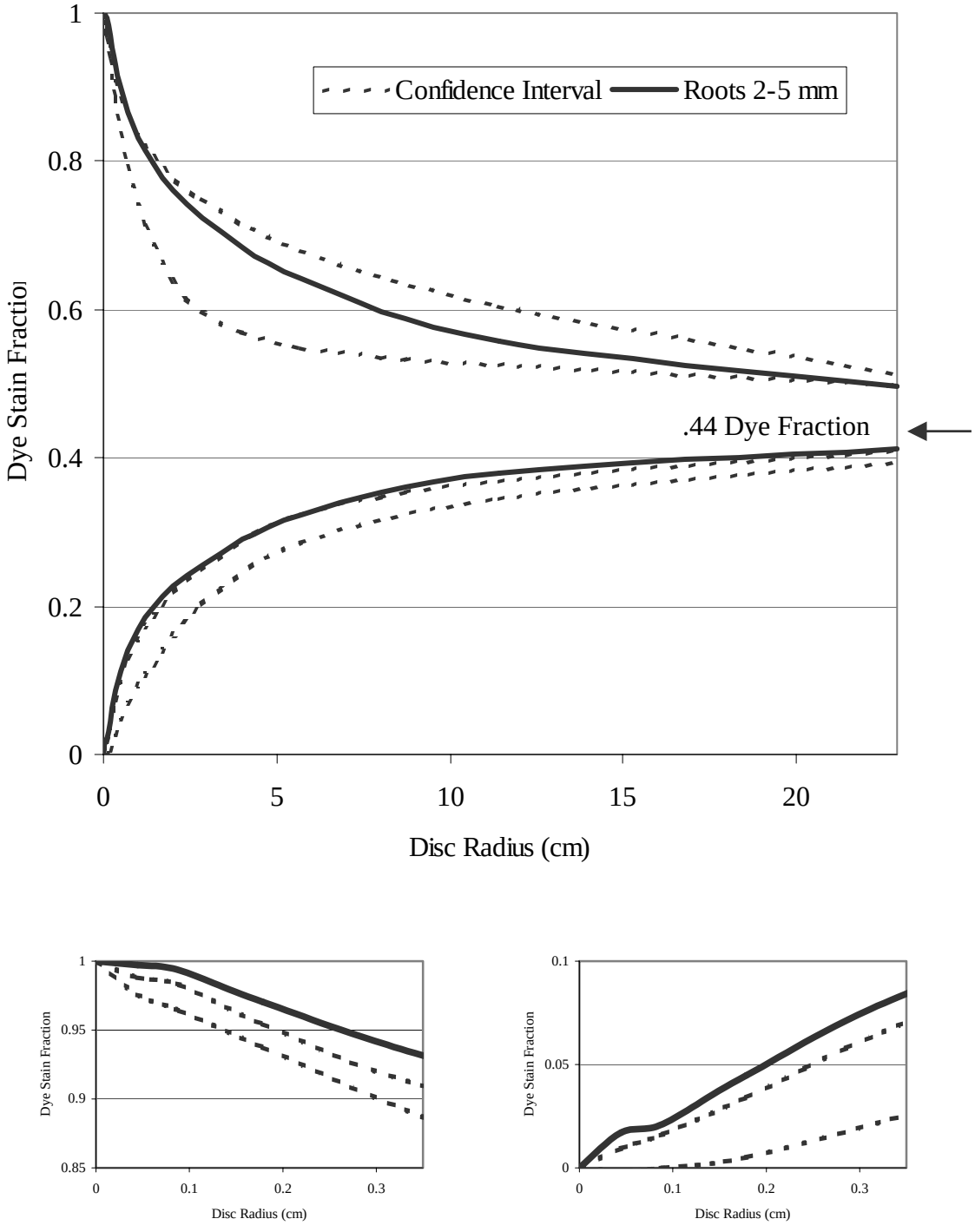

Figure 28. Fraction of area stained around roots in stained and unstained areas for roots 2-5 mm in the second plot at a depth of 25 cm. Plot had 0.44 m^2/m^2 stained.

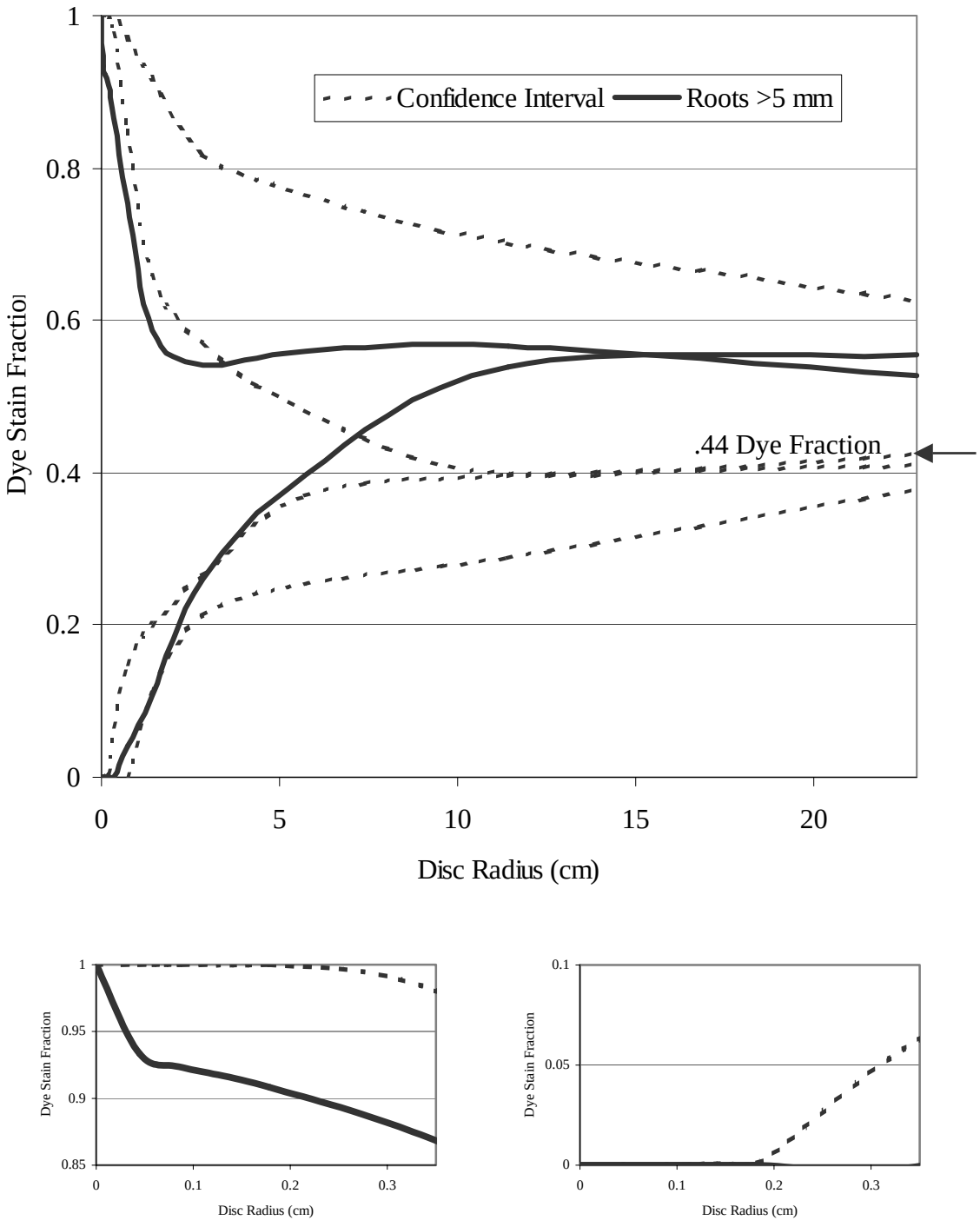

Figure 29. Fraction of area stained around roots in stained and unstained areas for roots >5 mm in the second plot at a depth of 25 cm. Plot had 0.44 m^2/m^2 stained.

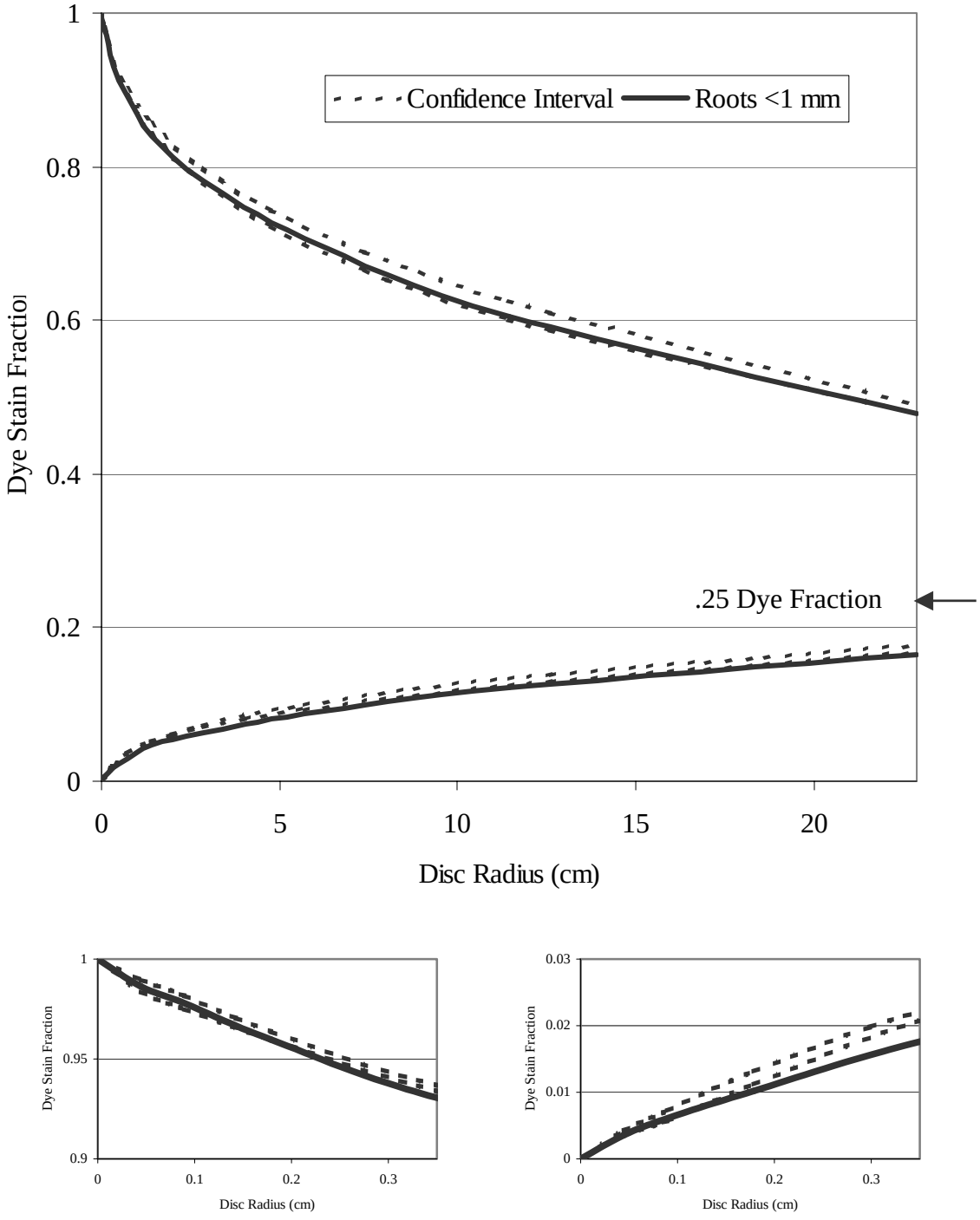

Figure 30. Fraction of area stained around roots in stained and unstained areas for roots <1 mm in the second plot at a depth of 45 cm. Plot had 0.44 m^2/m^2 stained.

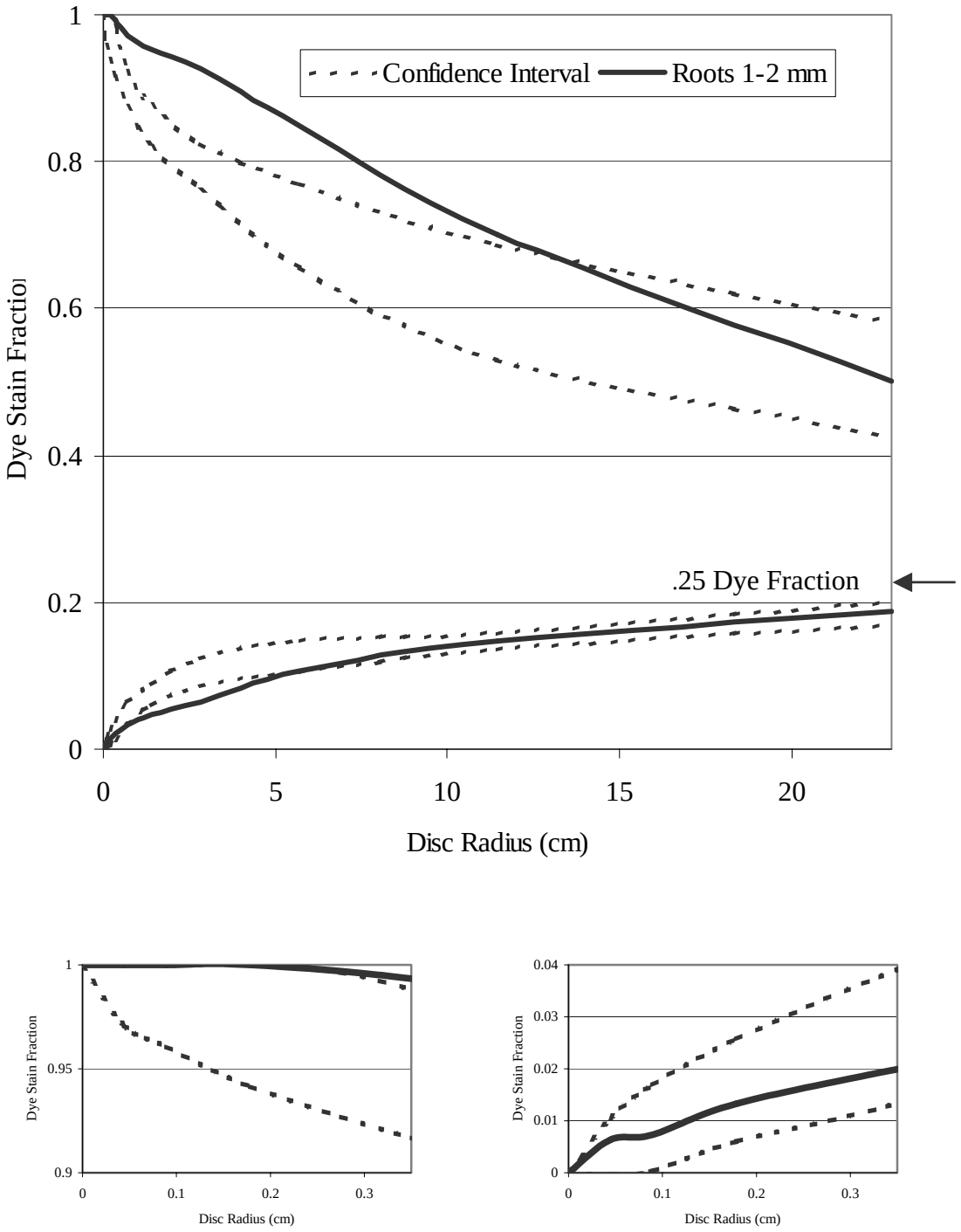

Figure 31. Fraction of area stained around roots in stained and unstained areas for Roots 1-2 mm in the second plot at a depth of 45 cm. Plot had 0.25 m^2/m^2 stained.

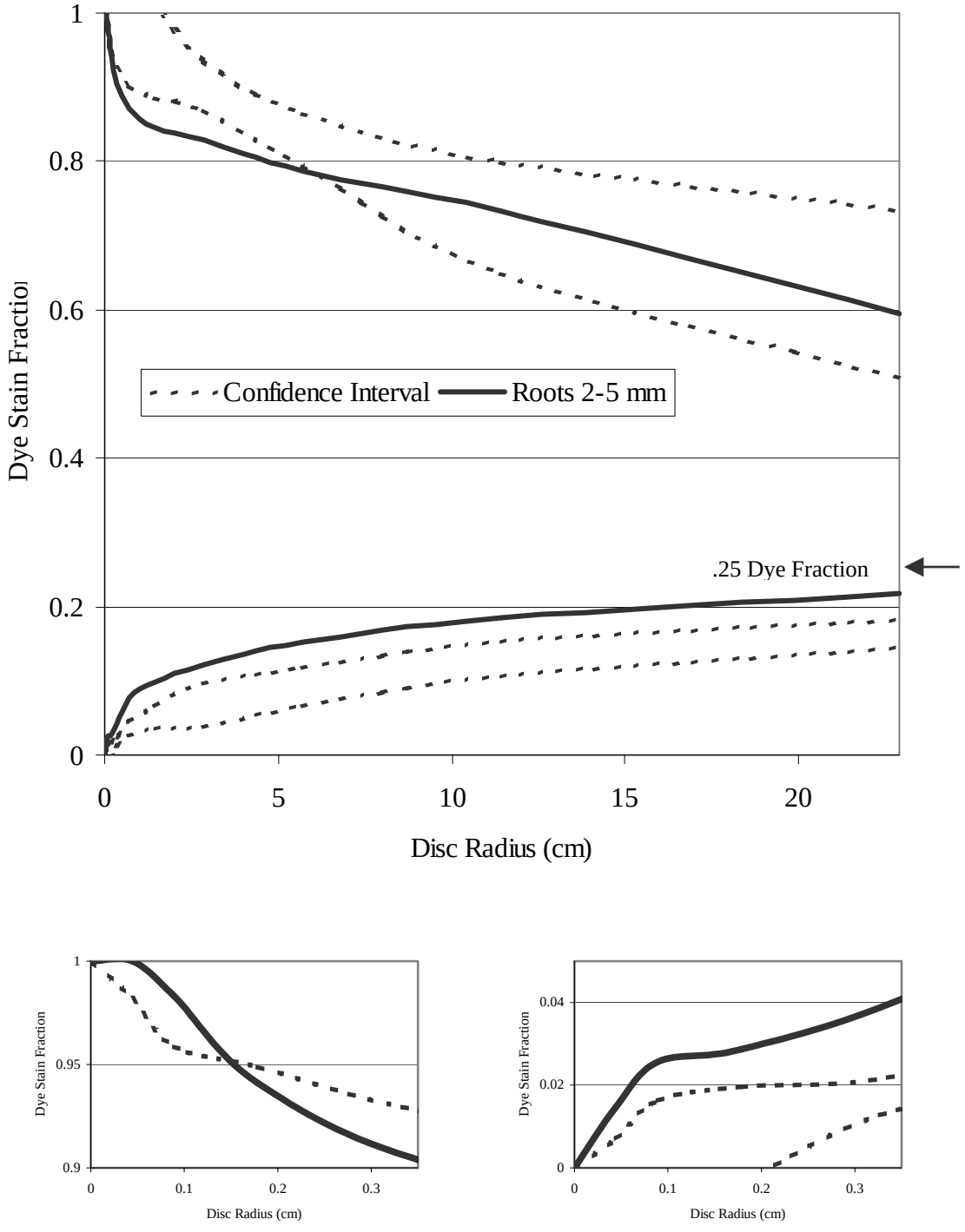

Figure 32. Fraction of area stained around roots in stained and unstained areas for roots 2-5 mm in the second plot at a depth of 45 cm. Plot had 0.25 m^2/m^2 stained.

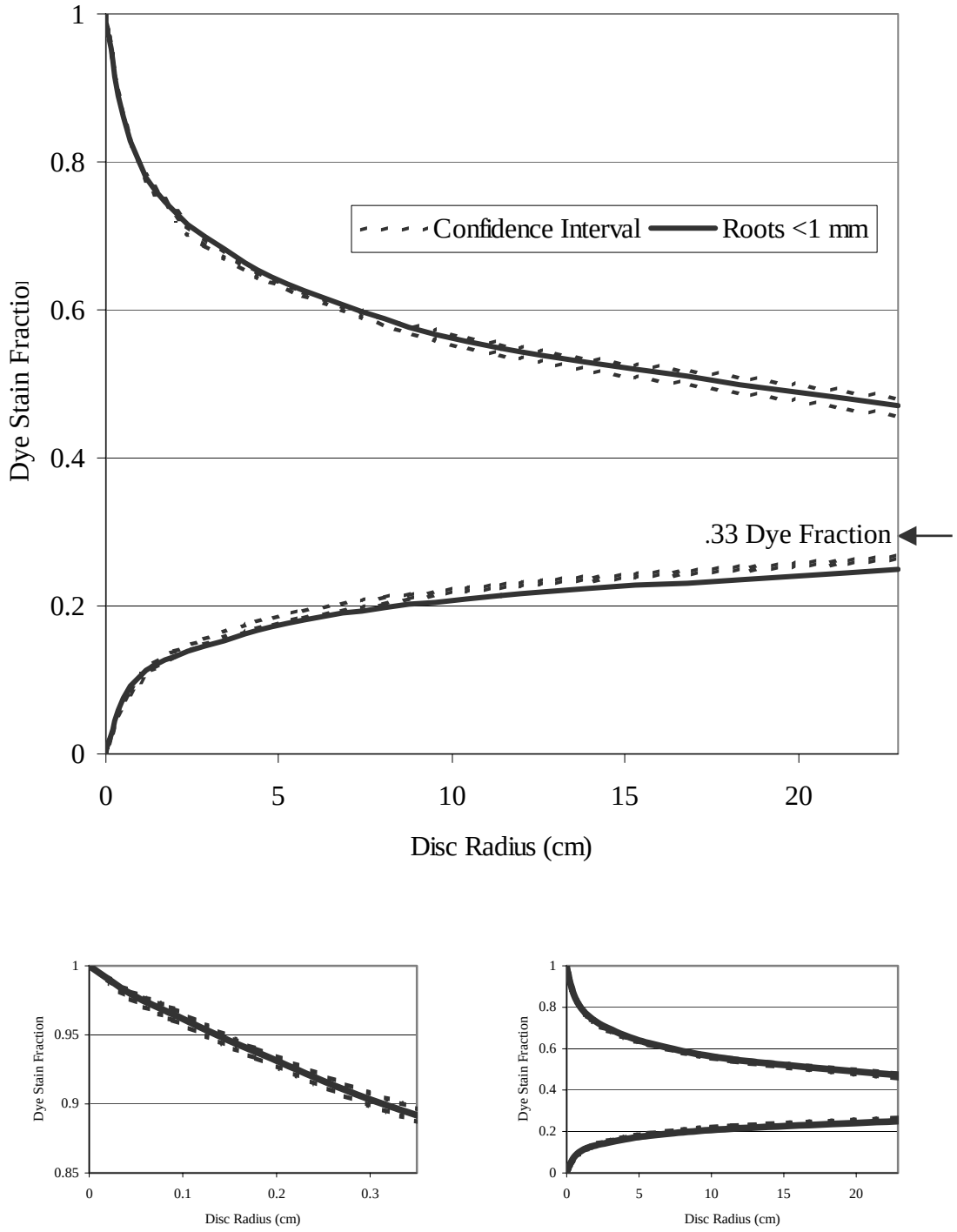

Figure 33. Fraction of area stained around roots in stained and unstained areas for roots <1 mm in the second plot at a depth of 75 cm. Plot had 0.33 m^2/m^2 stained.

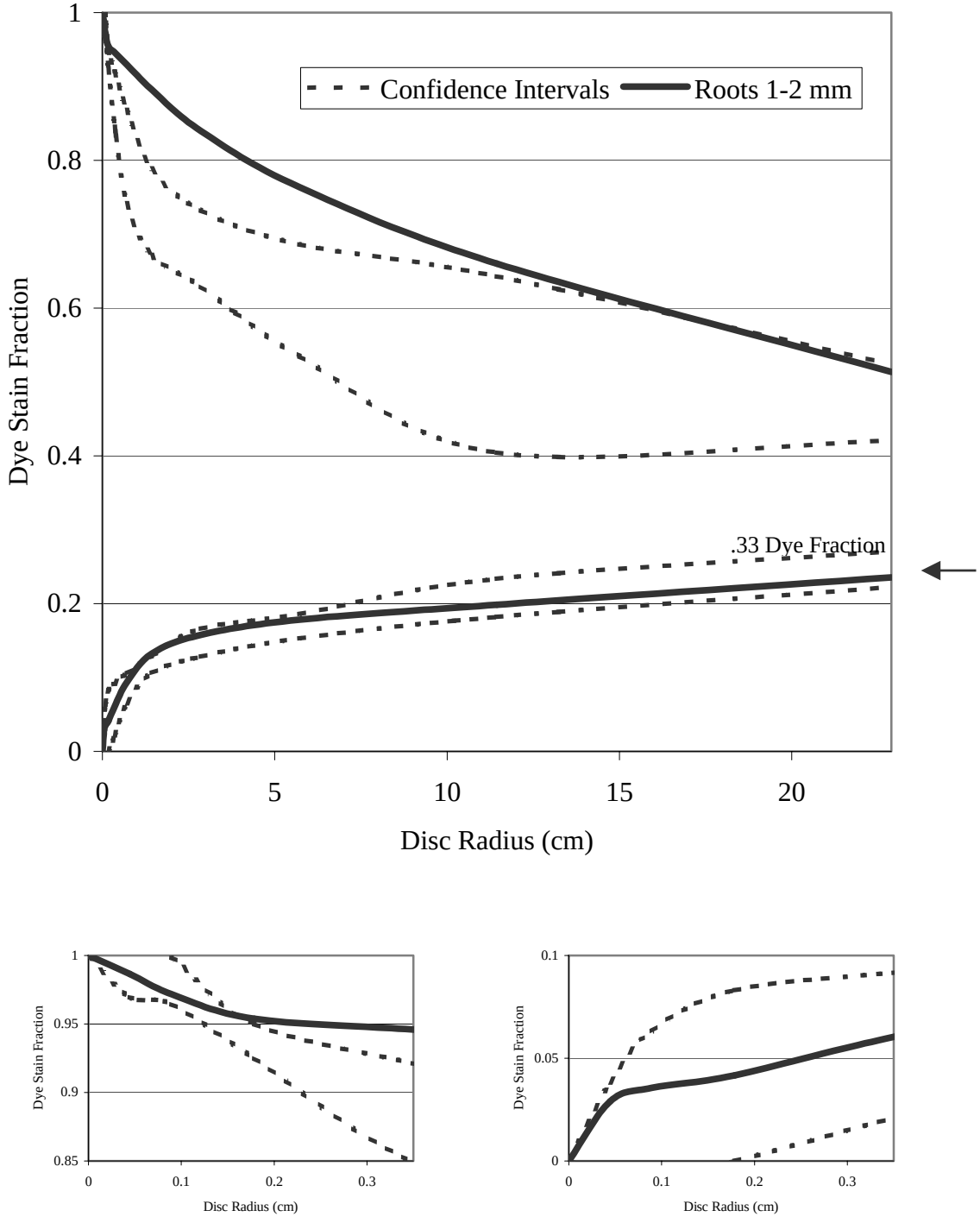

Figure 34. Fraction of area stained around roots in stained and unstained areas for roots 1-2 mm in the second plot at a depth of 75 cm. Plot had 0.33 m^2/m^2 stained.

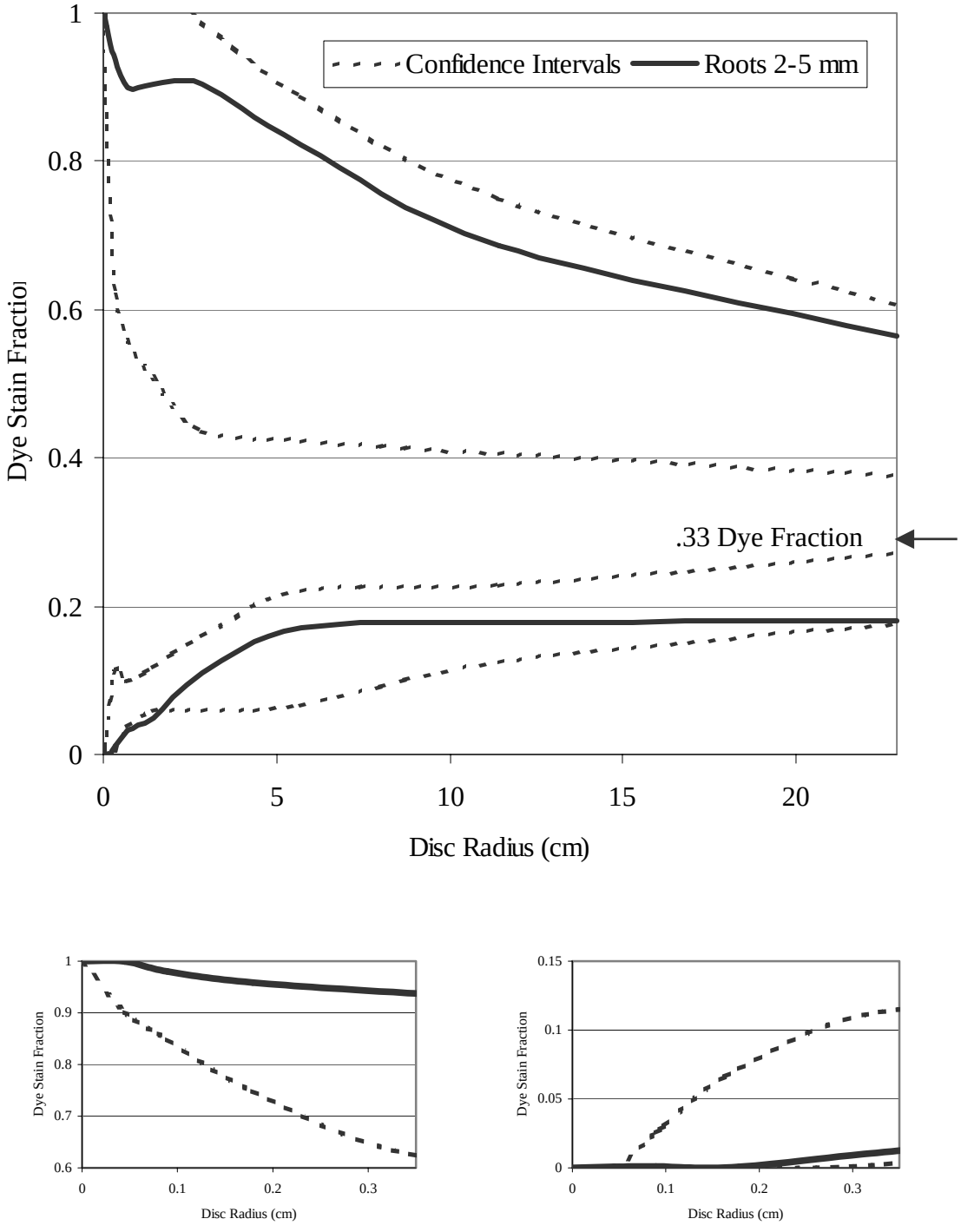

Figure 35. Fraction of area stained around roots in stained and unstained areas for roots 2-5 mm in the second plot at a depth of 75 cm. Plot had 0.33 m^2/m^2 stained.

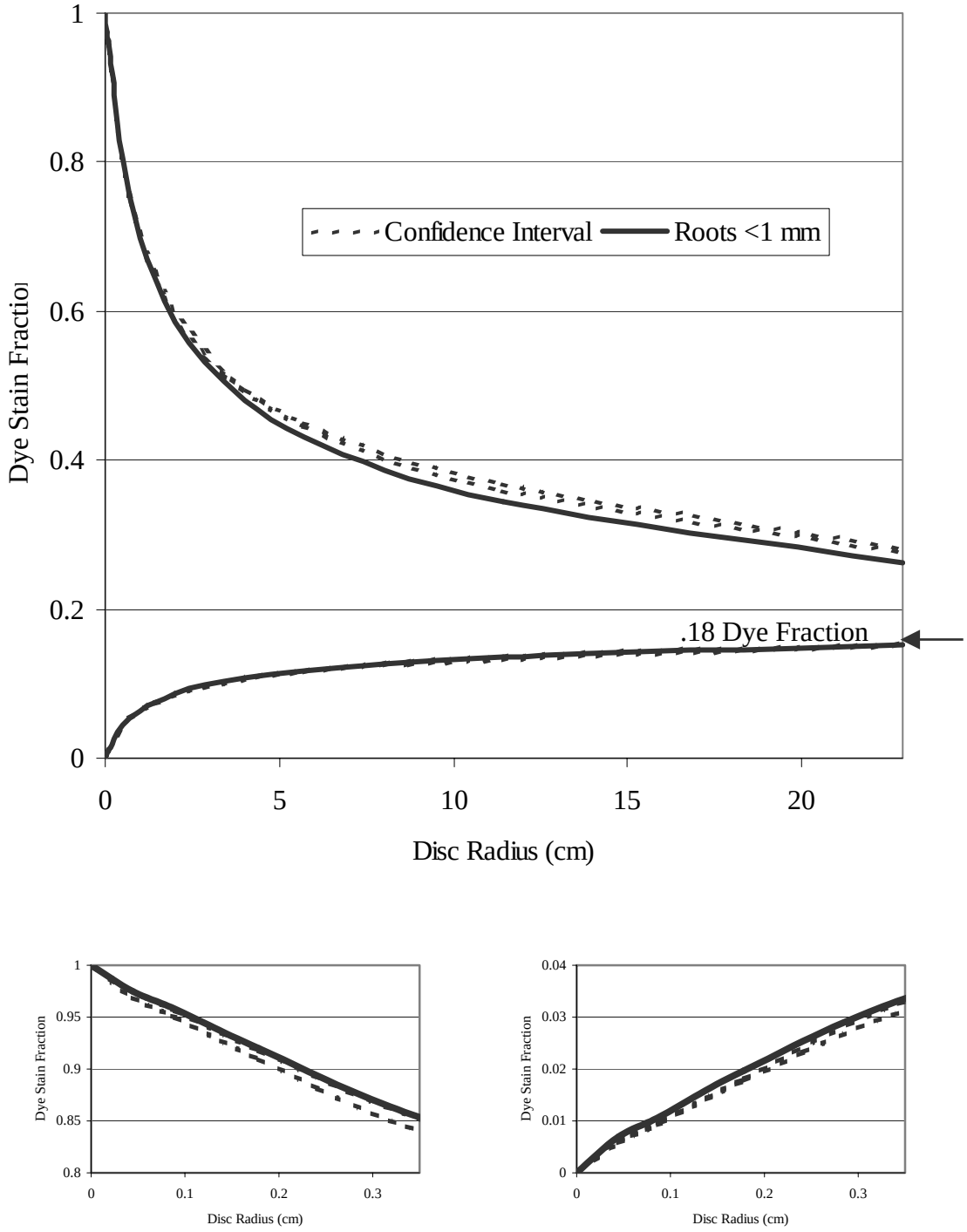

Figure 36. Fraction of area stained around roots in stained and unstained areas for roots <1 mm in the third plot at a depth of 25 cm. Plot had 0.18 m^2/m^2 stained.

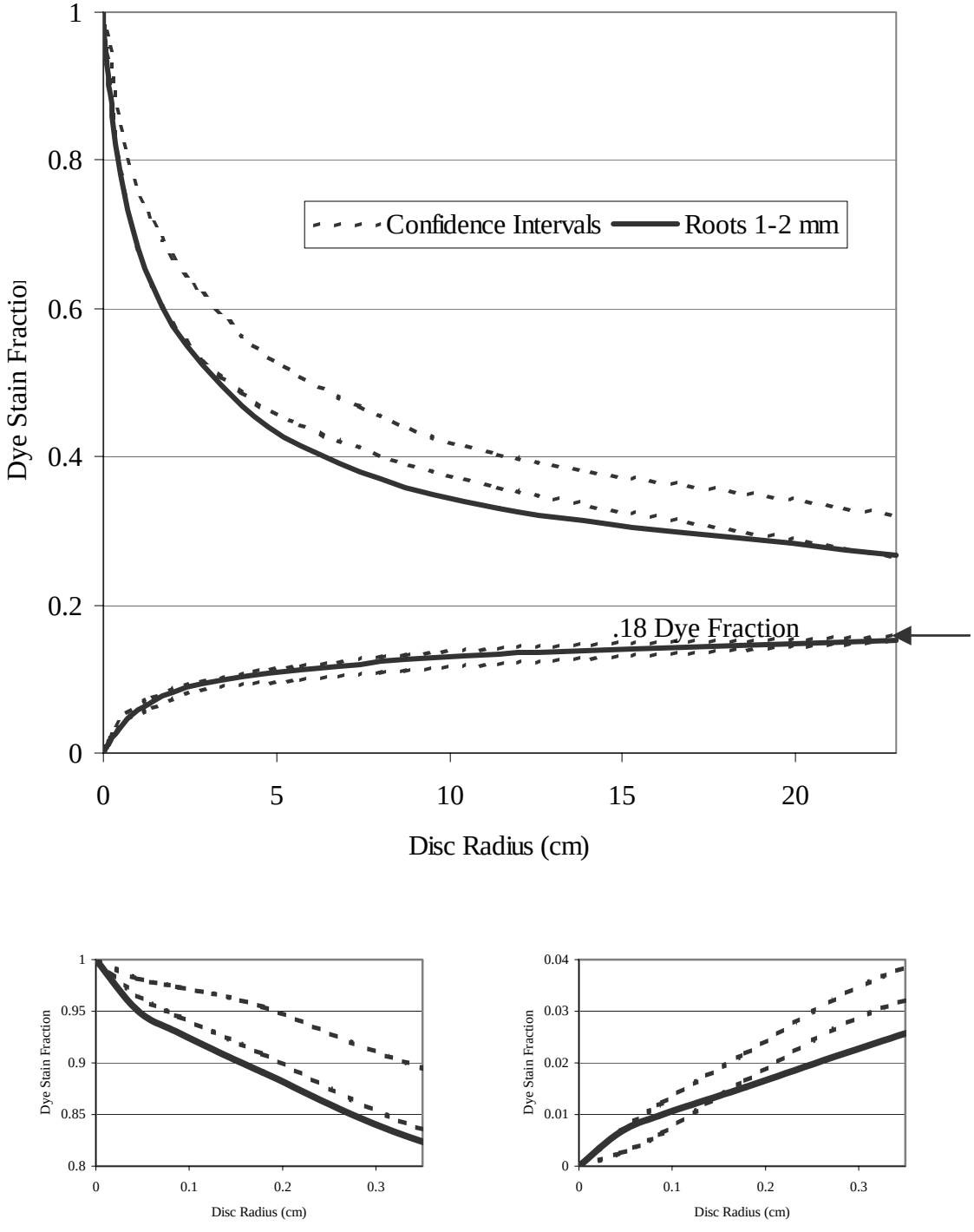

Figure 37. Fraction of area stained around roots in stained and unstained areas for roots 1-2 mm in the third plot at a depth of 25 cm. Plot had 0.18 m^2/m^2 stained.

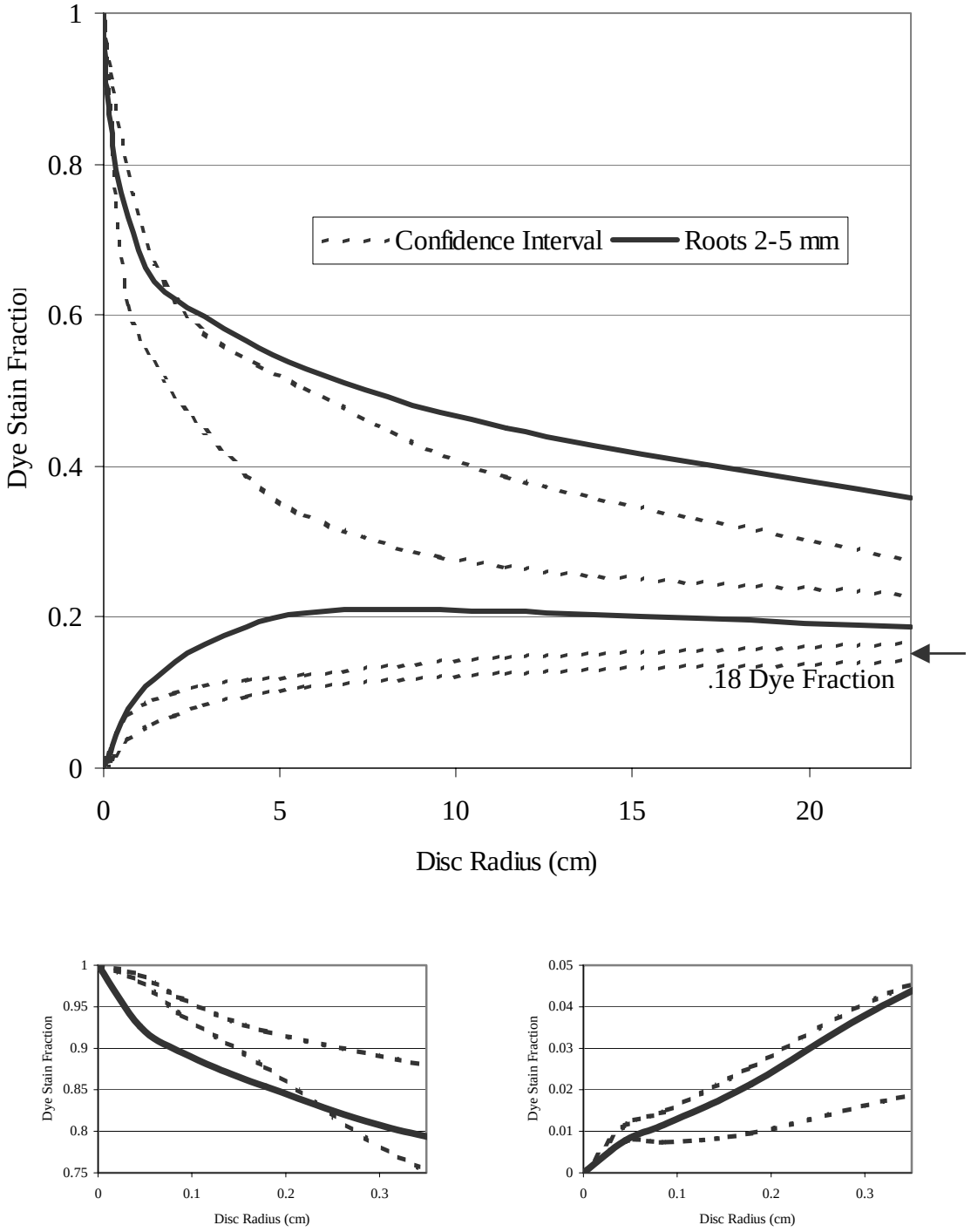

Figure 38. Fraction of area stained around roots in stained and unstained areas for roots 2-5 mm in the third plot at a depth of 25 cm. Plot had 0.18 m^2/m^2 stained.

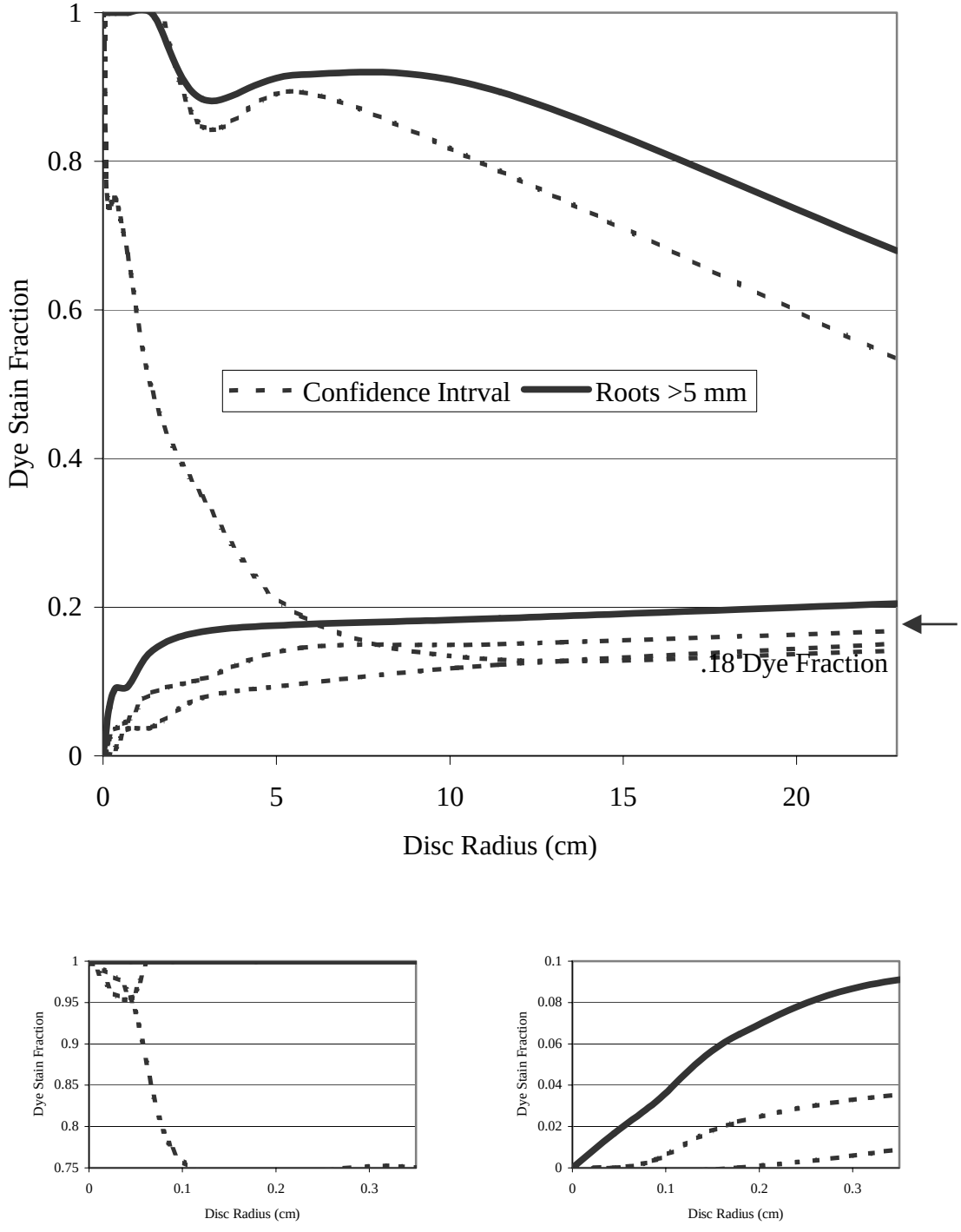

Figure 39. Fraction of area stained around roots in stained and unstained areas for roots >5 mm in the third plot at a depth of 25 cm. Plot had 0.18 m^2/m^2 stained.

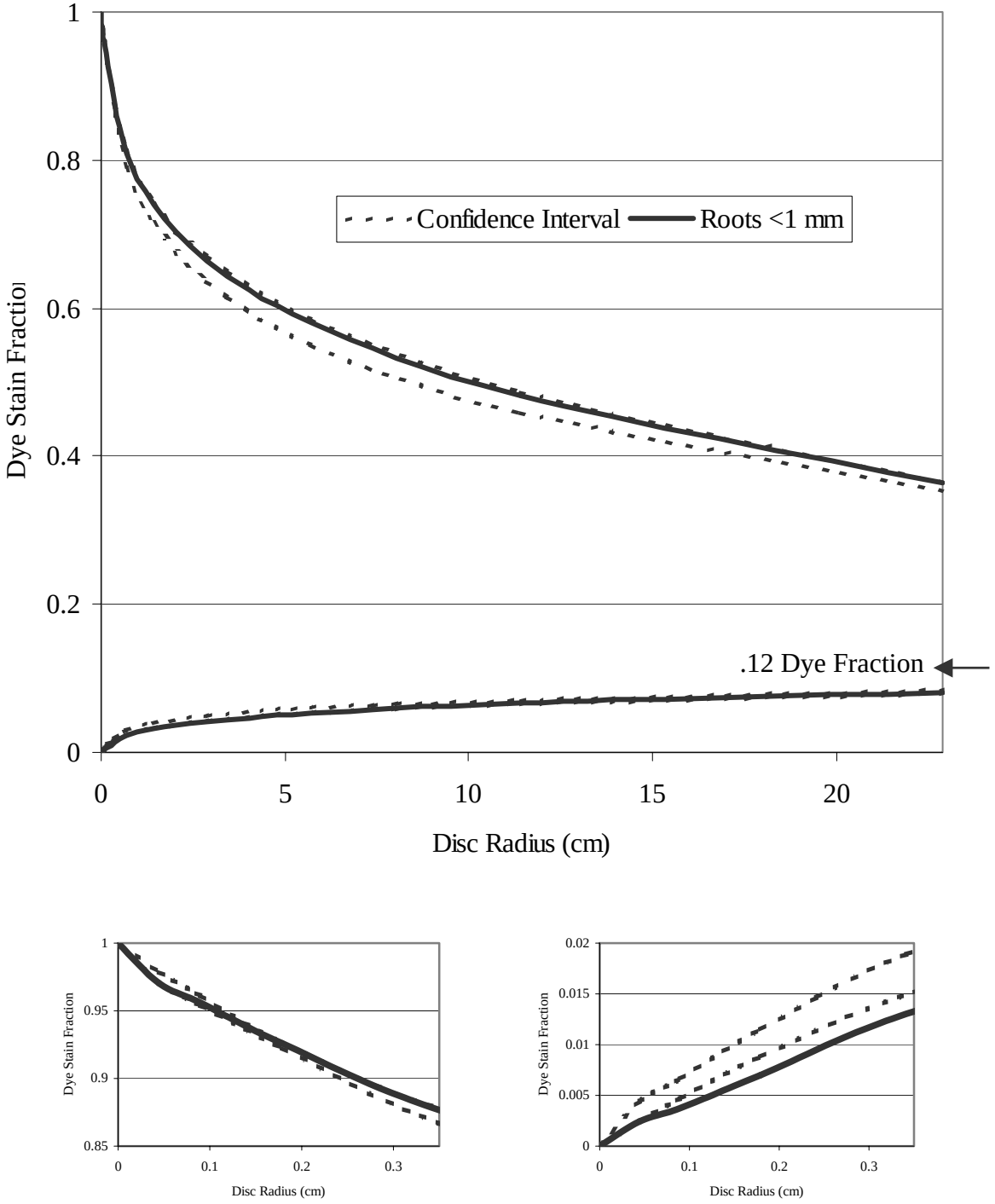

Figure 40. Fraction of area stained around roots in stained and unstained areas for roots <1 mm in the third plot at a depth of 45 cm. Plot had 0.12 m^2/m^2 stained.

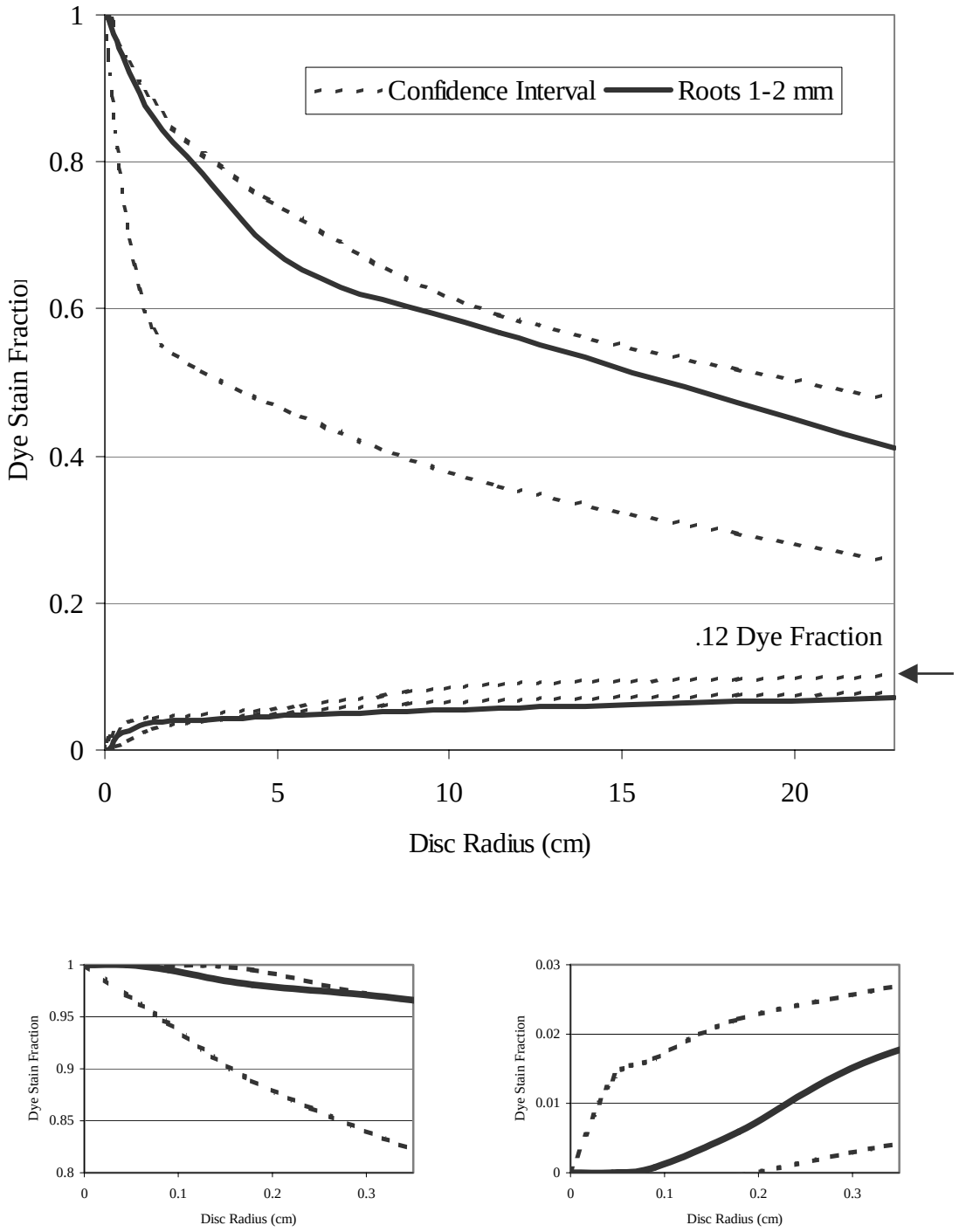

Figure 41. Fraction of area stained around roots in stained and unstained areas for roots 1-2 mm in the third plot at a depth of 45 cm. Plot had 0.12 m^2/m^2 stained.

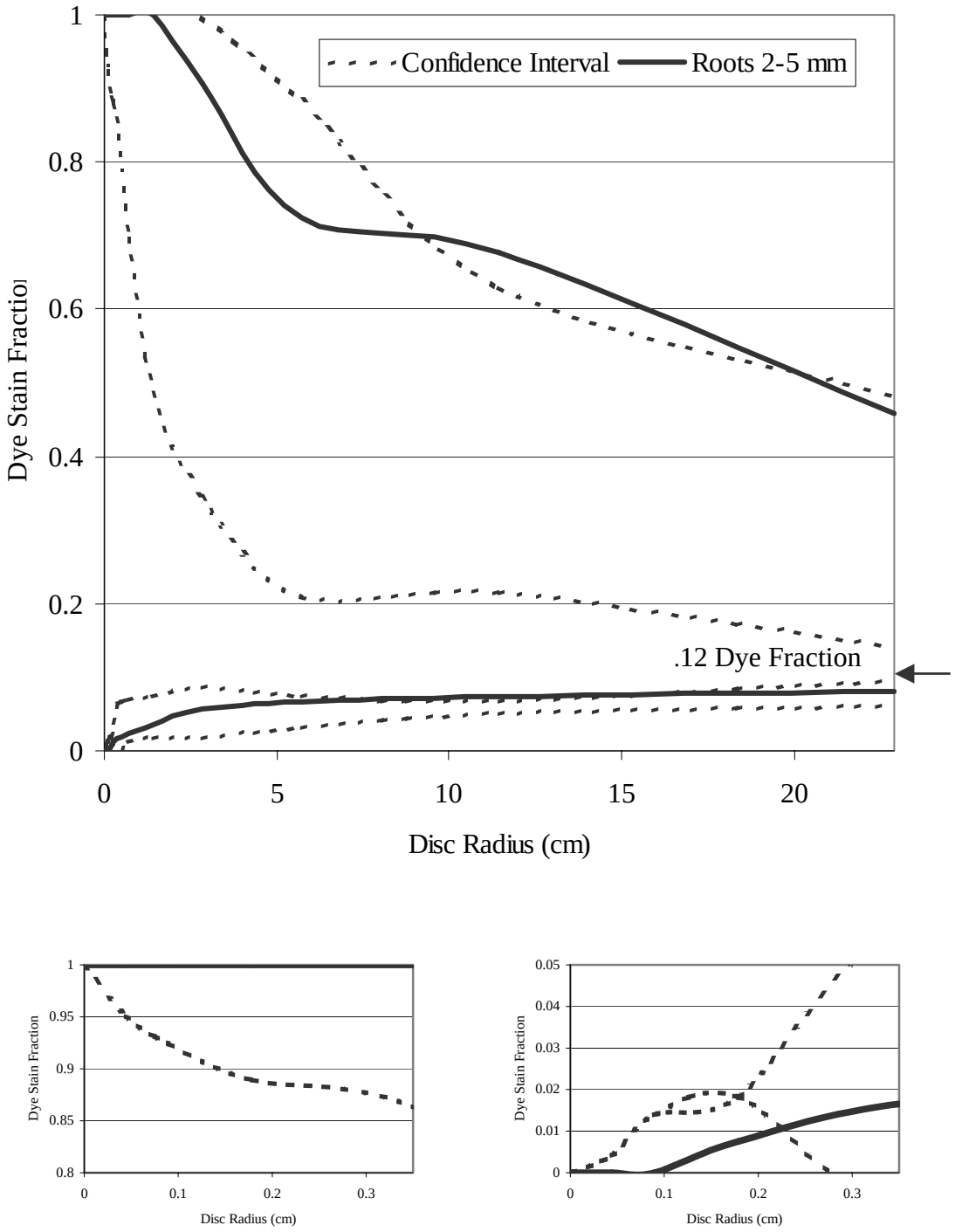

Figure 42. Fraction of area stained around roots in stained and unstained areas for roots 2-5 mm in the third plot at a depth of 45 cm. Plot had 0.12 m^2/m^2 stained.

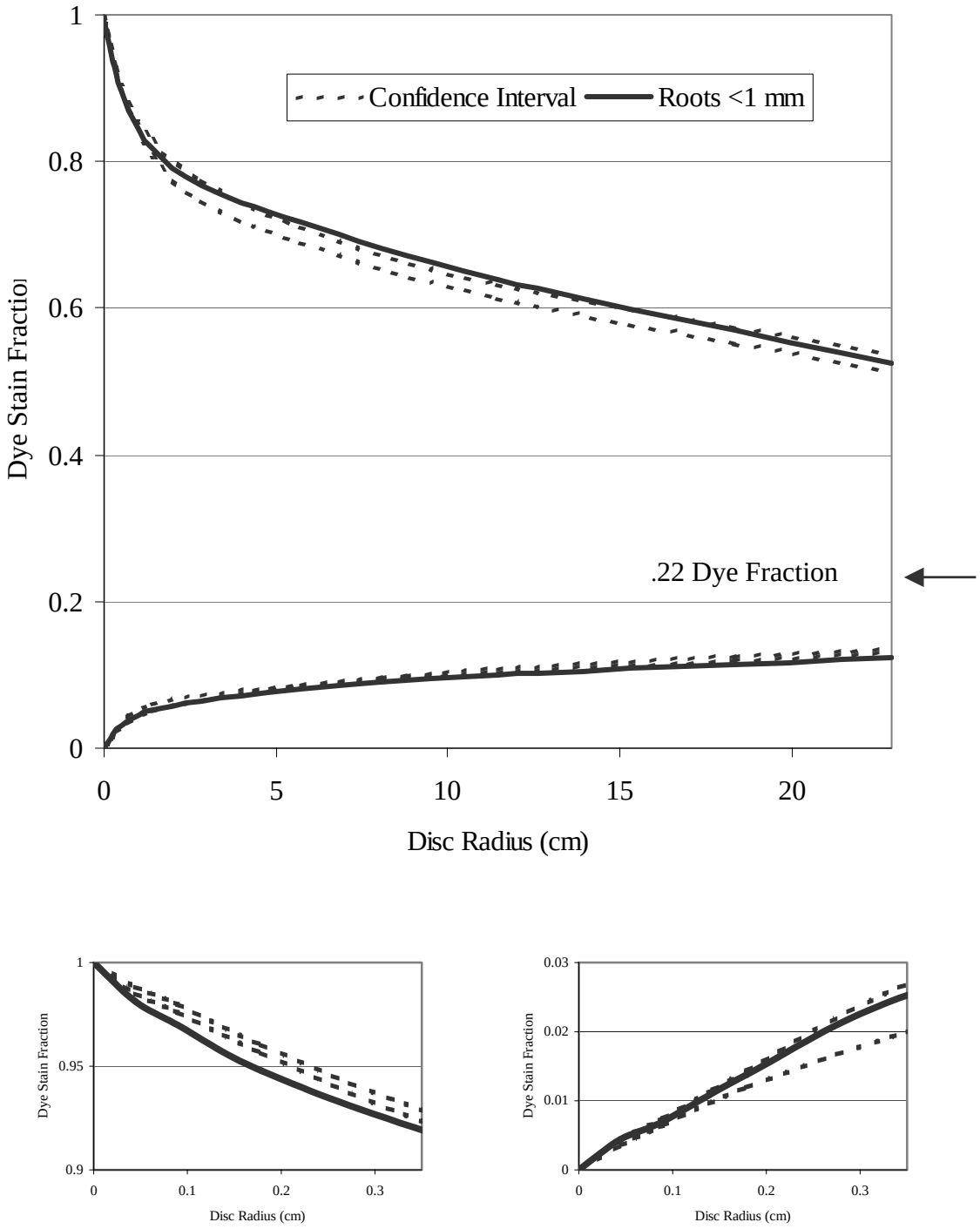

Figure 43. Fraction of area stained around roots in stained and unstained areas for roots <1 mm in the third plot at a depth of 75 cm. Plot had 0.22 m^2/m^2 stained.

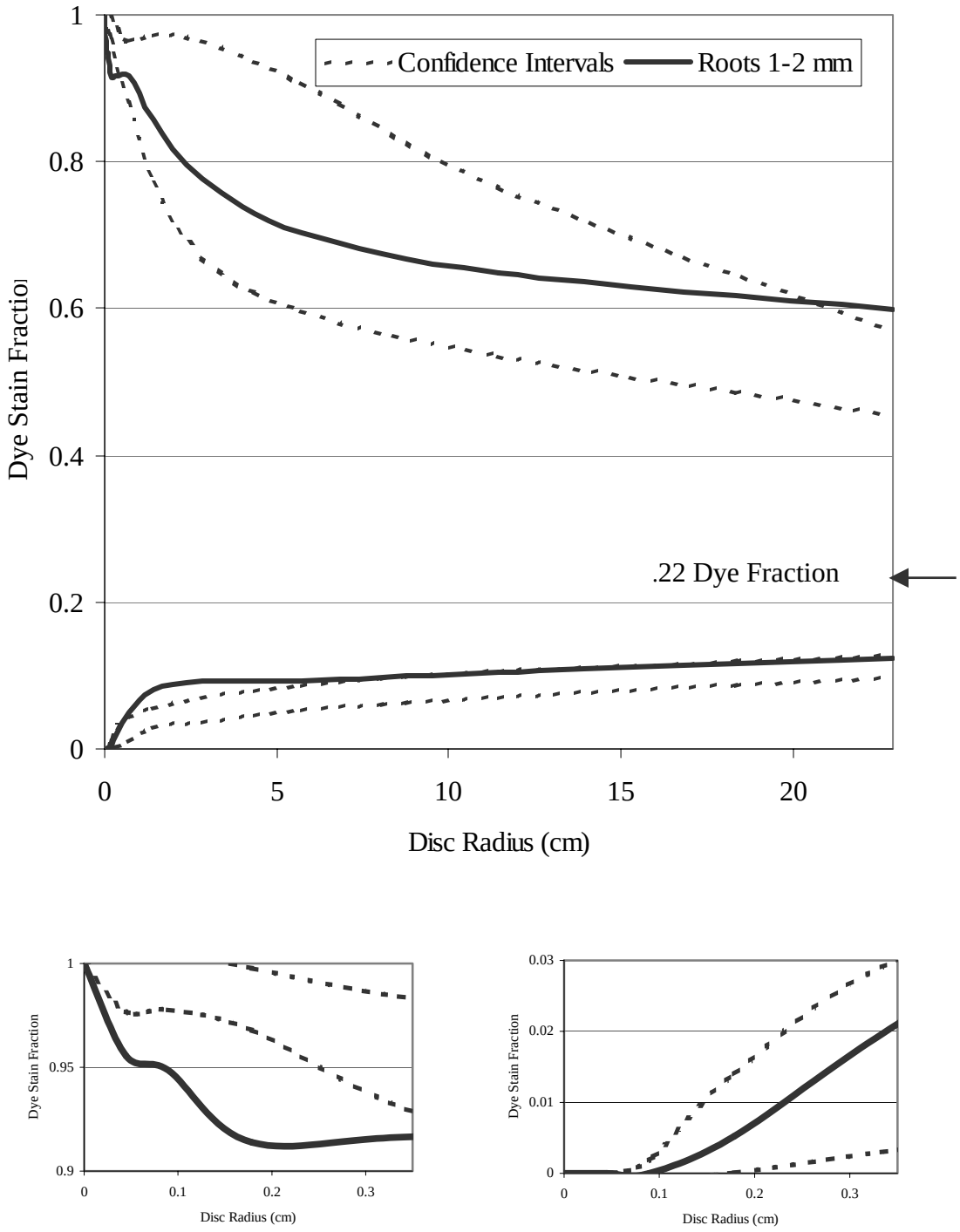

Figure 44. Fraction of area stained around roots in stained and unstained areas for roots 1-2 mm in the third plot at a depth of 75 cm. Plot had 0.22 m^2/m^2 stained.

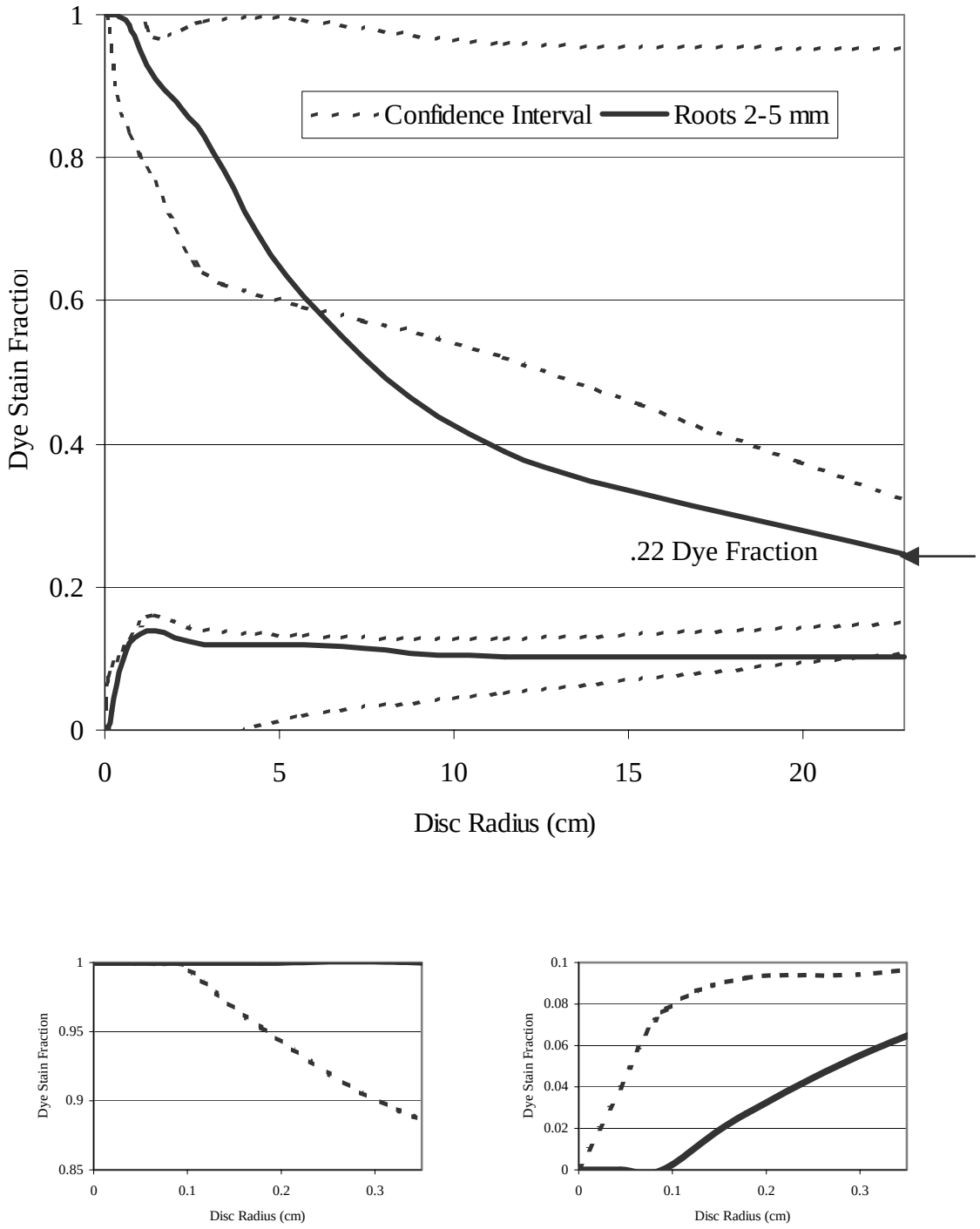

Figure 45. Fraction of area stained around roots in stained and unstained areas for roots 2-5 mm in the third plot at a depth of 75 cm. Plot had 0.22 m^2/m^2 stained.

Since the dye stain fraction in most plots is less than the unstained fraction, the unstained roots make up the bulk of most root categories. In the larger roots categories, compared to the stained roots, the unstained roots had smaller deviations from the curves generated from the randomly distributed roots. These deviations were nearly evenly mixed between above and below the confidence intervals, but most of the large deviations were above the confidence intervals (see Figures 32, 38, and 39). The larger deviations all came in the 2-5 mm root category. So the distribution of the unstained roots does not appear to be entirely random with respect to the dye stain pattern, and the data analysis weakly indicates a positive spatial association between the roots and dye stain pattern.

Looking at the results of the distribution analysis based on depth the data does not indicate that a spatial association tends to be stronger at one depth over the others. However, in the distribution analysis the 1-2 mm roots and the 2-5 mm roots behaved differently in relation to depth. The evidence for a spatial association of 1-2 mm roots came from the planes at 45 cm and 75 cm (see Figures 31, 34, and 44). The evidence for 2-5 mm roots was more even distributed throughout the profile but actually tended to be stronger near the surface (see Figures 19, 32, and 38).

It is possible to say two things. First, there does appear to be a higher concentration of larger roots within the dye stained areas than would be expected if the distributions were random. Second, the results from the distribution analysis graphs suggest that larger roots are clustering in or around the dye stain pattern.

Pitfalls

A number of problems arose during the experiment. In clearing and removing the soil we found the highly structured nature of the soil made it very difficult to obtain a perfectly level and smooth soil surface. Our 0.5 m by 0.5 m grid was marked using pushpins at the corners of each square. The slight variations in topography meant that at times the corners of our grid squares did not match perfectly with the corners on the plastic sheets used for mapping the roots. And more importantly, we found that the plastic sheets were prone to stretching or shifting during mapping, and then again when the root points were digitized. Even a slight shift or stretch in the plastic sheet could have resulted in a root map displaced by a few millimeters from its actual location. We experimented with thicker plastic, that was less likely to stretch or move, but the thicker plastic was less transparent and less flexible, making mapping more difficult. We opted for the thinner plastic with the associated uncertainties.

By visually comparing the plastic sheets, photographs and the roots graphs created with the digitized data it appears that in most cases the maps were off by less than 1 cm, but some roots were off by as much as 2 cm. The data shift appears to be fairly consistent within a given plastic sheet. Unfortunately not all photos have large visible roots that can be used as reference points to evaluate the root maps.

The photos of the grid squares were combined to create a mosaic of the entire plot. Great effort was taken to make sure the camera was centered, level, and at the same height for each photo, but slight variations existed in the photos. In addition conditions such as shadow and lighting differed among photos. As a result of differing

light conditions the threshold command varied slightly in sensitivity. This was particularly evident on the perimeter photos of the planes to a depth of 75 cm. Because of the depth, and shadow these photos tended to be darker, and as a result the threshold command overestimated dye coverage relative to the interior photos. The result was visible seams in the composite mosaic images.

As mentioned earlier, it is also important to point out that the percent dye cover of a given plot is partially dependent upon the amount of dye applied, and the time taken to apply it. In this experiment a relatively large amount of dye was applied over a period of six hours. The result was plots of roughly forty percent dye cover in the first layer, and down to about 15 percent in the third layer. If less dye had been applied over a shorter period of time, the percent dye cover would have been smaller at all levels.

Looking back the experiment may have been more effective if we had excavated layers closer to the surface. Beginning at 25 cm put us at a depth where the flow paths converge, but it also put us below much of the root zone. This resulted in low root counts in the second and third layer, and it is possible that significant clustering occurred above 25 cm. By excavating at shallower depths we could have avoided the low root counts in the larger roots categories at 45 cm and 75 cm, and saved ourselves hours of work.

It seems apparent from our initial observations during excavation and visual inspection of our photographs, that our lack of a spatial association at times may be as much the result of experimental error in overlaying the two datasets as anything else. It seems likely that we simply were not able to map the root distribution with sufficient

accuracy using this methodology. It may be possible to do so through meticulous preparation of the soil surface and improved mapping procedures. But, it may be more practical to simply photograph each grid with as high resolution as possible and then map roots directly from the photographs. If this was possible and each photo was analyzed individually instead of as a mosaic, much of the potential error could be eliminated.

CHAPTER VI

SUMMARY AND CONCLUSIONS

Neither the root count data, nor the distribution analysis graphs indicated that the distribution of the <1 mm pasture grass roots was anything but random with respect to the dye stain pattern. The data indicated that the distribution of the larger roots was not entirely random with respect to the dye stain pattern. Both the root count data and the position distribution graphs pointed toward signs that some localized clustering of the larger root categories had occurred in and around the dye stain pattern. However, this evidence was not statistically significant, and in no way established a spatial association between preferential flow paths and root location.

REFERENCES

Bengough, A. G., and C. E. Mullins. 1990. Mechanical impedance to root growth, a review of experimental techniques and root growth responses. J. Soil Sci. 41:341-358.

Bland, W. L. 1989. Estimating root length density by the core break method. Soil Sci. Soc. Am. J. 53:1595-1597.

Böhm, W. 1979. Methods of studying root systems. Springer-Verlag, New York.

Böhm, W., and U. Köpke. 1977. Comparative root investigations with two profile wall techniques. Z. Acker Pflanzebau 144:297-303.

Bouma, J. 1984. Using soil morphology to develop measurement methods and simulation techniques for water movement in heavy clay soil. p. 298-315. *In* J. Bouma and P.A.C. Raats (ed.) Water and solute movement in heavy clay soils. Proc. of an ISSS Symposium. ILRI publication No. 37, Wageningen, The Netherlands.

Bouma, J., and L. W. Dekker. 1978. A case study on infiltration into dry clay. I. Morphological observations. Geoderma 20:27-40.

Bui, E. N., and J. E. Box. 1992. Stemflow, rain throughfall, and erosion under canopies of corn and sorghum. Soil Sci. Soc. Am. J. 56:242-247.

Burken, J. G., and J. L. Schnoor. 1996. Phytoremediation: Plant uptake of atrazine and the role of exudates. J. Environ. Eng-ASCE 122:958-963.

Chang, Y. Y., and M. Y. Corapcioglu. 1998. Plant-enhanced subsurface bioremediation of nonvolatile hydrocarbons. J. Environ. Eng-ASCE 124:162-169.

Clothier, B. E., and S. R. Green. 1997. Roots: The big movers of water and chemicals in soil. Soil Sci. 162:534-543.

Cunningham, S. D., T. A. Anderson, A. P. Schwab, and F. C. Hsu. 1996. Phytoremediation of soils contaminated with organic pollutants. Adv. Agron. 56:55-114.

de Souza, M. P., E. A. H. Pilon-Smits, C. M. Lytle, S. Hwang, J. Tai, T. S. U. Honma, L. Yeh, and N. Terry. 1998. Rate-limiting steps in selenium assimilation and volatilization by Indian mustard. Plant Physiol. 117:1487-1494.

Ehlers, W., U. Köpke, F. Hesse, and W. Böhm. 1983. Penetration resistance and root growth of oats in tilled and untilled loess soil. Soil Tillage Res. 3:261-275.

Flury, M., and H. Flühler. 1994. Brilliant blue FCF as a dye tracer for solute transport studies - a toxicological overview. J. Environ. Qual. 23:1108-1112.

Flury, M., and H. Flühler. 1995. Tracer characteristics of brilliant blue FCF. Soil Sci. Soc. Am. J. 59:22-27.

Gardner, W. R. 1960. Dynamic aspects of water availability to plants. Soil Sci. 89:63-73.

Gish, T. J., D. Gimenez, and W. J. Rawls. 1998. Impact of roots on ground water quality. Plant Soil 200:47-54.

Godfrey, C.L., G.S. McKee, and H. Oakes. 1973. General soil map of Texas. Texas Agri. Exp. Sta., Texas A&M Univ. in cooperation with SCS, USDA.

Hasegawa, S., and T. Sato. 1987. Water uptake by roots in cracks and water movement in clayey subsoil. Soil Sci. 143:381-386.

Heuvelman, W. J., and K. J. McInnes. 1997. Spatial variability of water fluxes in soil: A field study. Soil Sci. Soc. Am. J. 61:1037-1041.

Heuvelman, W. J., and K. J. McInnes. 1999. Solute travel time distributions in soil: A field study. Soil Sci. 164: 2-9

Hubert, L. J., R. G. Gollege, C. M. Constanzo, and N. Gale. 1985. Measuring association between spatially defined variables: An alternative procedure. Geographical Analysis 17:36-46.

Isaaks, E. H., and R. M. Srivastava. 1989. Applied Geostatistics. Oxford University Press, New York.

Journel, A. G. 1983. Non-parametric estimation of spatial distribution. Math. Geol. 15:445-468.

Juang, K. W., D. Y. Lee, and C. H. Hsiao. 1998. Kriging with cumulative distribution function of order statistics for delineation of heavy metal contaminated soils. Soil Sci. 163:797-804.

Kamara, L., R. Zartman, and R. H. Ramsey. 1991. Cotton-root distribution as a function of trickle irrigation emitter depth. Irrigation Science. 12: 141-144.

Keys, J. R., A. M. Tarquis, and K. J. McInnes. 1997. Flow path characterization of a structured soil by dye-staining technique. p. 177. *In* Agronomy abstracts. ASA, Madison, WI.

Kung, K. J. S. 1990. Preferential flow in a sandy vadose zone: 1. Field observation. Geoderma 46: 51-58.

Lascano, R. J., J. T. Vorheis, R. L. Baumhardt, and D. R. Salisbury. 1997. Computer-controlled variable intensity rain simulator. Soil Sci. Soc. Am. J. 61:1182-1189.

Lin, H. S. and K. J. McInnes. 1995. Water flow in a clay soil beneath a tension infiltrometer. Soil Sci. 159:375-382.

Lin, H. S., K. J. McInnes, L. P. Wilding, and C. T. Hallmark. 1996. Effective porosity and flow rate with infiltration at low tensions into a well-structured subsoil. Transactions of the ASAE 39:131-135.

Lin, H. S., K. J. McInnes, L. P. Wilding, and C. T. Hallmark. 1998. Macroporosity/moisture effect on infiltration rates in vertisols and vertic intergrades. Soil Sci. 163:2-8.

Logsdon, S. D., and R. R. Allmaras. 1991. Maize and soybean root clustering as indicated by root mapping. Plant Soil 131:169-176.

Mitchell, A. R., T. R. Ellsworth, and B. D. Meek. 1995. Effect of root systems on preferential flow in swelling soil. Commun. Soil Sci. Plant Anal. 26:2655-2666.

Ott, R. L., and Longnecker, M. 2001. An Introduction to Statistical Methods and Data Analysis. Duxbury. Pacific Grove, CA.

Passioura, J. B. 1991. Soil structure and plant growth. Aust. J. Soil Res. 29:717-728.

Passioura, J. B. 1996. Simulation models: Science, snake oil, education or engineering. Agron. J. 88: 690-694.

Pellerin, S. and L. Pagès. 1996. Evaluation in field conditions of a three-dimensional architectural model of the maize root system: Comparison of simulated and observed horizontal root maps. Plant Soil 178:101-112.

Shaffer, K. A., D. D. Fritton, and D. E. Baker. 1979. Drainage water sampling in a wet, dual-pore soil system. J. Environ. Qual. 8:241-246.

Smucker, A. J. M., S. L. McBurney, and A. K. Srivastava. 1982. Quantitative separation of roots from compacted soil profiles by the hydropneumatic elutriation system. Agron. J. 74:500-503.

Soil Survey Staff. 1993. Soil survey manual. US Dept. Agri. Handbook No. 18. U.S. Government Printing Office, Washington, DC.

Tardieu, F. 1987. Etat structural, enracinement et alimentation hydrique du maïs. III. Disponibilité des réserves en eau du sol. Agronomie 7:279-288.

Tardieu, F. 1988a. Analysis of the spatial variability of maize root density. I. Effect of wheel compaction on the spatial arrangement of roots. Plant Soil 107:259-266.

Tardieu, F. 1988b. Analysis of the spatial variability of maize root density. II. Distance between roots. Plant Soil 107:267-272.

Tardieu, F., L. Bruckler, and F. Lafolie. 1992. Root clumping may affect the root water potential and the resistance to soil-root water transport. Plant Soil 140:291-301.

Tardieu, F., and H. Manichon. 1986. Caractérisation en tant que capteur d'eau de l'enracinement du maïs en parcelle cultivée. II. Une méthode d'étude de la répartition verticale et horizontale des racines. Agronomie 6:415-425.

Taylor, H. M., and H. R. Gardner. 1963. Penetration of cotton seedling taproots as influenced by bulk density, moisture, and strength of soil. Soil. Sci. 96:153-156.

Taylor, H. M., and L. F. Ratliff. 1969. Root elongation rates of cotton and peanuts as a function of soil strength and soil water content. Soil Sci. 108:113-119.

van Ommen, H. C., L. W. Decker, R. Dijksma, J. Hulshof, and W. H. van der Molen. 1988. A new technique for evaluating the presence of preferential flow paths in nonstructured soils. Soil Sci. Soc. Am. J. 52:1192-1194.

Vogel, H. J. 1997. Morphological determination of pore connectivity as a function of pore size using serial sections. Europ. J. Soil Sci. 48:365-377.

Vogel, H. J., and A. Kretzschmar. 1996. Topological characterization of pore space in soil - sample preparation and digital image-processing. Geoderma 73:23-38.

Wang, J., J. D. Hesketh, and J. T. Woolley. 1986. Preexisting channels and soybean rooting patterns. Soil Sci. 141:432-437.

Warrick, A. W., D. E. Meyers, and D. R. Nielsen. 1986. Geostatistical methods applied to soil science. p. 53-82. *In* A. Klute (ed.) Methods of soil analysis. Part 1. 2nd ed. Agron. Monogr. 9. ASA and SSSA, Madison, WI.

Watson, K. W., and R. J. Luxmoore. 1986. Estimating macroporosity in a forest watershed by use of a tension infiltrometer. Soil Sci. Soc. Am. J. 50:578-582.

Whiteley, G. M., and A. R. Dexter. 1983. Behaviour of roots in cracks between soil peds. Plant Soil 74:153-162.

APPENDIX

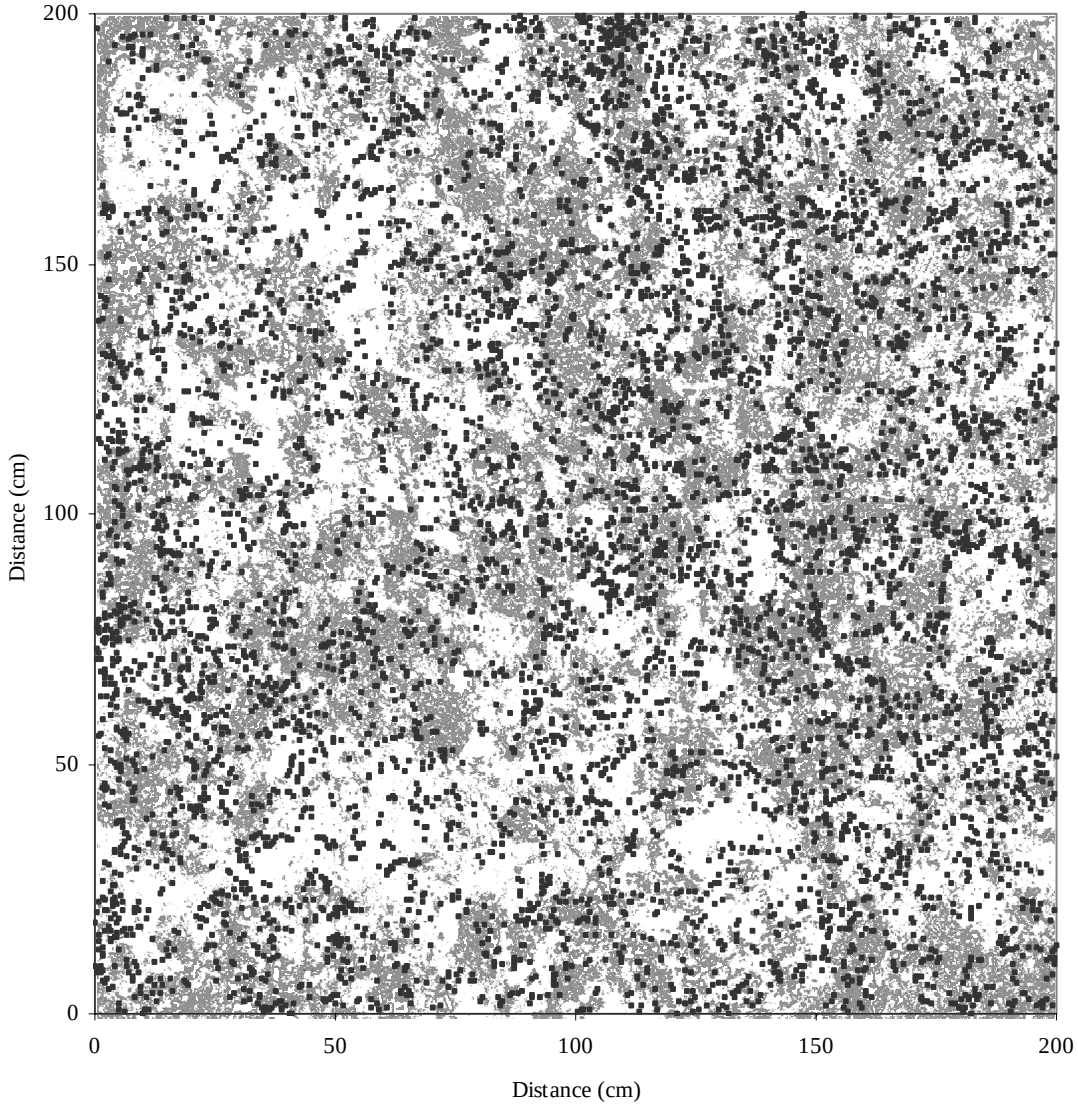

First plot at a depth of 25 cm. Roots <1 mm.

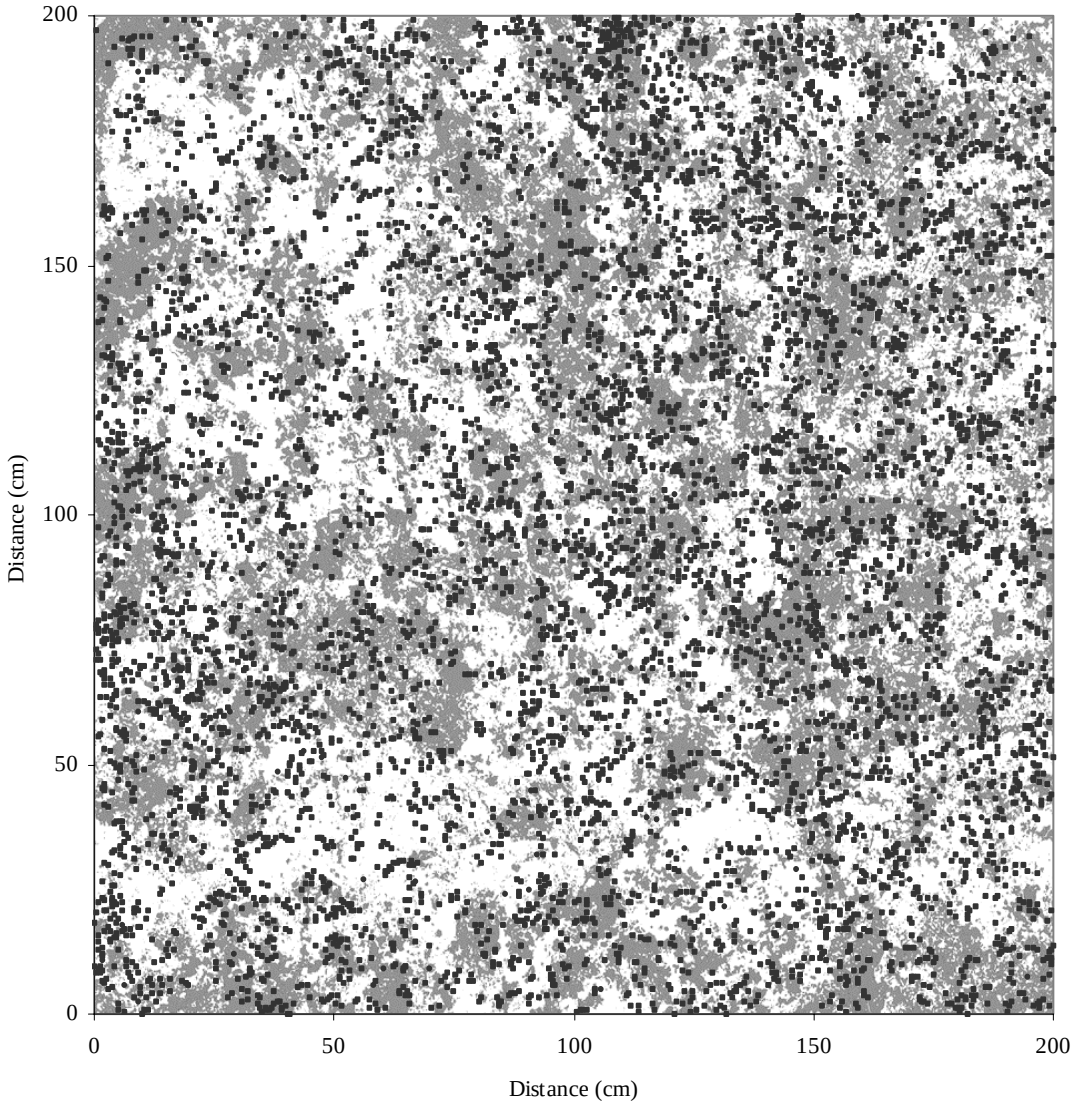

First plot at a depth of 25 cm. Roots 1-2 mm.

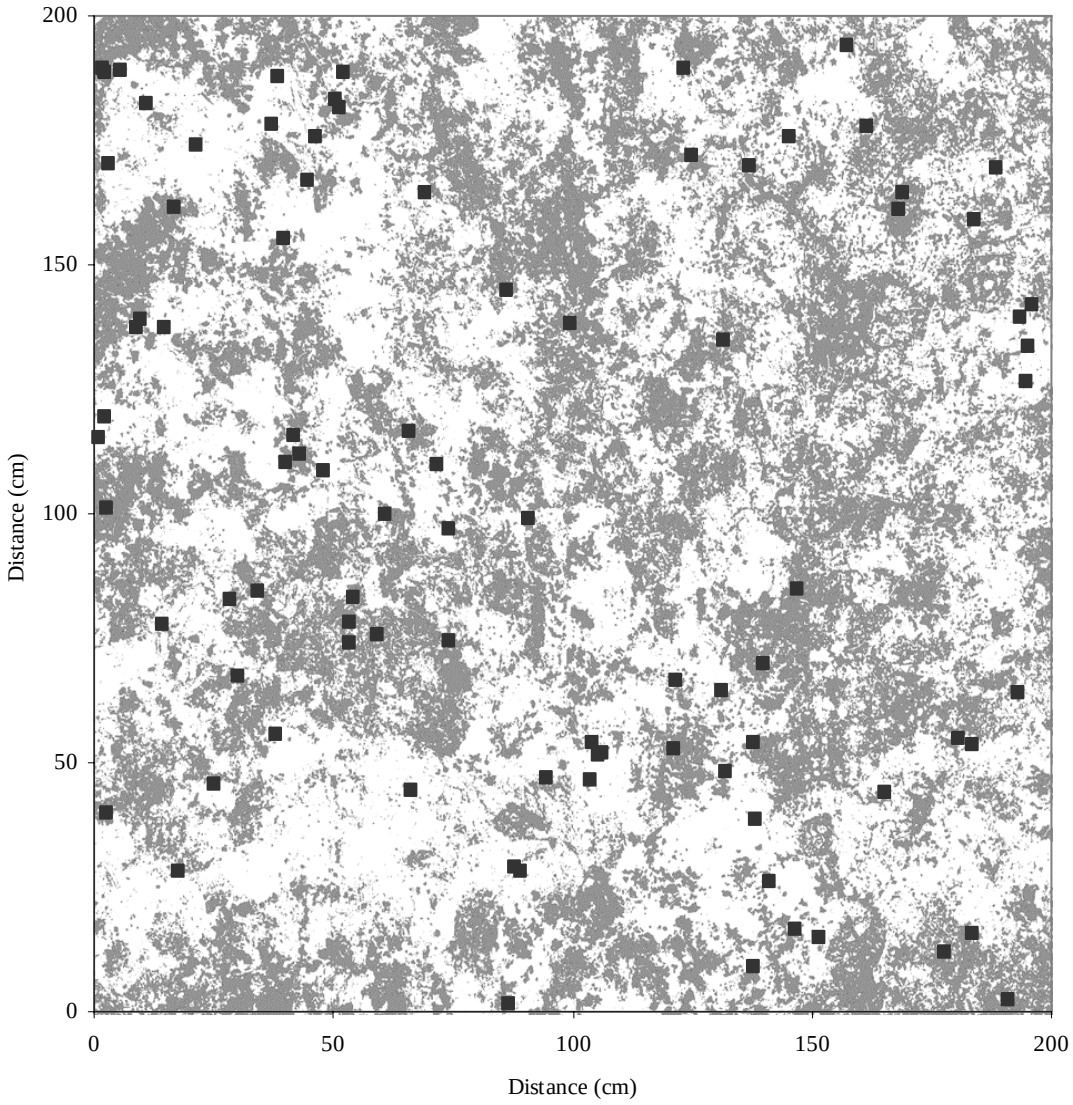

First plot at a depth of 25 cm. Roots 2-5 mm.

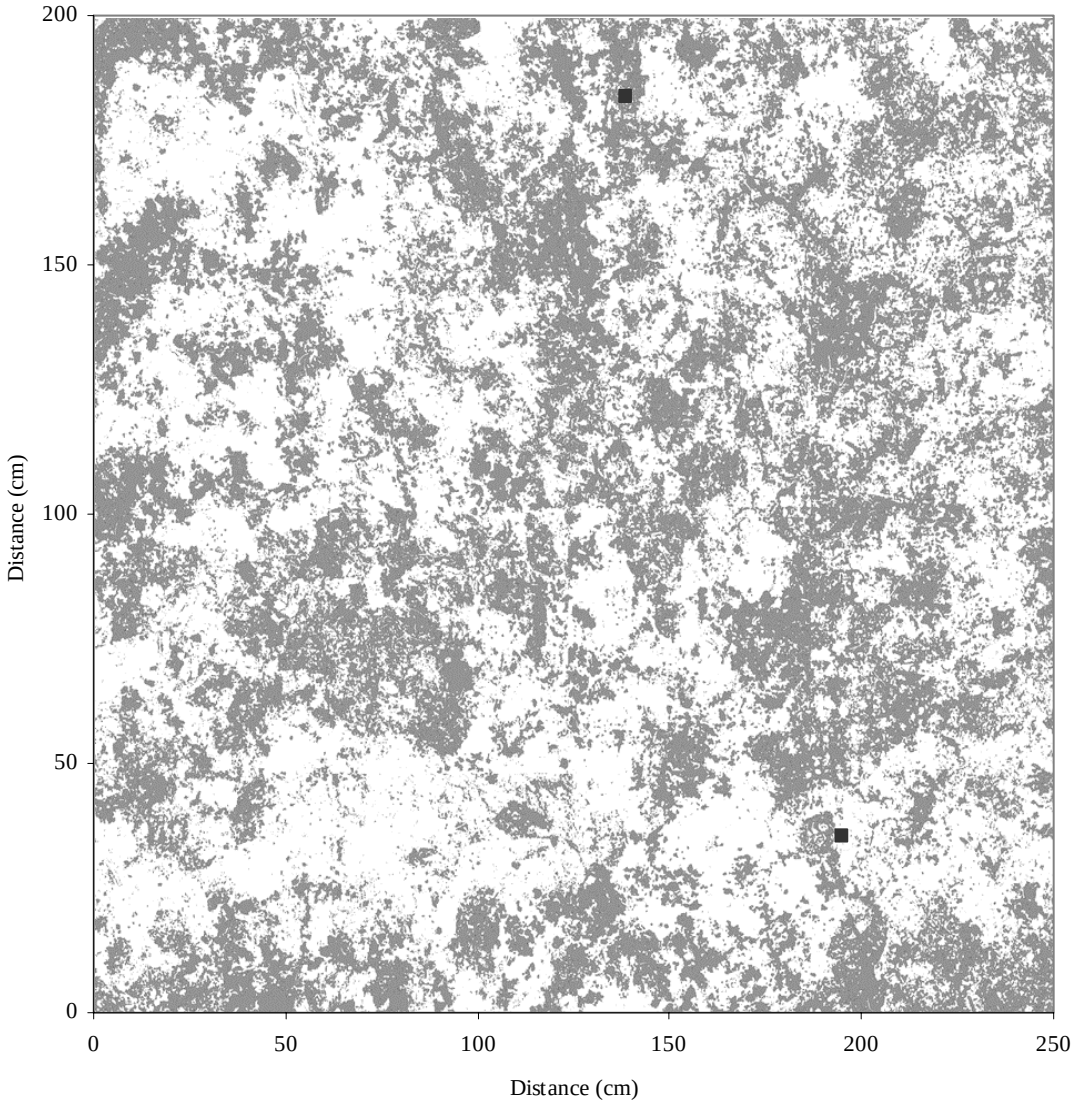

First plot at a depth of 25 cm. Roots >5 mm.

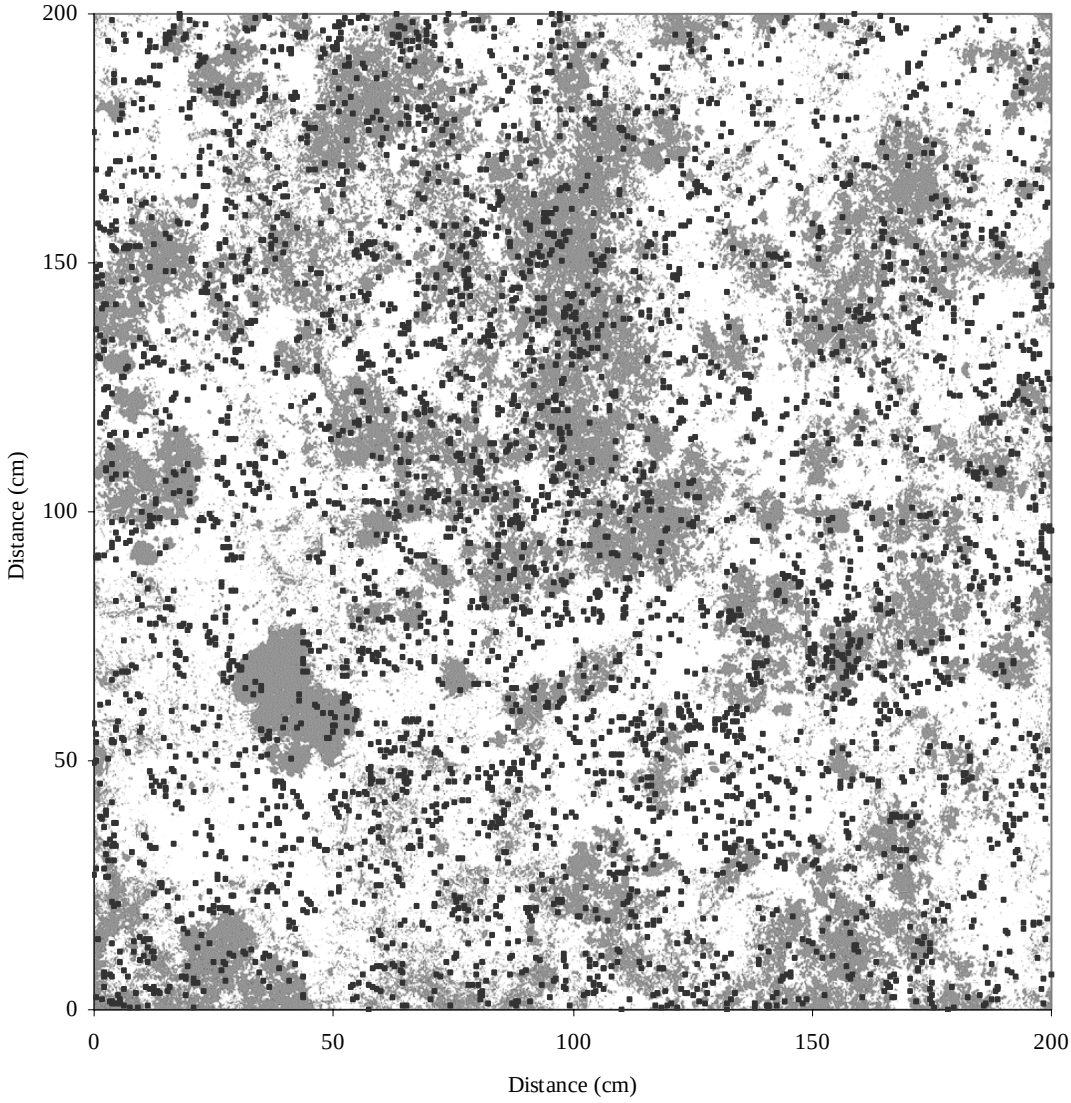

First plot at a depth of 45 cm. Roots <1 mm.

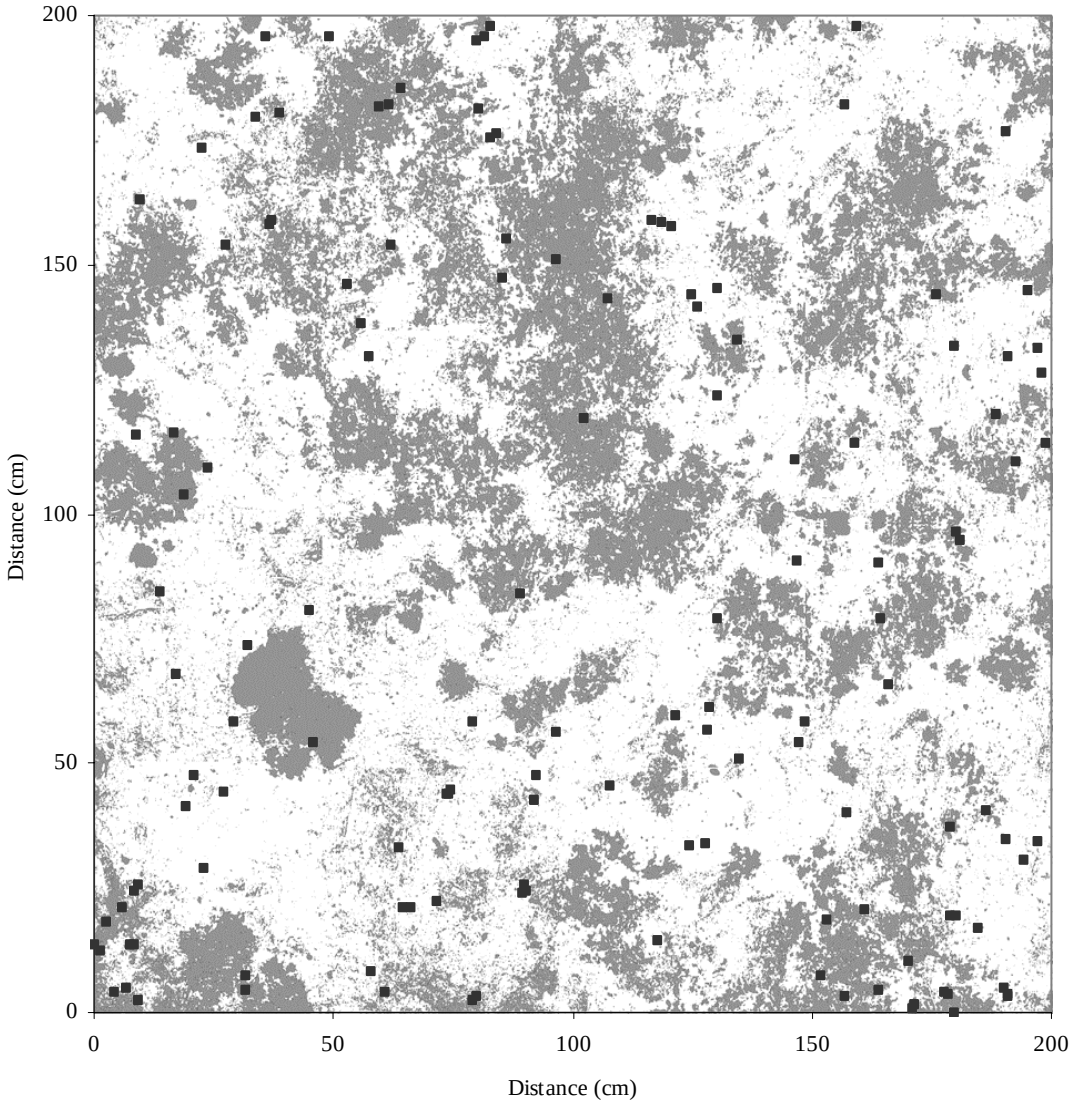

First plot at a depth of 45 cm. Roots 1-2 mm.

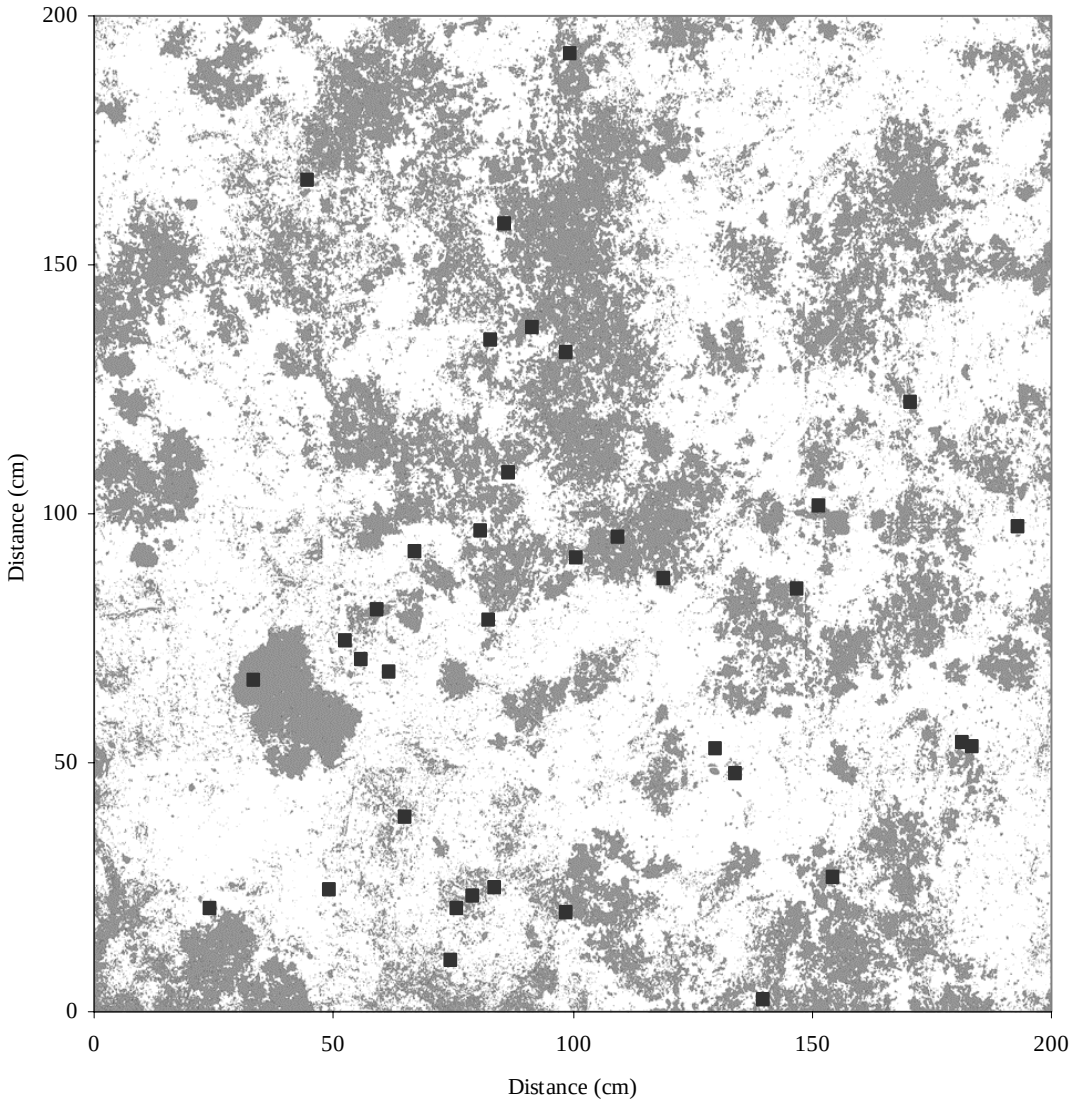

First plot at a depth of 45 cm. Roots 2-5 mm.

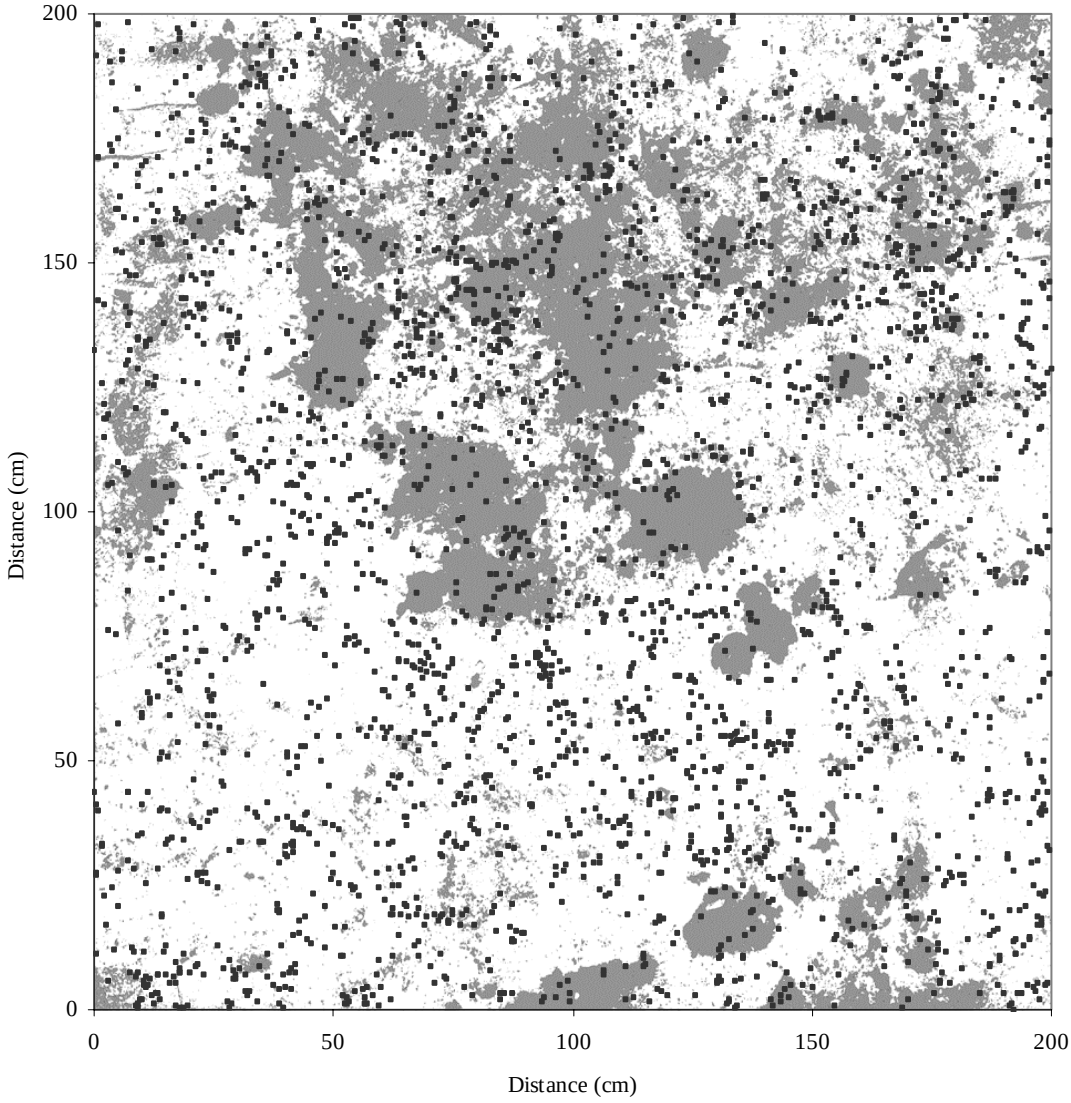

First plot at depth of 75 cm. Roots <1 mm.

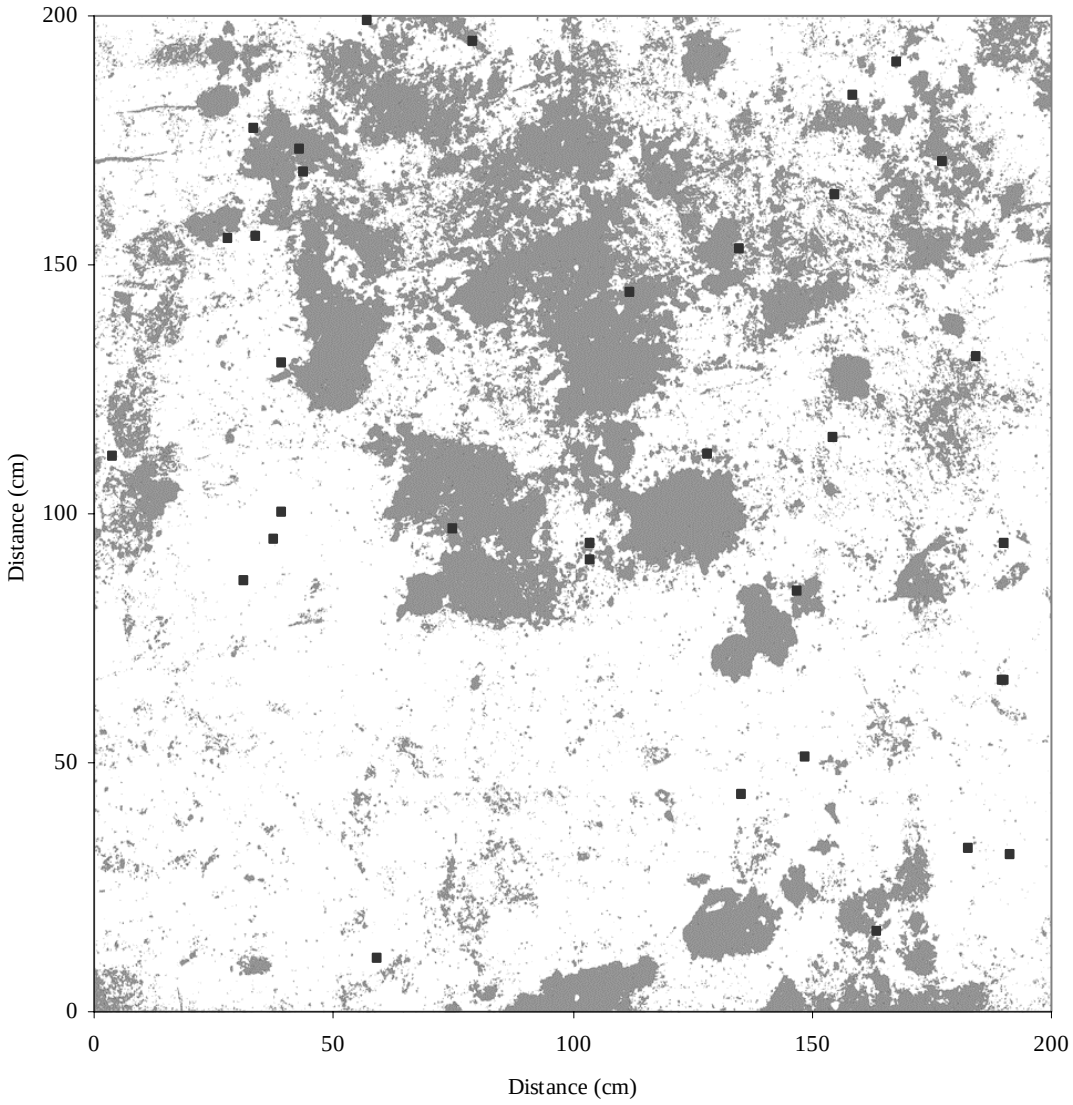

First plot at depth of 75 cm. Roots 1-2 mm.

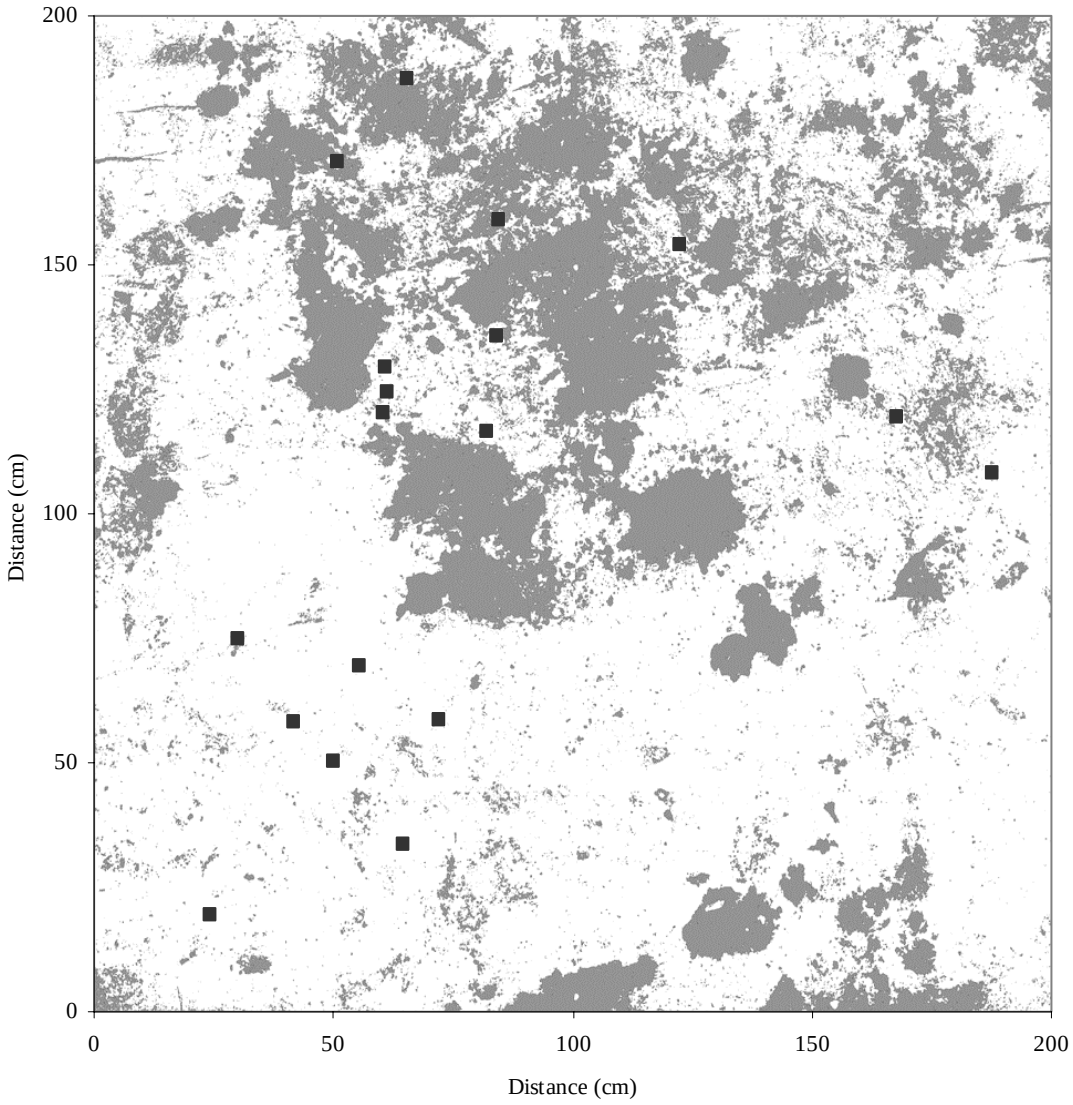

First plot at a depth of 75 cm. Roots 2-5 mm.

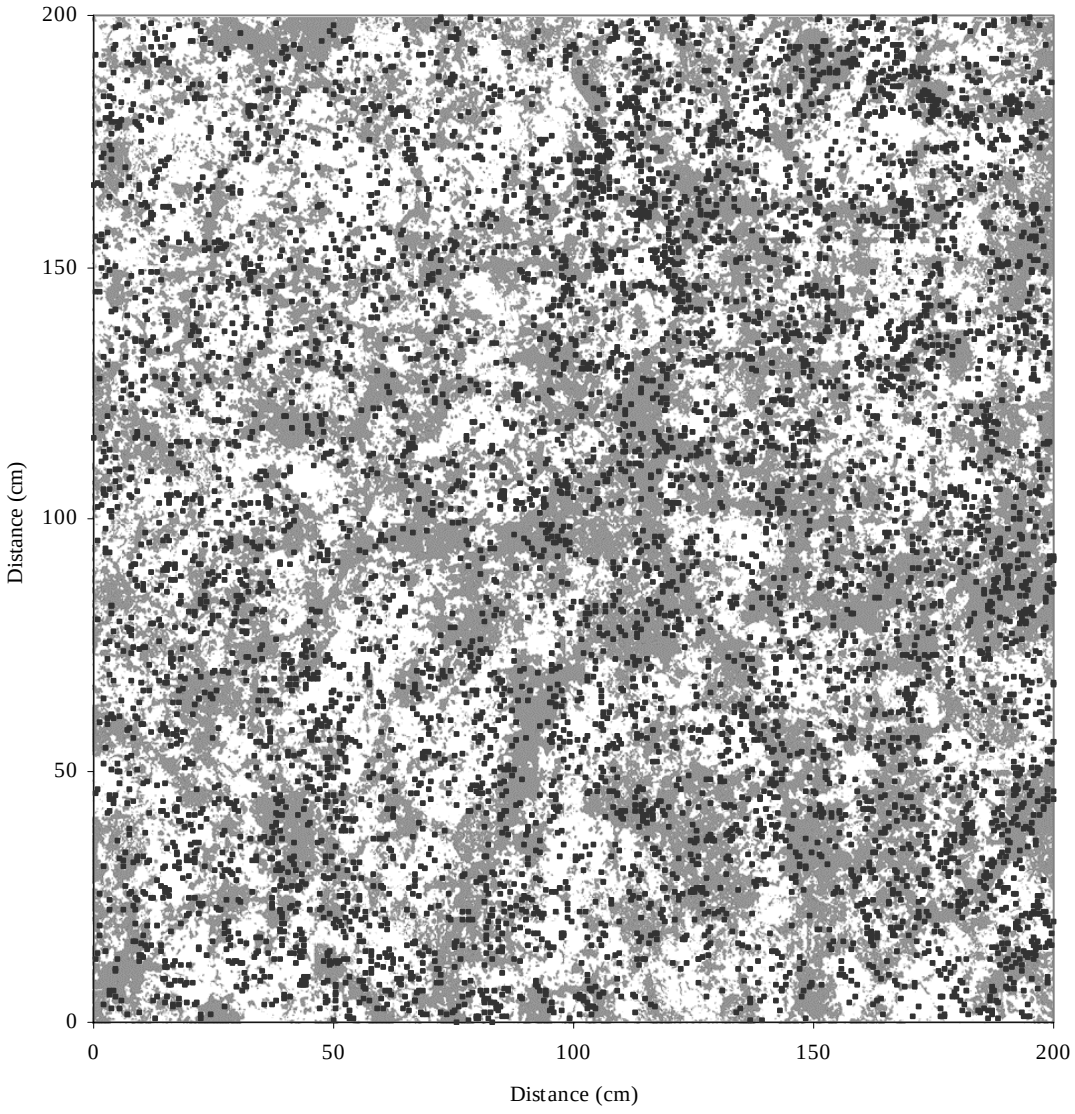

Second plot at depth of 25 cm. Roots <1 mm

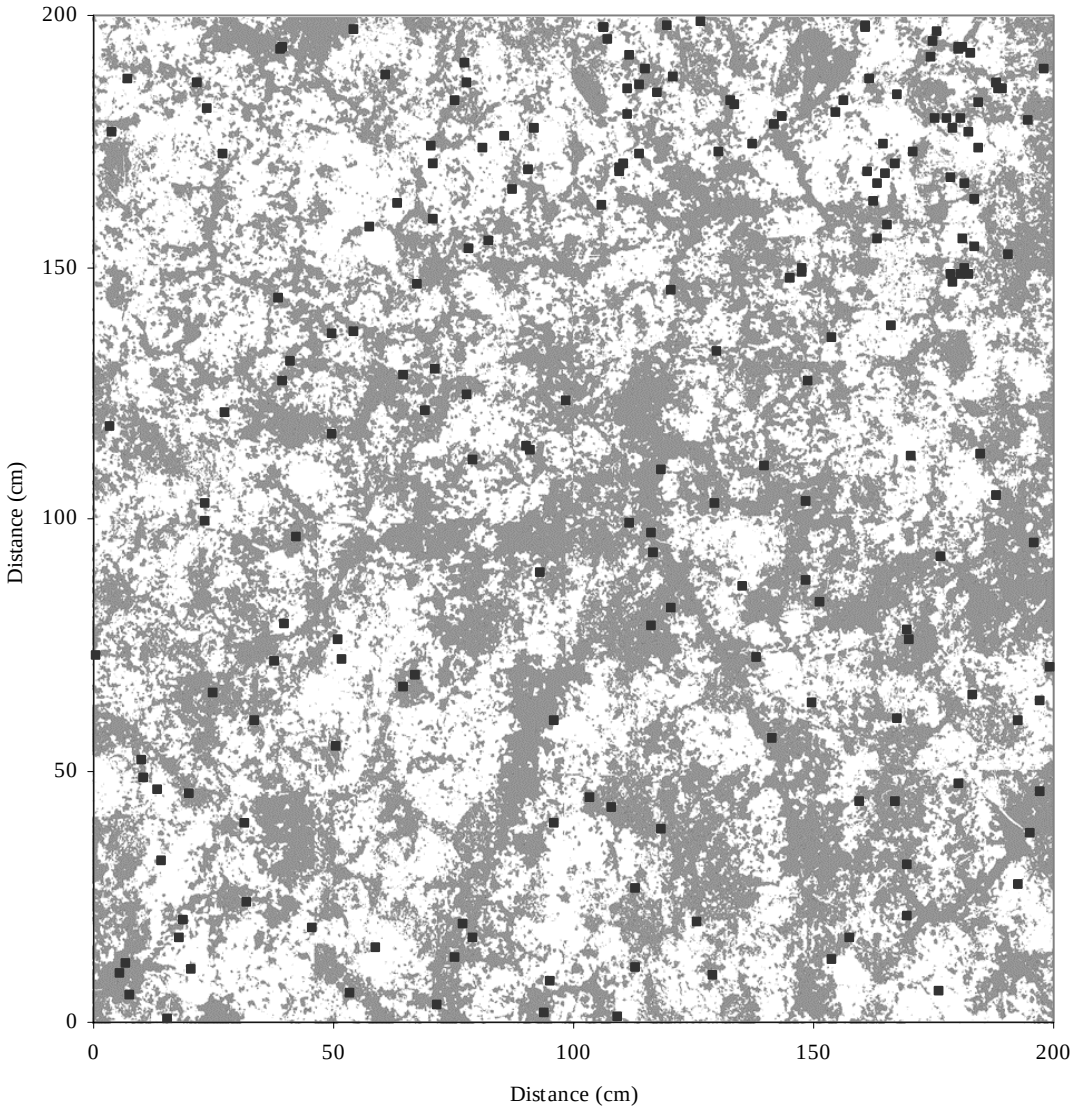

Second plot at a depth of 25 cm. Roots 1-2 mm

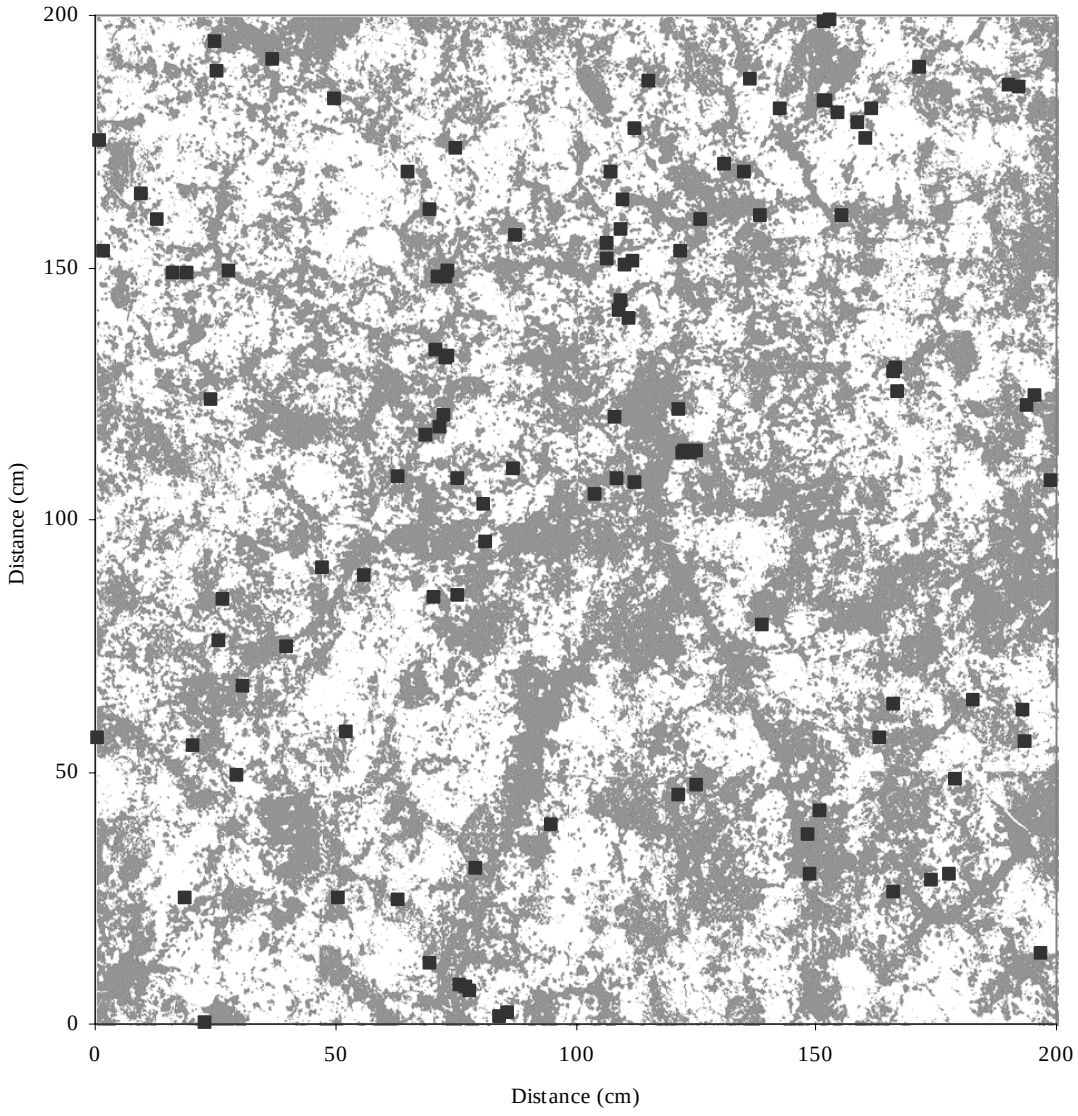

Second plot at a depth of 25 cm. Roots 2-5 mm

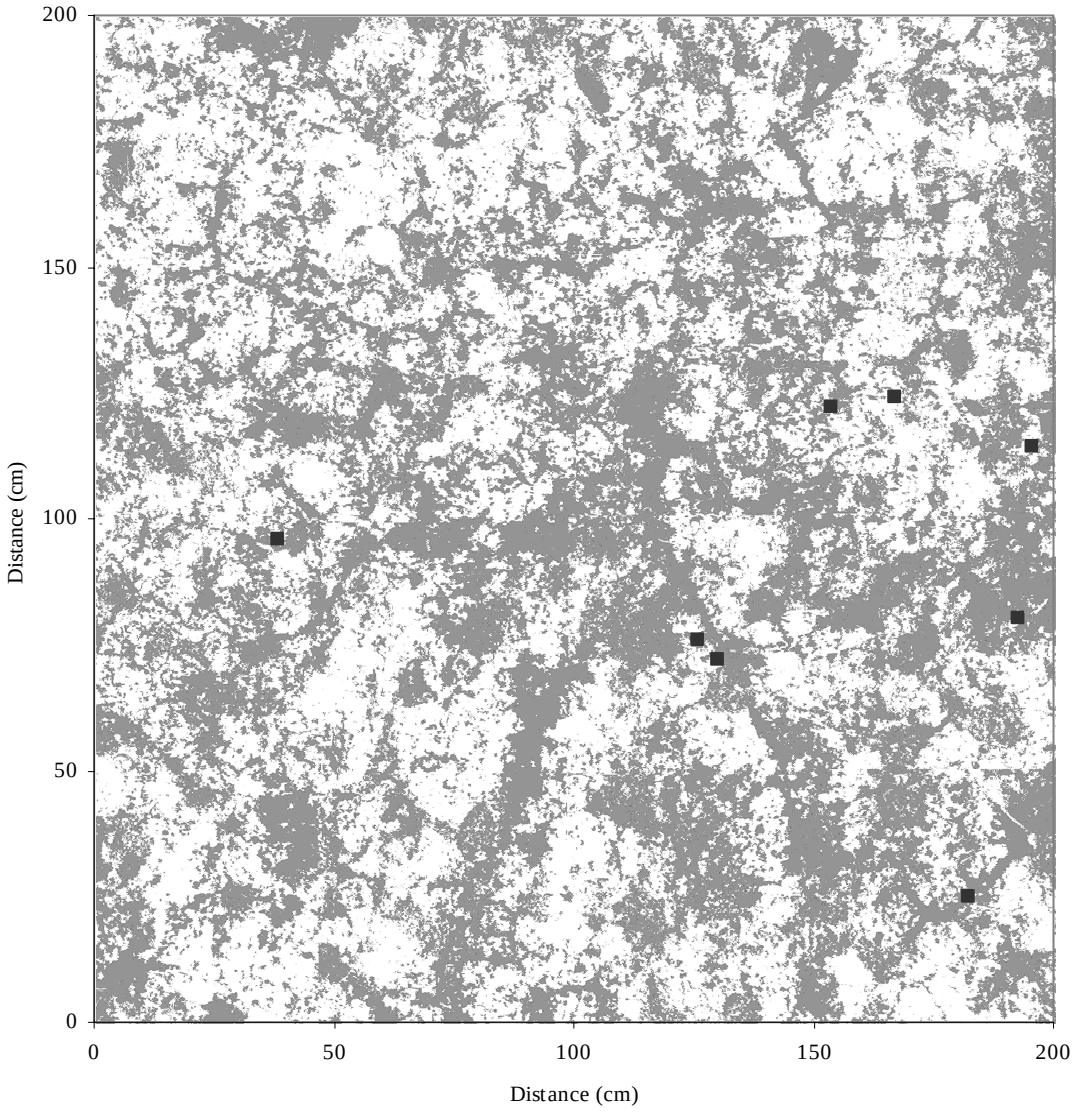

Second plot at a depth of 25 cm. Roots >5 mm

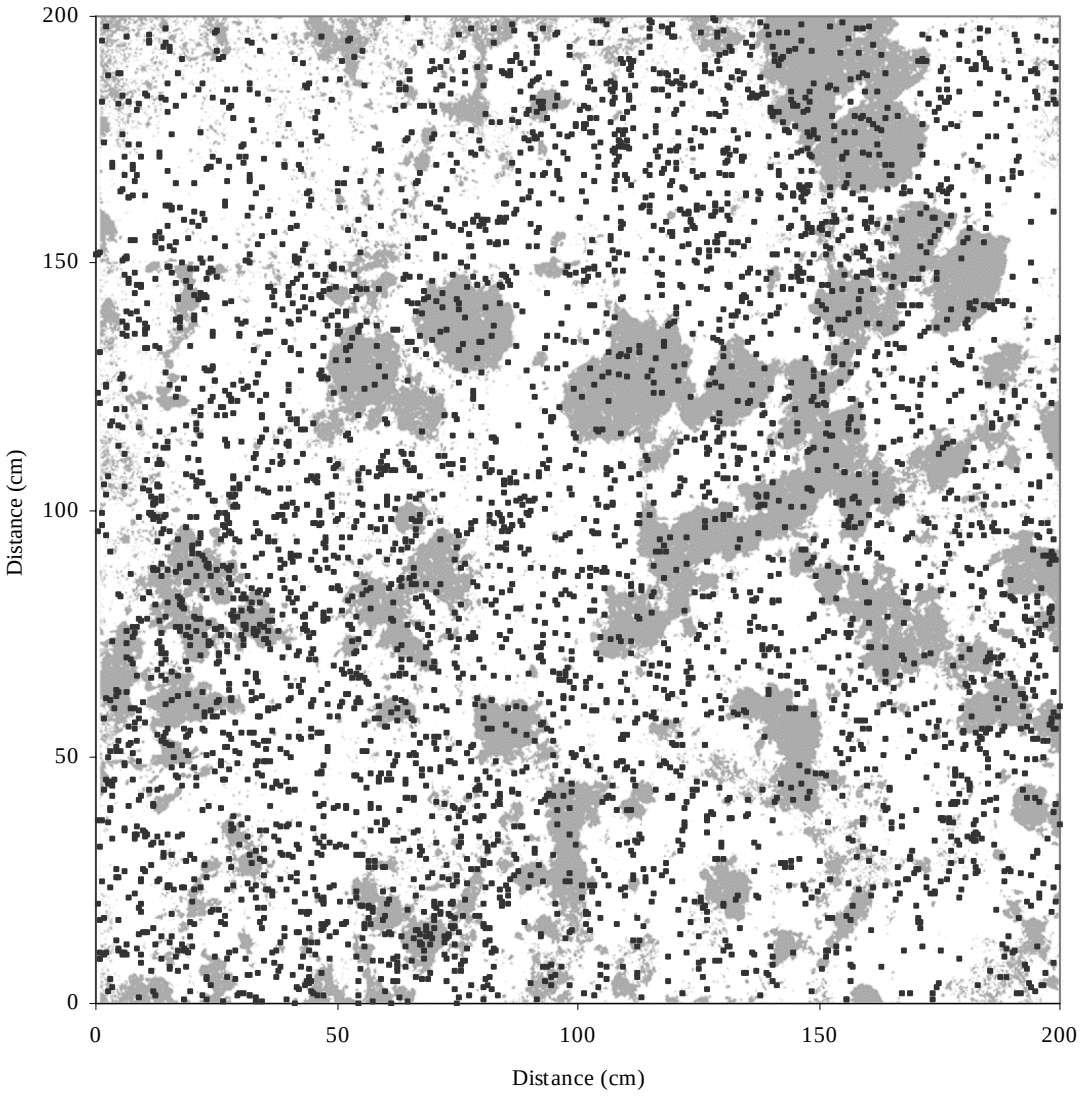

Second plot at a depth of 45 cm. Roots <1 mm

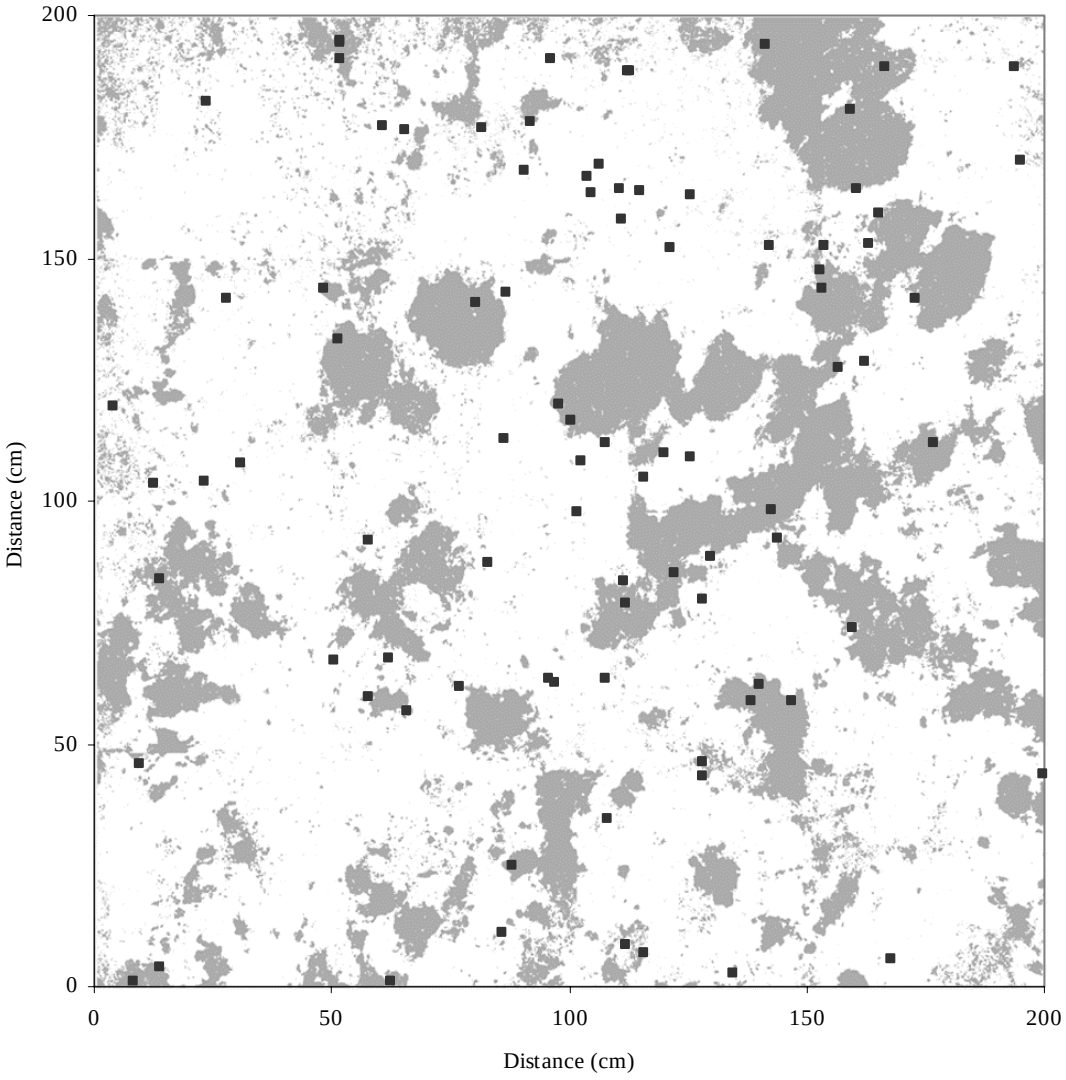

Second plot at a depth of 45 cm. Roots 1-2 mm

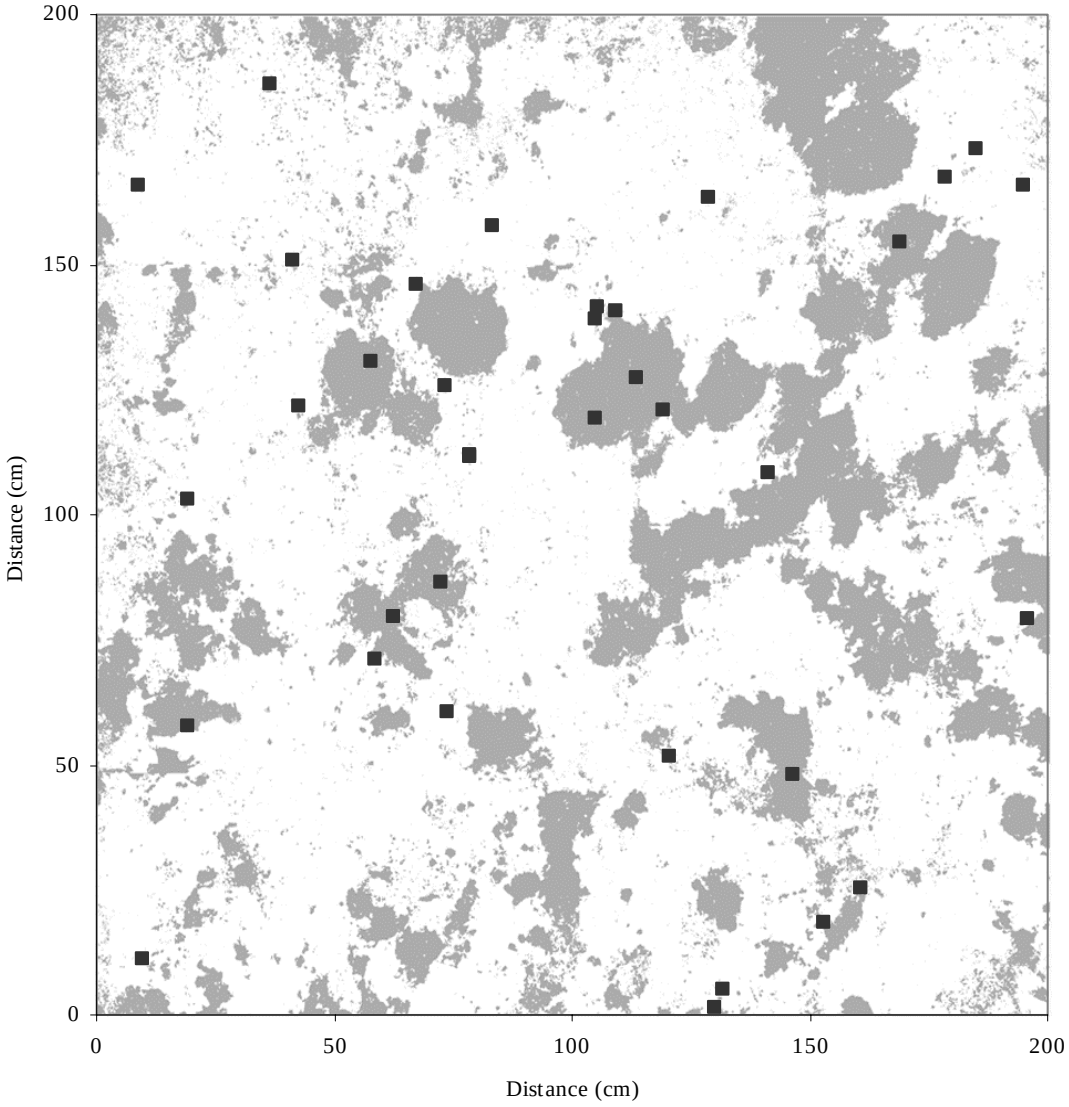

Second plot at a depth of 45 cm. Roots 2-5 mm

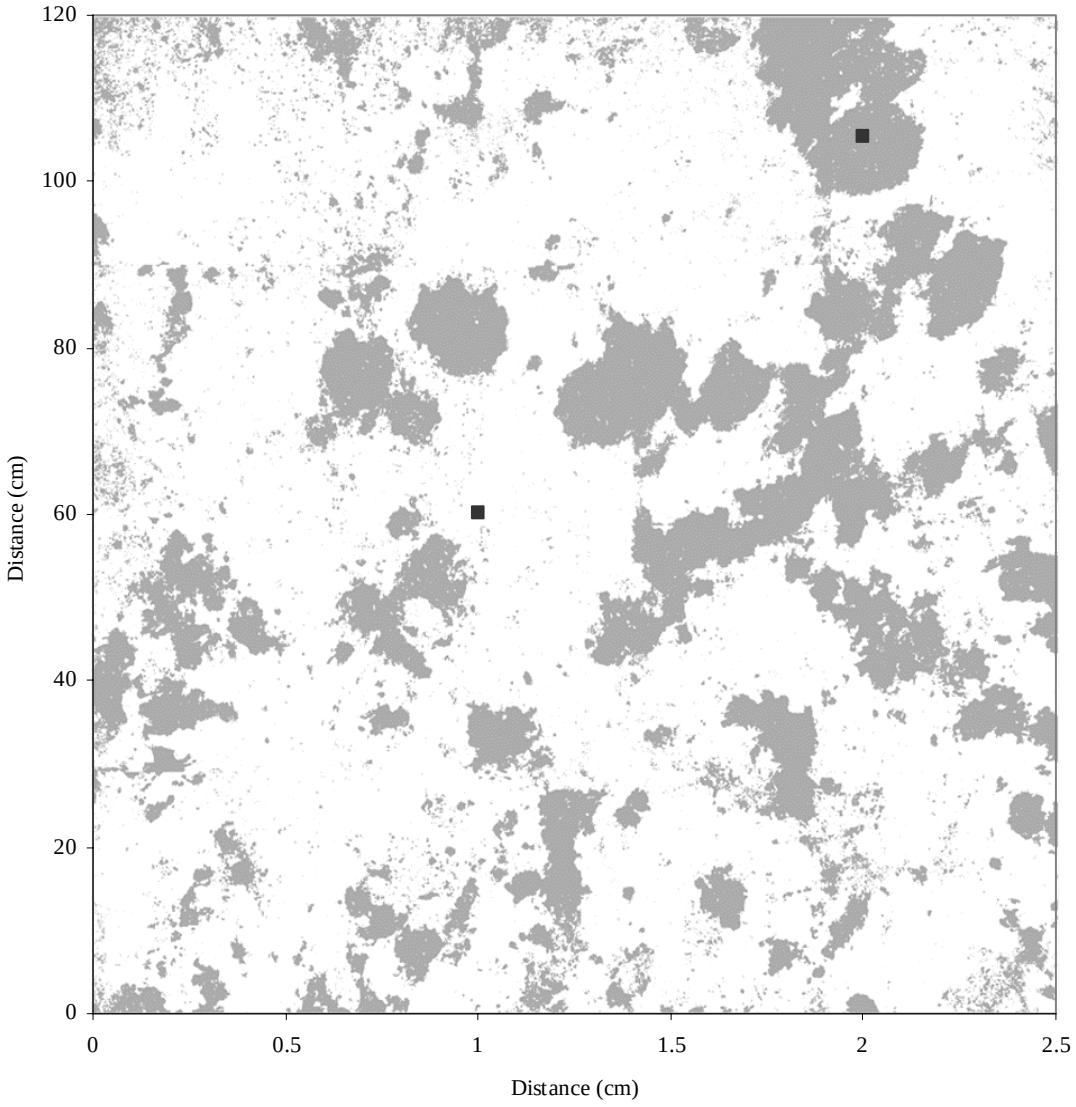

Second plot at a depth of 45 cm. Roots >5 mm

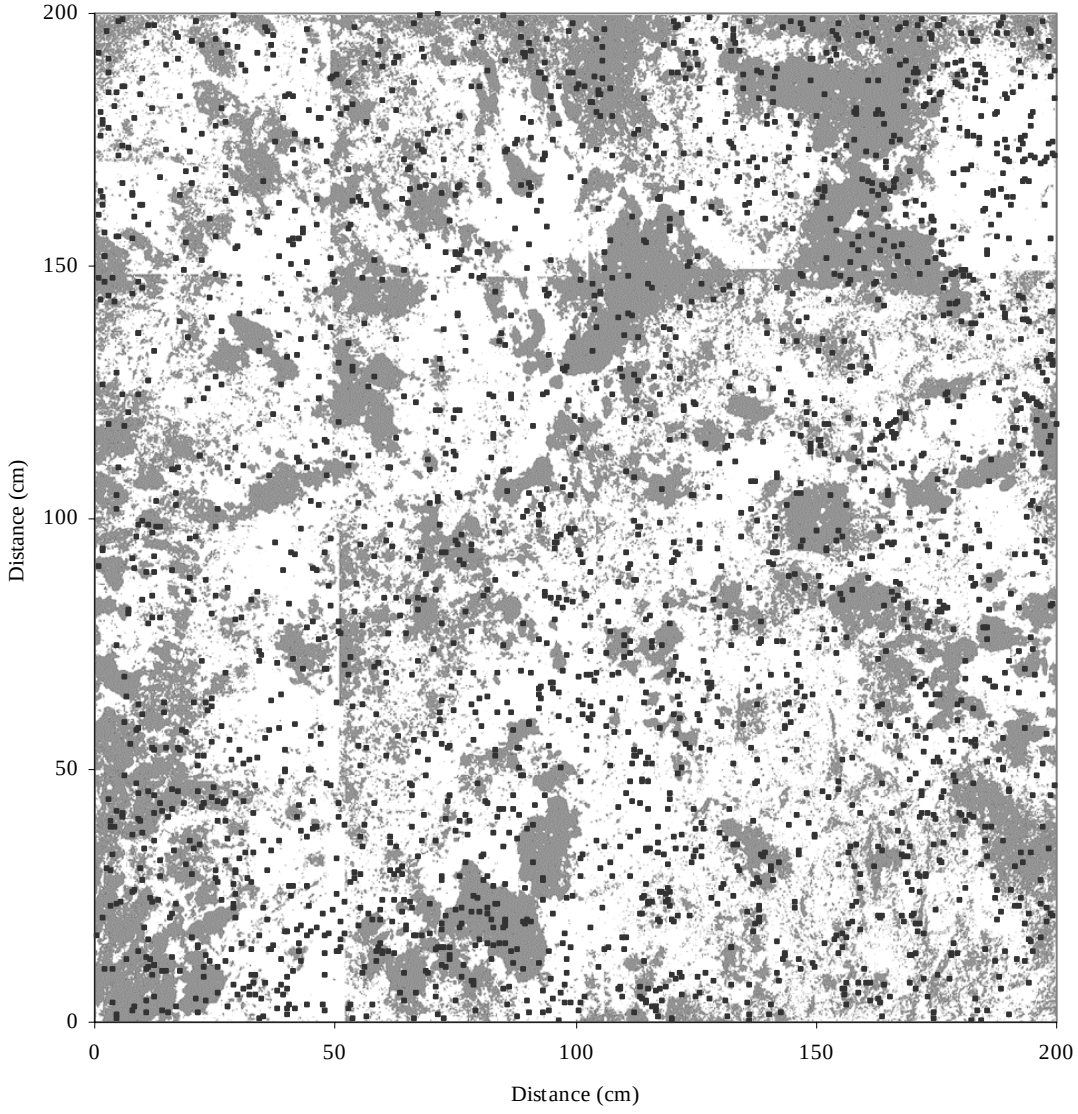

Second plot at a depth of 75 cm. Roots <1 mm

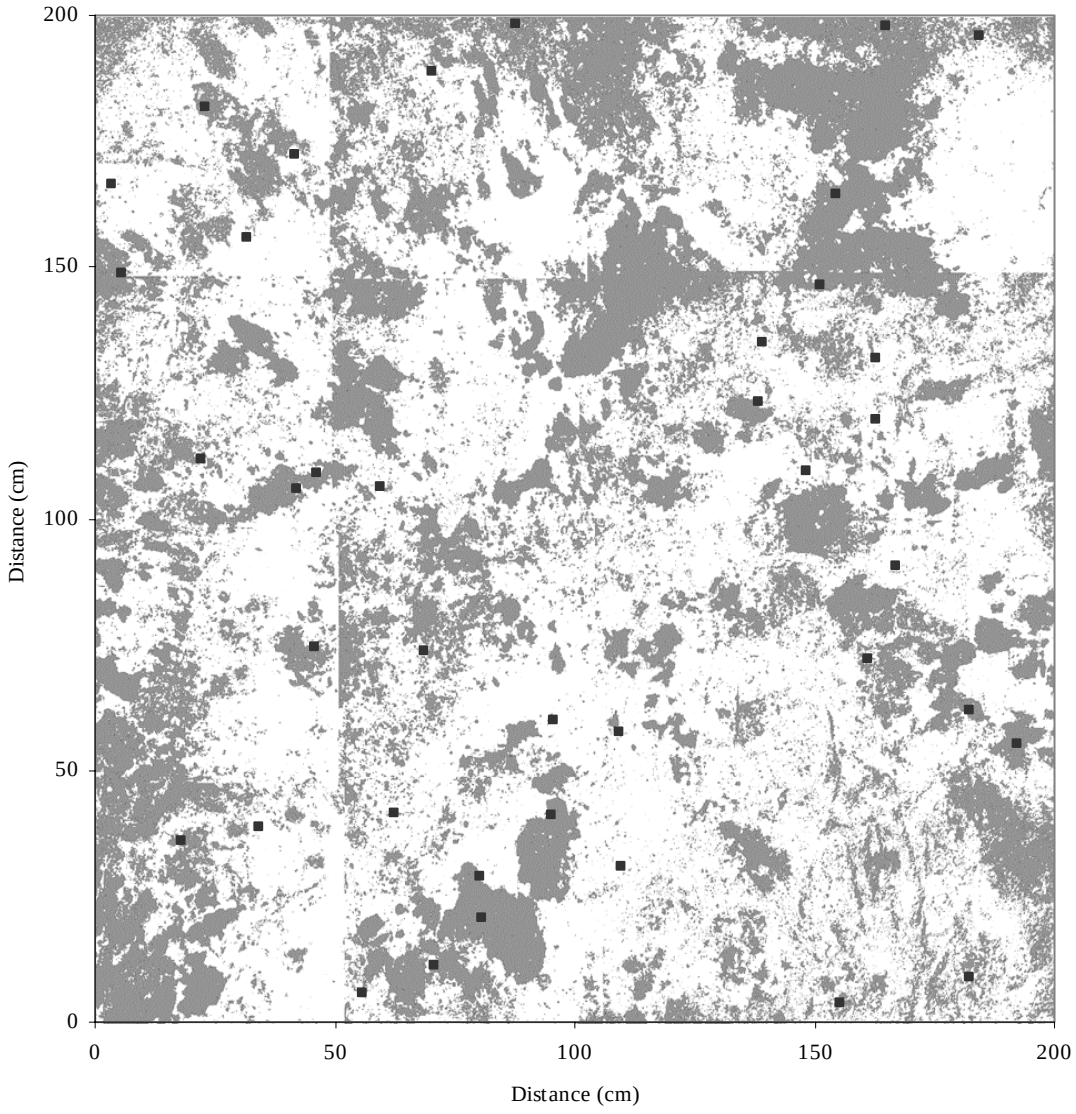

Second plot at a depth of 75 cm. Roots 1-2 mm

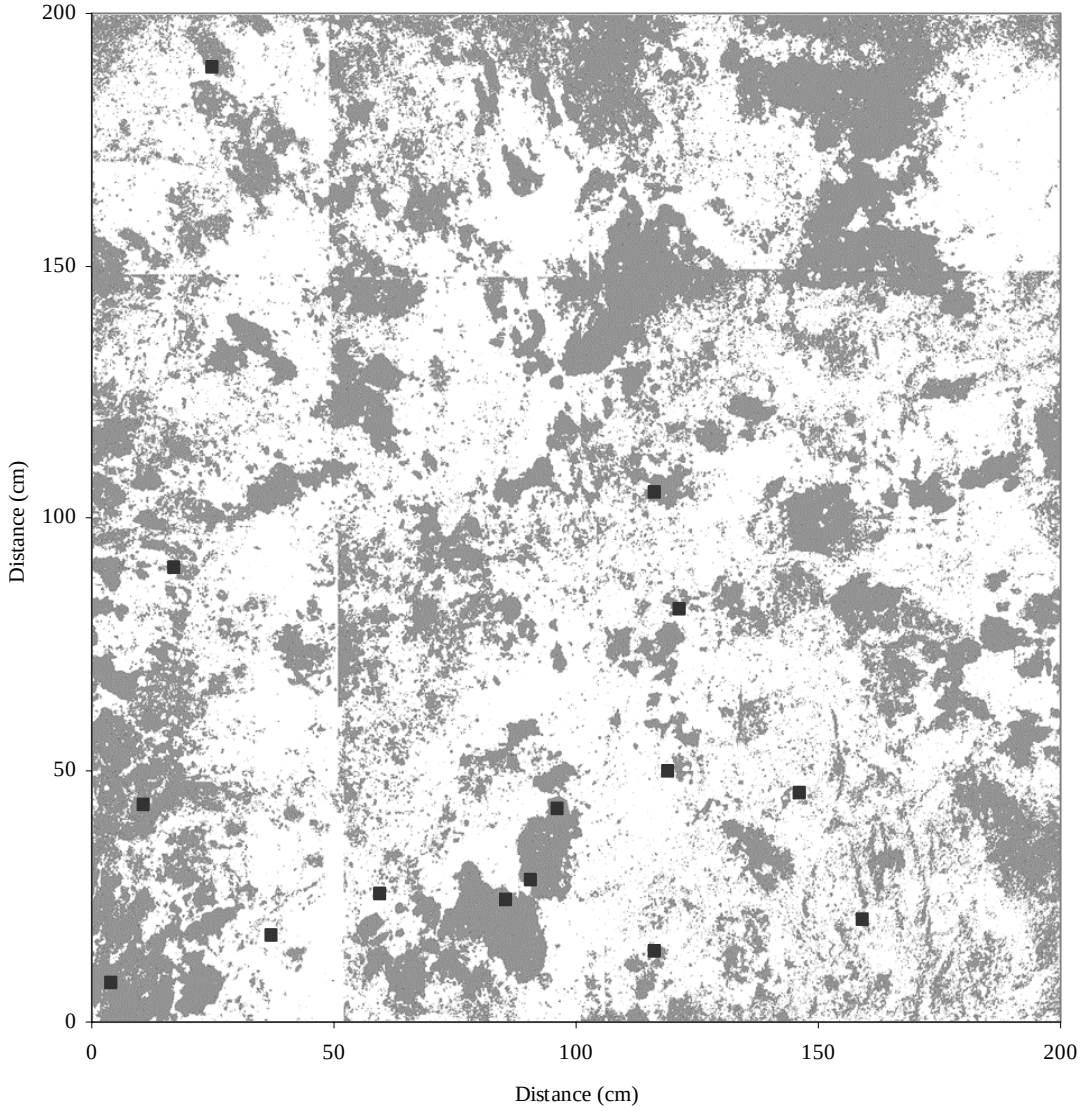

Second plot at a depth of 75 cm. Roots 2-5 mm

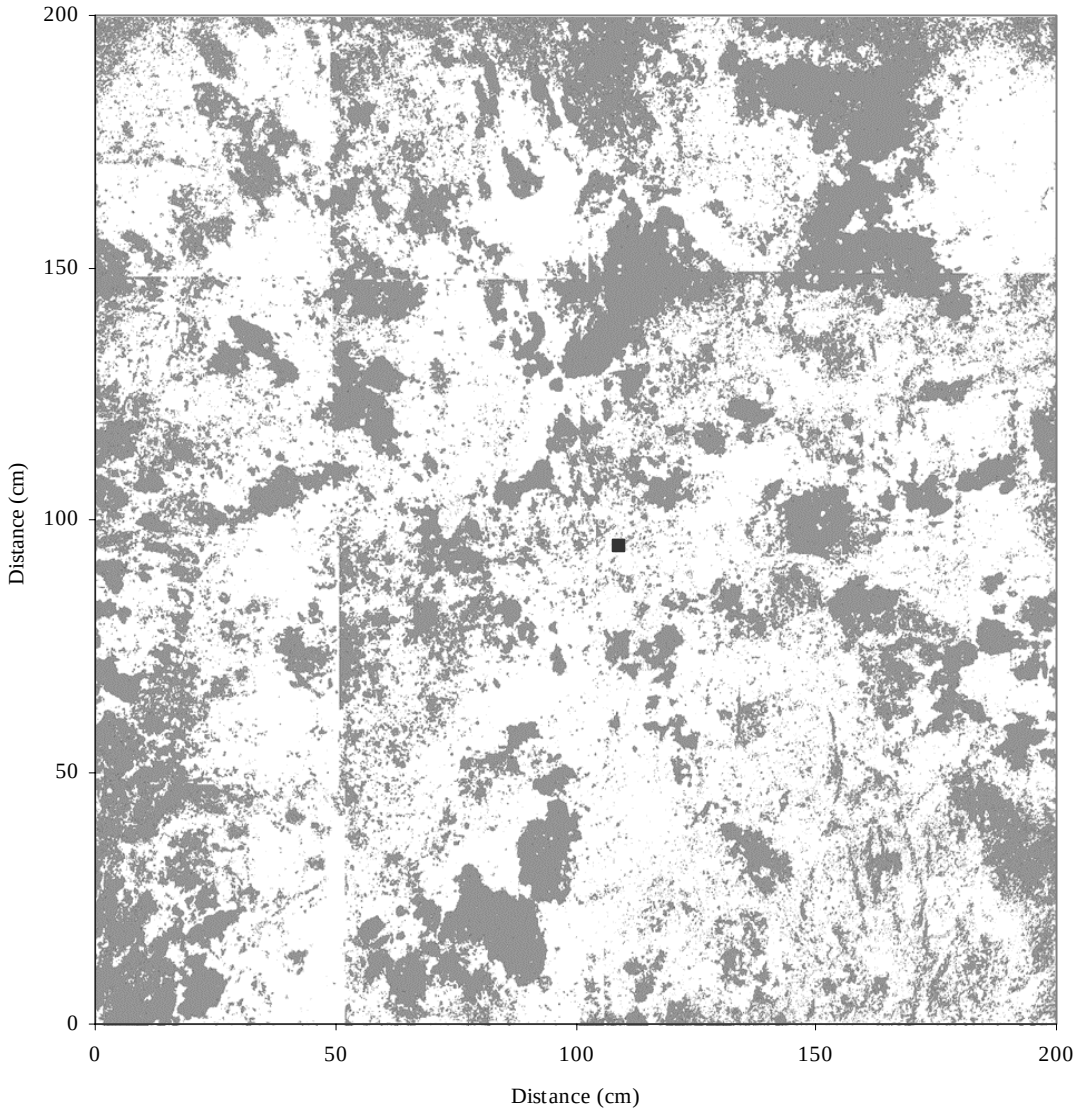

Second plot at a depth of 75 cm. Roots >5 mm

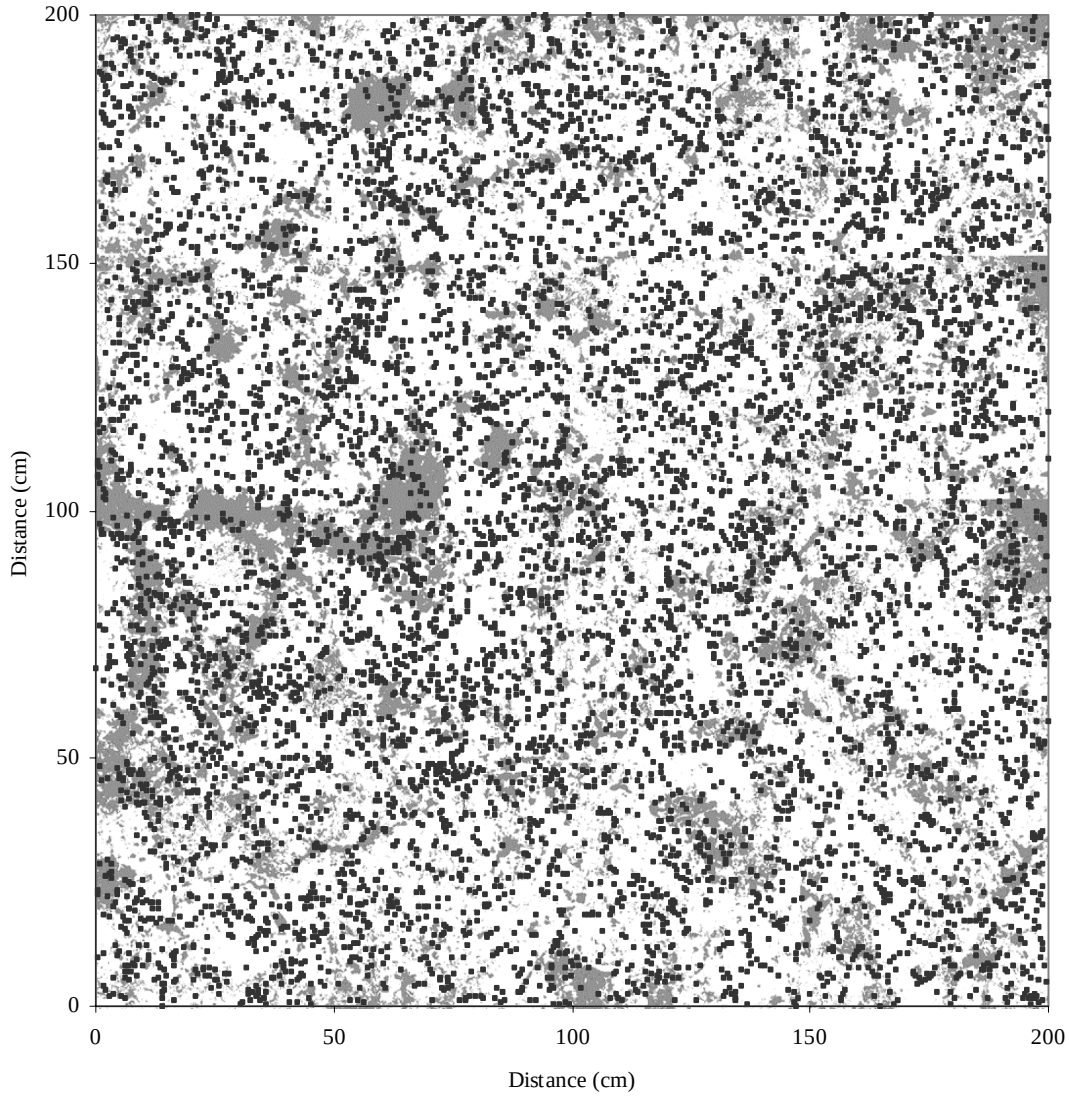

Third plot at a depth of 25 cm. Roots <1 mm

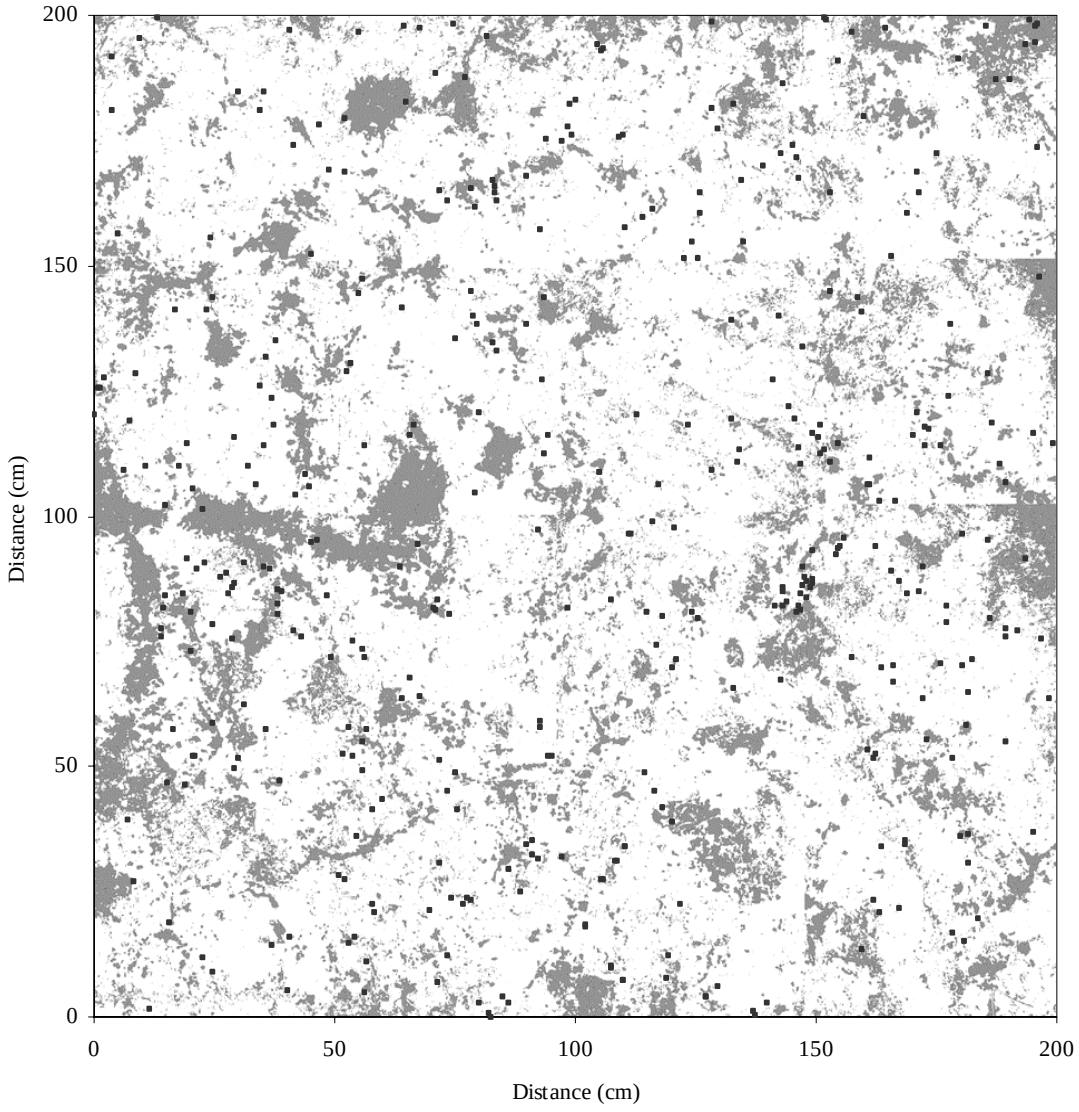

Third plot at a depth of 25 cm. Roots 1-2 mm

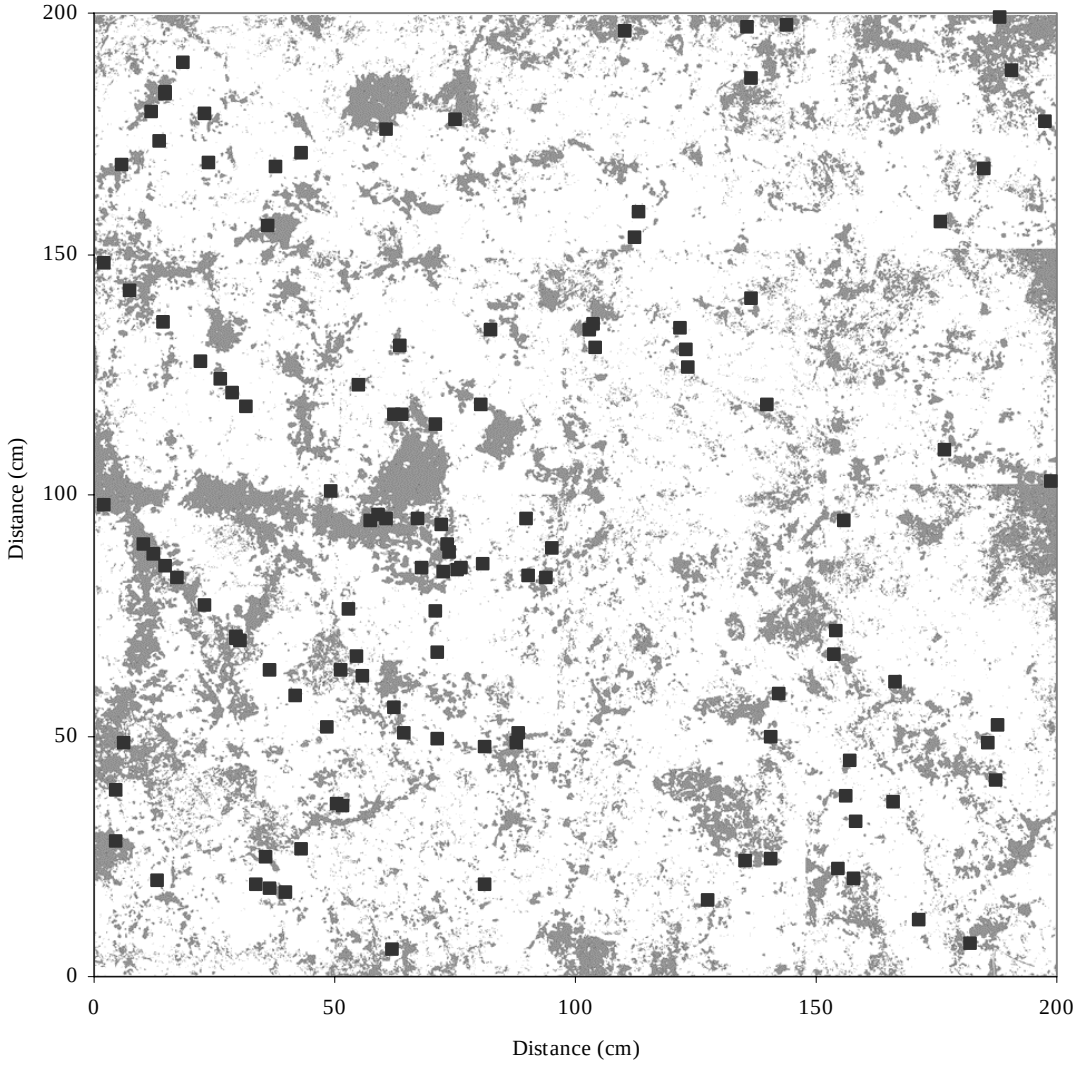

Third plot at a depth of 25 cm. Roots 2-5 mm

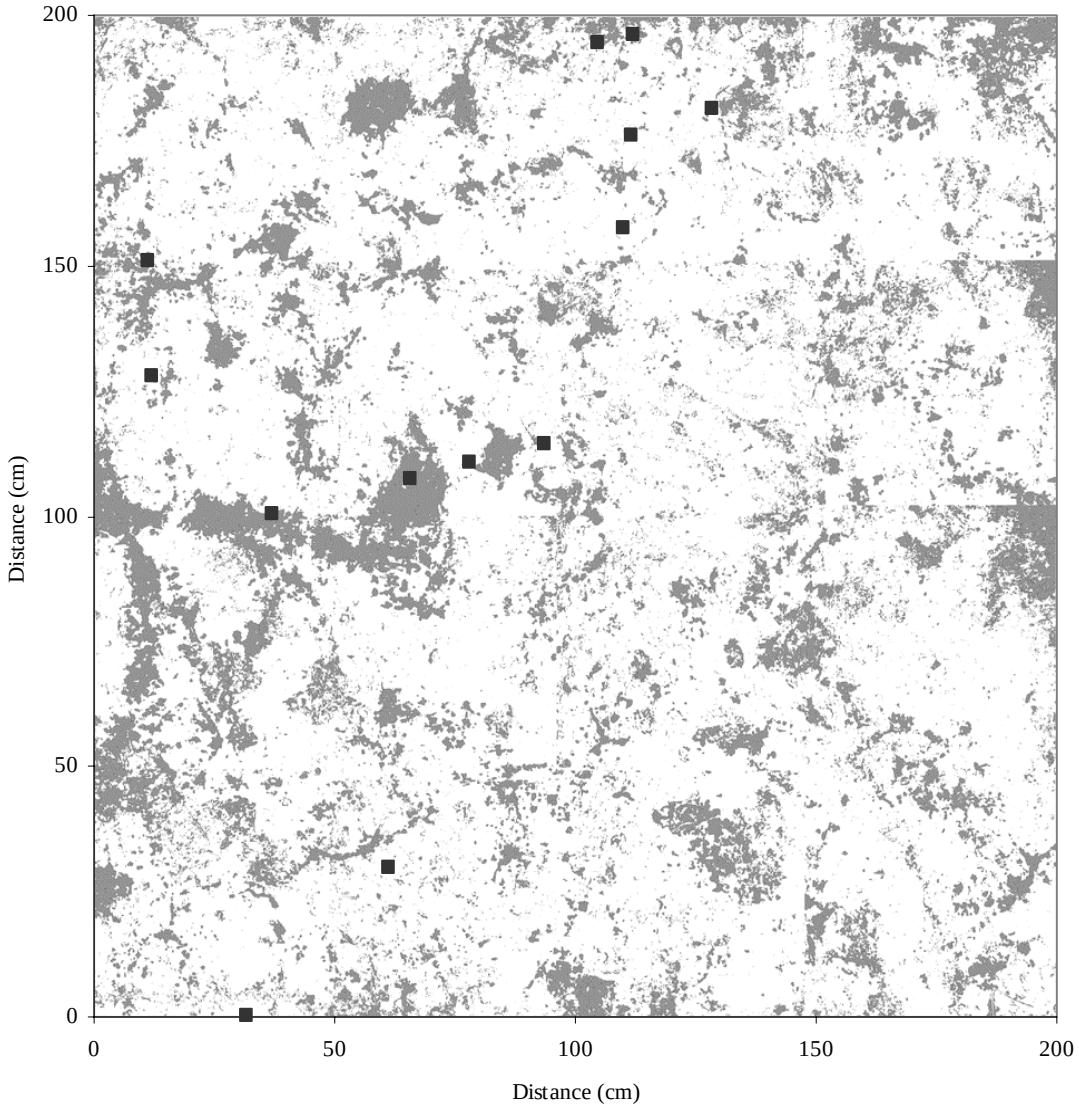

Third plot at a depth of 25 cm. Roots >5 mm

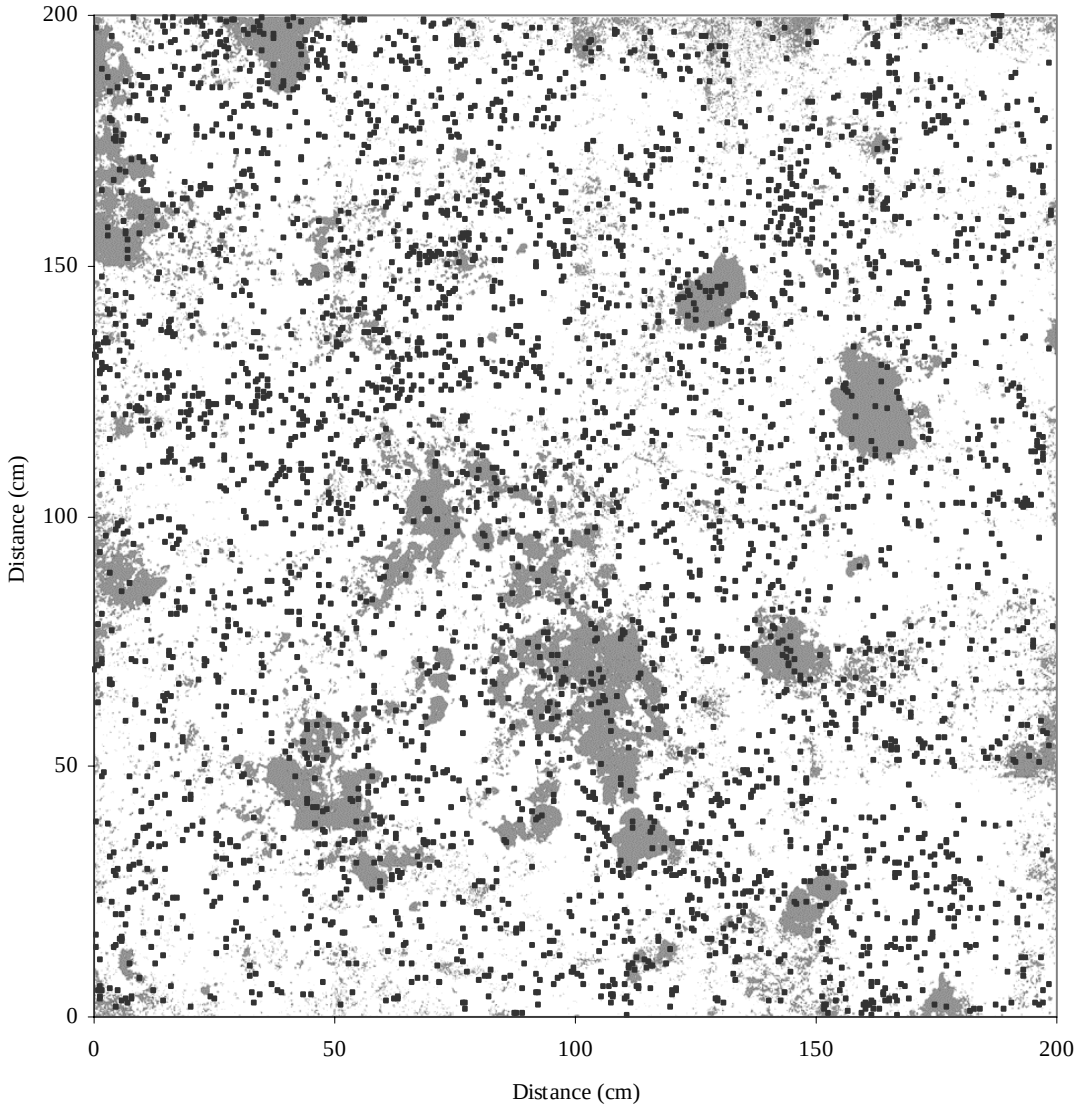

Third plot at a depth of 45 cm. Roots <1 mm

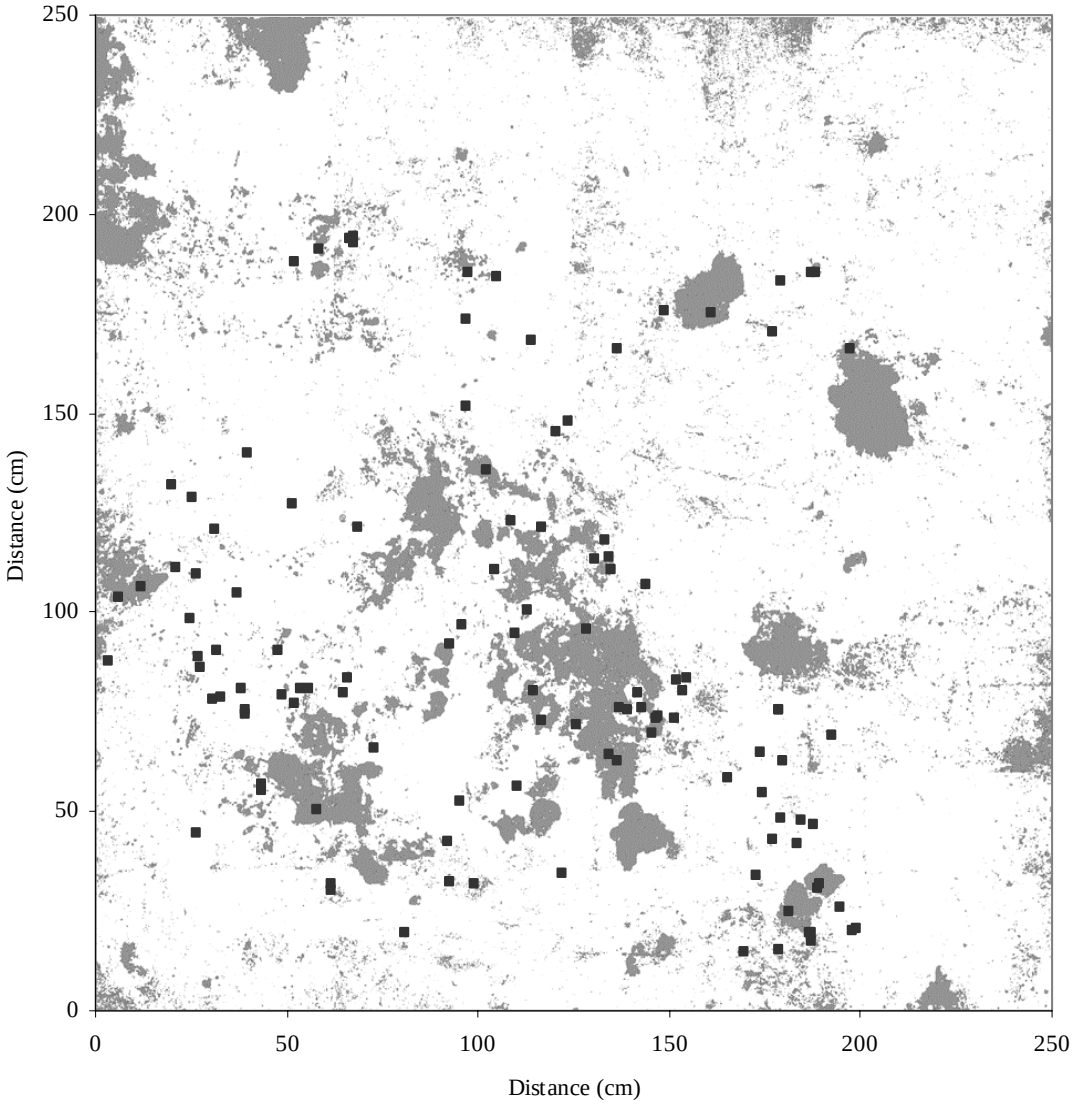

Third plot at a depth of 45 cm. Roots 1-2 mm

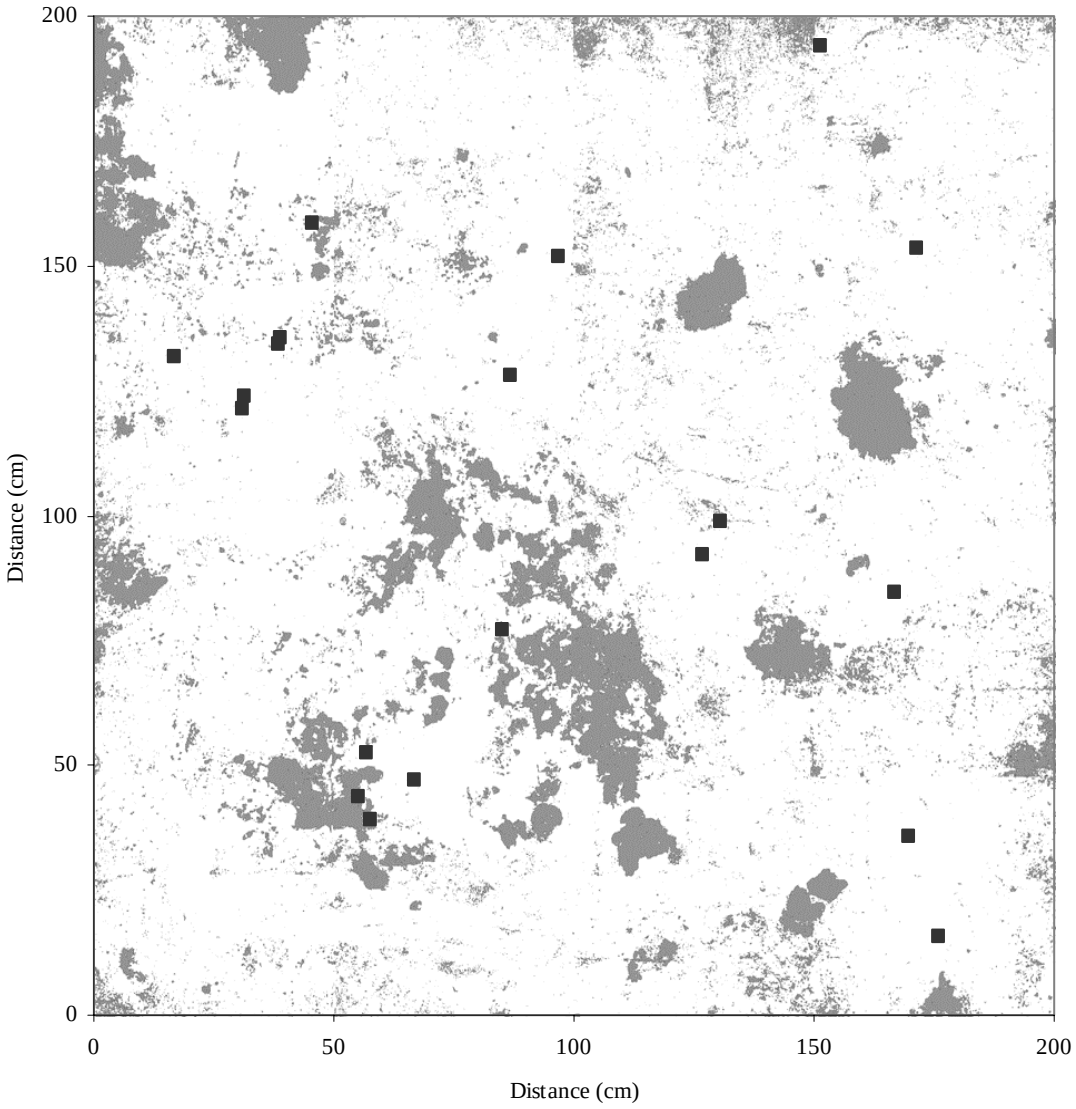

Third plot at a depth of 45 cm. Roots 2-5 mm

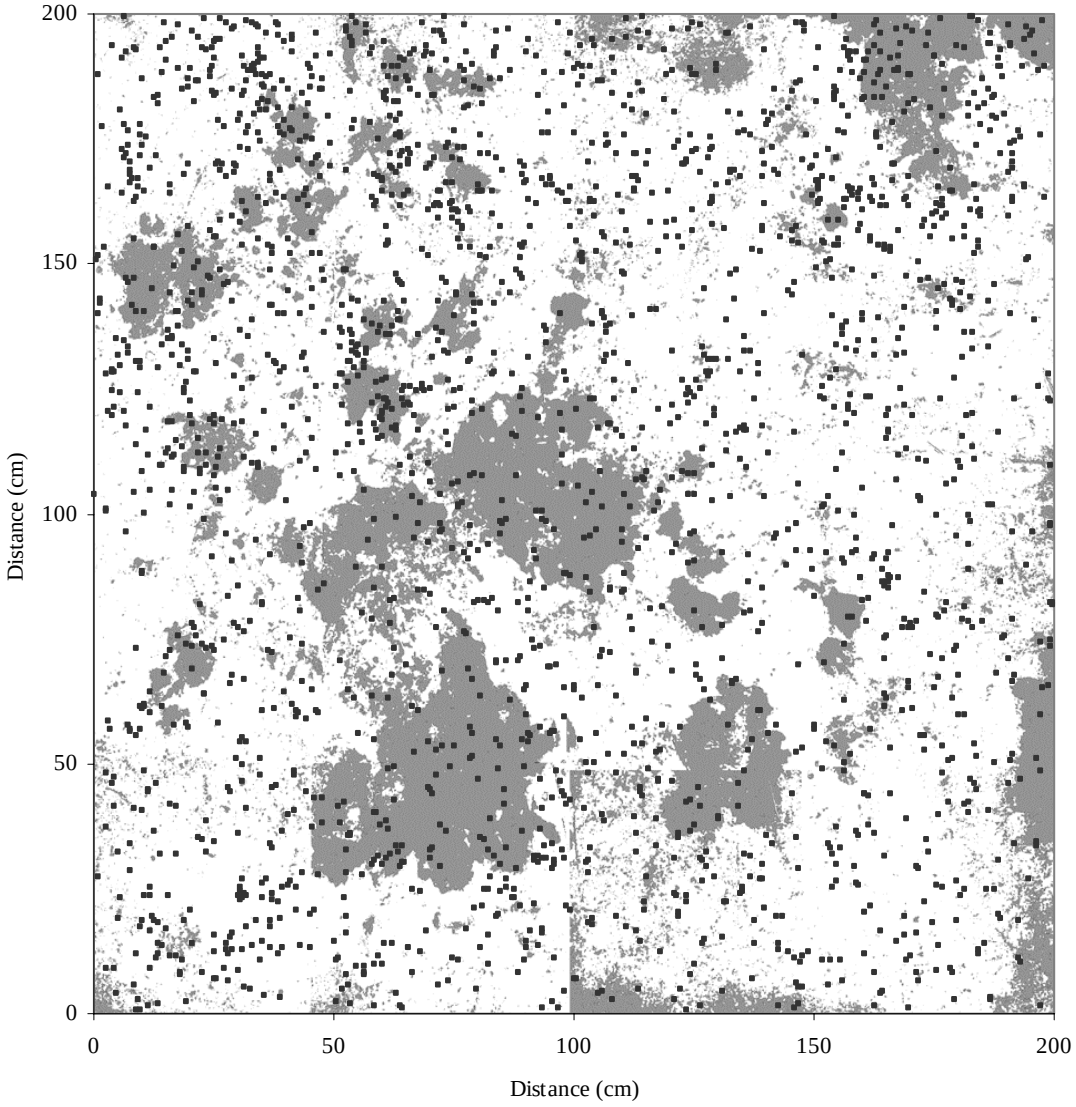

Third plot at a depth of 75 cm. Roots <1 mm

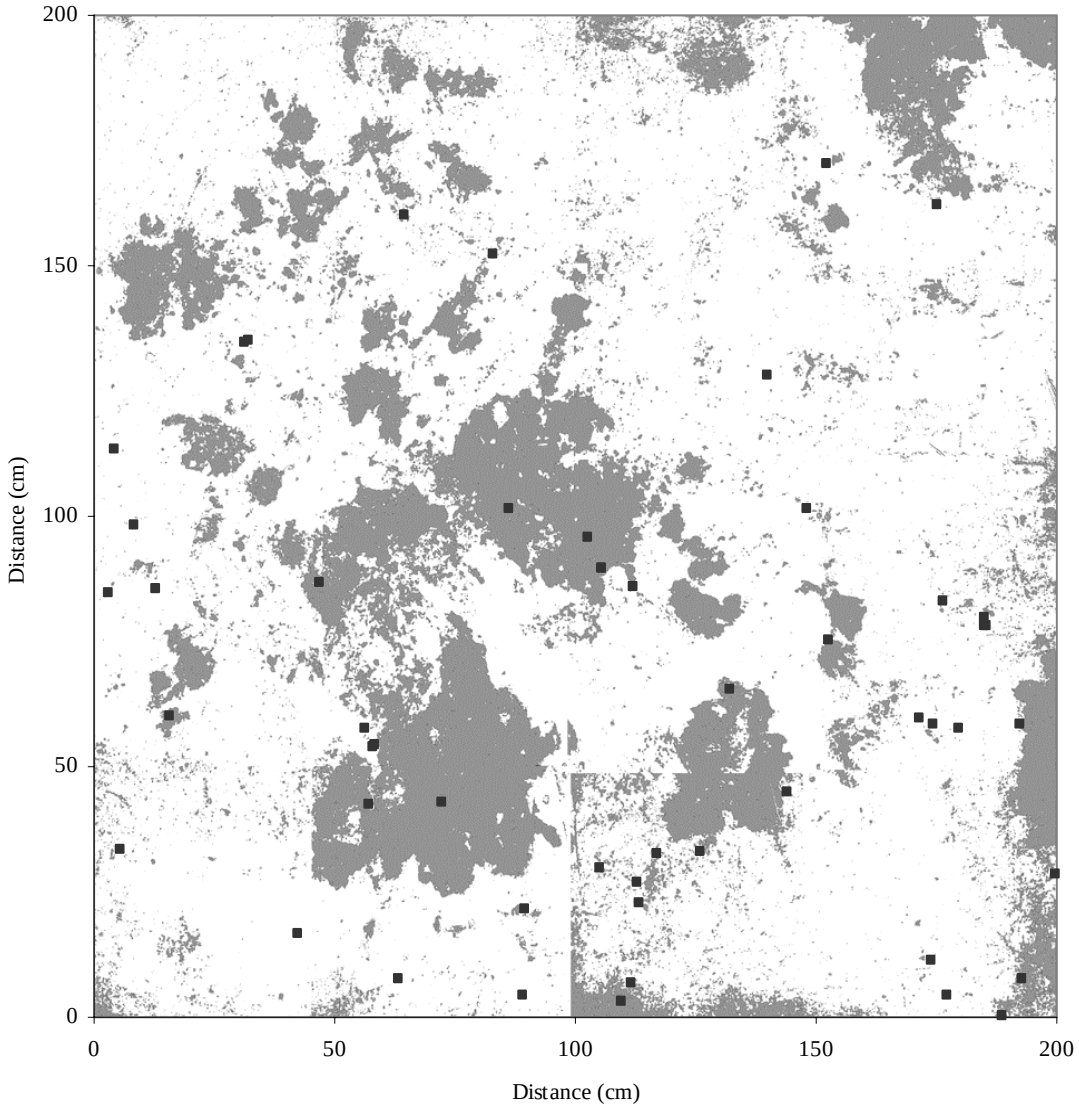

Third plot at a depth of 75 cm. Roots 1-2 mm

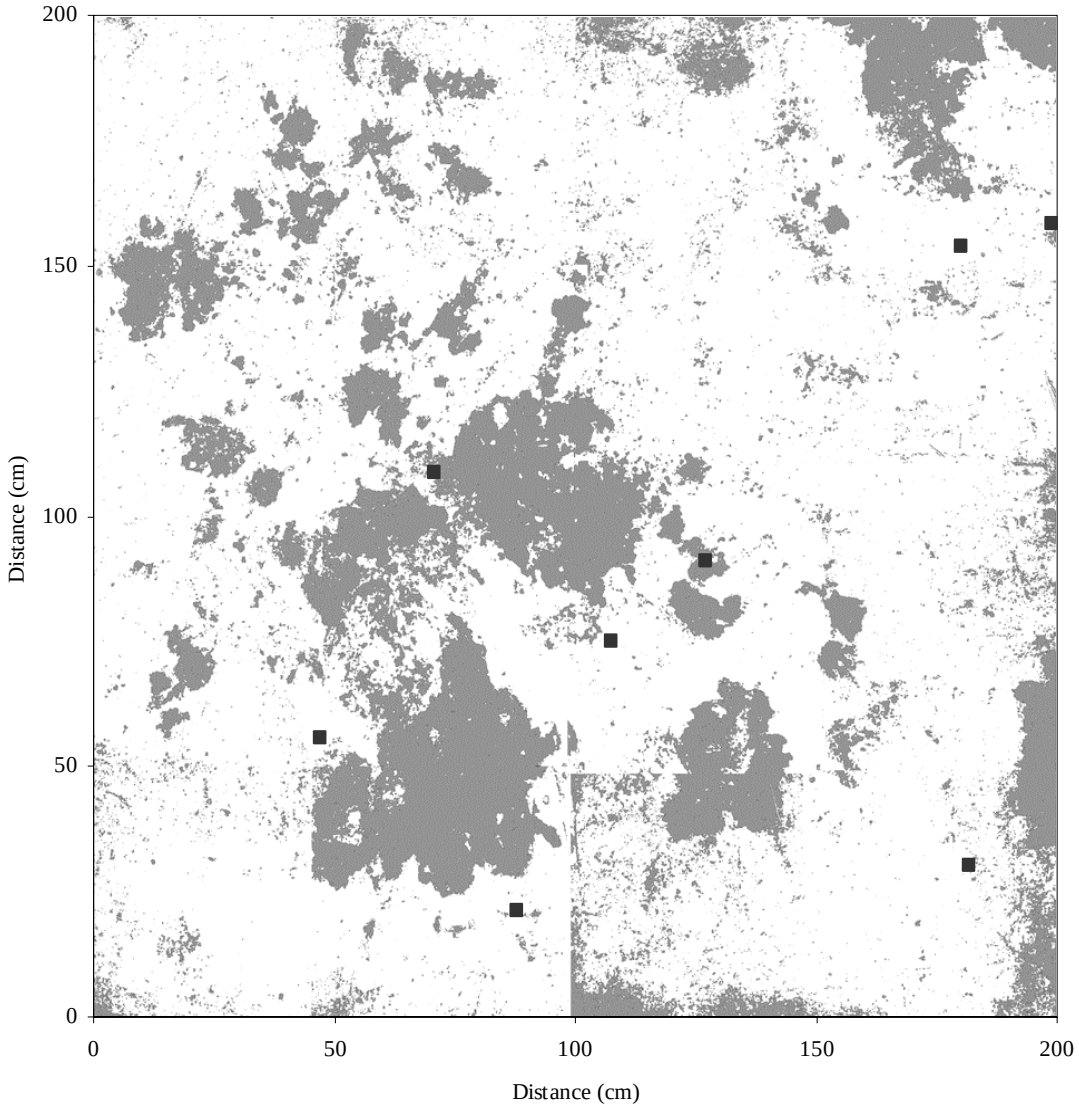

Third plot at a depth of 75 cm. Roots 2-5 mm

VITA

Nathan T. Gardiner

BIOGRAPHICAL:

Born April 9, 1977 in Logan, Utah, son of Duane and Trudy Gardiner.

EDUCATION:

2000 B.S. in Conservation Biology, Brigham Young University, Provo, UT

2003 M.S. in Soil Science, Texas A&M University, College Station, TX

PERMANENT ADDRESS:

1313 Brenda Ave, Kingsville TX 78363